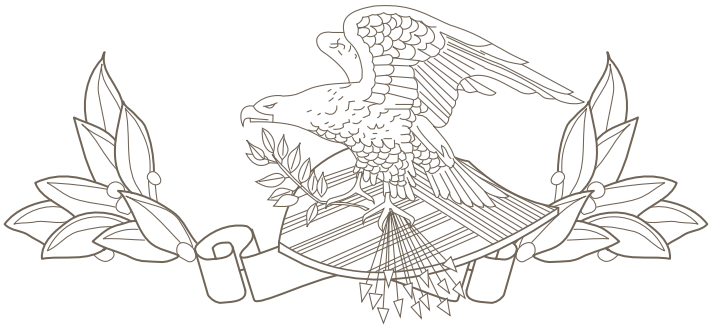

This technical report has been made electronically available on the World Wide Web through a contribution from

Anonymous Donor

Office of Scientific and Technical Information
Office of Science
U.S. Department of Energy
April, 2009

U.S. DEPARTMENT OF ENERGY

Office of Science

osti.gov

ANL-6633

Argonne National Laboratory

CONTRIBUTION TO THE THEORY OF TWO-PHASE, ONE-COMPONENT CRITICAL FLOW

by

Hans K. Fauske

Price $2.75 . *Available from the Office of Technical Services, Department of Commerce, Washington 25, D.C.*

DISCLAIMER

ANL-6633
Engineering and Equipment
(TID-4500, 18th Ed.)
AEC Research and
Development Report

ARGONNE NATIONAL LABORATORY
9700 South Cass Avenue
Argonne, Illinois

CONTRIBUTION TO THE THEORY OF TWO-PHASE, ONE-COMPONENT CRITICAL FLOW

by

Hans K. Fauske

Reactor Engineering Division

October, 1962

Operated by The University of Chicago
under
Contract W-31-109-eng-38
with the
U. S. Atomic Energy Commission

PREFACE

The experimental part of these investigations was carried out during the time from June 1959 to August 1960 at the Chemical Engineering Department, University of Minnesota, Minnesota.

First of all, I want to express my sincere gratitude to my teacher, Professor Dr. Herbert S. Isbin, University of Minnesota. He initiated my interest in two-phase flow in general and in critical flow in particular. He has never hesitated in placing at my disposal his profound experience in the fundamental problems of two-phase flow. I am especially grateful for the opportunity of becoming acquainted with his methods of approach to scientific problems, as well as his attitude toward science in general.

The extension of experimental studies was made possible by an Argonne National Laboratory contract, and the development of the theory and interpretation of the data was continued under an Atomic Energy Commission contract on Reactor Containment Studies. The author is also grateful for the Research Assistantship provided on these two contracts with the Chemical Engineering Department, University of Minnesota, Minnesota.

I furthermore wish to express my sincere appreciation to Mr. John B. Antolak for his advice and criticisms on the building of the equipment.

Finally, I wish to thank Graduate Students Stanley L. Gordon and Henry H. Chien for assistance with the numerical calculations.

TABLE OF CONTENTS

TABLE OF CONTENTS

TABLE OF CONTENTS

LIST OF FIGURES

LIST OF FIGURES

LIST OF TABLES

NOMENCLATURE

A	Cross-sectional area of flow, ft^2
A_g	Cross-sectional area occupied by the vapor phase, ft^2
A_l	Cross-sectional area occupied by the liquid phase, ft^2
a	Constant in the empirical relation, $v_g = aP^{-n}$
c_p	Specific heat at constant pressure, $Btu/lb_m\text{-}^\circ F$
c_v	Specific heat at constant volume, $Btu/lb_m\text{-}^\circ F$
D	Equivalent diameter or diameter of test section, ft
f	One- and two-phase friction factor, dimensionless
f_m	Average friction factor, dimensionless
F	Total frictional force, lb_f
F_{fg}	Friction force (shear force) in the vapor phase, lb_f
F_{fl}	Friction force (shear force) in the liquid phase, lb_f
G	Mass flow rate, $lb_m/sec\text{-}ft^2$
g	Gravitational constant, 32.2 ft/sec^2
g_c	Conversion factor, 32.2 $lb_m\text{-}ft/lb_f\text{-}sec^2$
H_m	Total enthalpy of the two-phase mixture, Btu/lb_m
H_s	Enthalpy of superheated steam, Btu/lb_m
h_f	Enthalpy of saturated liquid, Btu/lb_m
h_{fg}	The change in enthalpy going from liquid to vapor state, Btu/lb_m
h_{sL}	Enthalpy of subcooled water, Btu/lb_m
J	Conversion factor, 778 $ft\text{-}lb_f/Btu$
$K = c_p/c_v$	Ratio of the specific heats at constant pressure and volume, dimensionless
$k = u_g/u_l$	Slip ratio, dimensionless
L	Length in direction of flow, ft
l	Length in direction of flow, ft
n	Constant in the empirical relation, $v_g = aP^{-n}$
P	Static pressure, lb_f/ft^2
Q	Heat loss, Btu/hr
S_f	Entropy of saturated liquid, $Btu/lb_m\text{-}^\circ F$

S_{fg}	The change in entropy going from liquid to vapor state, Btu/lb_m-°F
S_m	Total entropy of the two-phase mixture, Btu/lb_m-°F
T	Temperature, °F
t	Time, sec
u_g	Average linear velocity of the vapor phase, ft/sec
u_l	Average linear velocity of the liquid phase, ft/sec
v	The specific volume of the two-phase mixture, ft^3/lb_m
v_g	The specific volume of saturated vapor, ft^3/lb_m
v_l	The specific volume of saturated water, ft^3/lb_m
W	Total mass rate, lb_m/sec
W_g	Weight of vapor flowing, lb_m/sec
W_l	Weight of liquid flowing, lb_m/sec
W_o	Shaft work, ft-lb_f/lb_m
x	Quality, lb_msteam/lb_mmixture, dimensionless, or length in direction of flow, ft
z	Height, ft

Greek Letters

α	Void fraction, dimensionless
$\Gamma = \frac{1-x}{x} v_l k$	ft/sec
ρ	Density, lb_m/ft^3

Subscripts

Ann	Annular flow
e	Exit of pipe
f	Liquid phase
fg	1. Change in properties between the vapor and liquid state 2. Indicates friction in vapor phase
fl	Indicates friction in liquid phase
g	gas phase
Hom	Refers to the "Homogeneous Flow Model"
KE	Kinetic energy
l	Liquid phase

m	Two-phase mixture
ob	Refers to observed conditions
s	Refers to steam
sm	Refers to constant entropy
sl	Refers to subcooled liquid
TP	Refers to two-phase flow
TH	Refers to either (1) the theoretical mass velocity calculated from the "Homogeneous Flow Model" or (2) the per cent steam calculated assuming homogeneous flow.
th	Refers to conditions at the throat of the conduit
1 to 6	Refers to location of pressure taps along the test section

CHAPTER I

INTRODUCTION TO TWO-PHASE FLOW

The term two-phase flow encompasses a vast field. In general, two-phase flow refers to the fluid flow of countercurrent and cocurrent mixtures of any two of the three phases - gas, liquid, and solid. The field of two-phase flow can be further subdivided into two-component and one-component flow. The second of these is complicated by mass exchange between phases, accentuated by heat transfer.

The flows of gas-liquid systems always have not only definite external bounding surfaces, but also internal interfaces between the flowing media, which are generally variable in space and time. Interactions of forces, and, in nonisothermal flow, thermal interactions as well arise at interfaces. These interactions fundamentally affect the changes in the fields of flow velocities, pressures, temperatures, and thermal and diffusion fluxes transferring from one point of space to another point separated from the first by an interface.

The existence of twice as many flow and property variables than in single-phase flow intimates that even the simplest physical model will produce intricate relationships. The simplest of models has not been adequate. Thus, the challenge is to construct new physical models, based on data, which retain enough rigor to describe the phenomena but do not become so intractible mathematically as to render them useless. This is, of course, the goal of engineering research in all fields. Unfortunately, in two-phase flow we are a bit farther behind than in most other fields.

The material now available in this field, which can best be described as data accumulation, is so large that we may speak of a new broad field of hydrodynamics, "the hydraulics of two-phase flow." It is, therefore, beyond the scope of this work to carry out a comprehensive investigation of every aspect concerning two-phase flow.

From the very beginning of confrontation with fluid-flow problems of this kind, a phenomenon resembling critical flow in a gaseous system in particular apprehended the author's heedfulness. This was at a time when a shortage of experimental data existed and a fundamental understanding of the mechanism causing two-phase critical flow was altogether missing. This type of flow has become of vital importance in nuclear reactor technology due to the trend toward progressively higher fluid temperatures in coolant applications. The two-phase, critical-flow phenomenon is a factor which limits the amount of coolant which can travel through piping geometries. Exact knowledge of this phenomenon is necessary since it is a factor vital to the determination of the overall hydraulic characteristics of a reactor cooling system.

The design of efficient and economic reactor-containment systems is in many instances dependent upon predictions of critical flow behavior for a reactor coolant. Typically, the primary coolant contains considerable energy and contamination in a water-cooled reactor. Upon the incident of a rupture of some part of the primary coolant system, the escaping coolant must be contained in order to prevent the release of radioactive materials to the environs. Since the critical-flow phenomenon plays an important role in the rate of loss of the primary coolant, exact technical knowledge of its mechanism is required for the design of efficient and economic containment, and of pressure-suppression systems.

Critical two-phase fluid flow is encountered in other engineering and industrial operations. It occurs commonly in cascade drain pipes of boilers and turbines, in traps of steam heating plants, in the low-temperature flow of refrigerants and condensed gases, in the high-temperature flow of rocket propellants, and could take place in almost any fluid-flow system.

Critical flow in a gaseous system, which is quite often in the literature referred to either as maximum or sonic flow, is defined as the flow phenomenon characterized by having the fluid velocity equal to the rate of pressure propagation. As the pressure on the downstream side of

an orifice or nozzle is reduced, the velocity in the throat increases until a maximum value is obtained. At this point, the rate of pressure propagation up the pipe is equal to the fluid velocity down the pipe. Discharges greater than the critical value can be obtained in expanding nozzles. Single-phase critical flow can be predicted by thermodynamic equilibrium theory. However, thus far no reliable theory has been established to predict two-phase critical flow.

The purpose of the experimental work presented here was to procure data for critical two-phase, one-component flow at higher pressures. As far as the author knows, there exist no unclassified data for critical two-phase flow for critical pressures over 100 psia.

A new method of achieving two-phase critical flow data on the flow of steam and water was developed, which involved the use of a high-pressure, high-temperature steam generator and a high-pressure water pump to premix a steam-water mixture. This method required an extensive period of planning, ordering, and building the high-pressure equipment, followed by a long period of overcoming difficult engineering problems to get the equipment operating properly. Only investigators with substantial experience in building and operating two-phase flow loops can really appreciate the many design problems encountered.

The range of experimental variables covered here is as follows:

Total flow rates:	500-4300 $lb_m/sec\text{-}ft^2$
Qualities:	0.01-0.7
Critical outlet pressures:	40-360 psia.
Pipe sizes:	0.4825, 0.269, and 0.125-in. inside diameter and with lengths of 56¼ and 110 in.

The author has also presented a new theory for critical two-phase flow. This includes a new definition of the specific volume of the two-phase mixture. Furthermore, a new postulate for two-phase critical flow

is introduced, which leads directly to an expression of void fraction as a function of quality and pressure only. Hence, a theoretical expression for predicting the critical flow rate was derived. The model can also be used to calculate two-phase friction coefficients for critical-flow conditions.

CHAPTER II

LITERATURE SURVEY

2.1. Past Work on Slip, Void Fraction, and Flow Patterns

One of the most laborious problems associated with two-phase flow in general, both in using existing models and promoting new ones, is knowing the fraction of the cross-sectional area occupied by each phase. The fractional area occupied by the gas phase is often referred to as the void fraction. Unfortunately, the void fraction cannot be calculated from the mass flow rates of the individual phases alone, since it is generally accepted that the gas travels at a velocity greater than that of the liquid. The void fraction depends, therefore, upon the difference in phase velocities or the so-called slip velocity. The slip velocity, in turn, is presumably influenced by many interacting variables, such as mixture quality, the total and the individual phase-flow rates, temperature, pressure, physical properties of the phases, direction of flow, means of circulation (natural or forced), heat lost or gained, and the size and shape of the confining cross section. Because of the inherent complexity of the problem, no satisfactory method of predicting void fractions has yet been devised. Consequently, empirical and semi-empirical approaches have attained unusual prominence.

Literature surveys, such as those of Ambrose[5] and Galson,[37] show that virtually no slip, void-fraction, or flow-pattern data have been taken at the velocities found in critical flow, with the exception of one investigator.[66] In that case no attempt at correlation was made. Pattie[79] cites the recent void-fraction investigations available and discusses correlations for predicting void fractions which have been proposed by Martinelli et al.,[70] Armand,[7] Yagi et al.,[104] Untermeyer,[100] and Zmola and Bailey.[10] A table is also presented which gives for each investigation the system geometry, phases used, means of circulation, pressure and quality ranges studied, and the method employed for measuring void fractions. Larson[62] gives in his work a good resumé of different methods adopted for measuring void fractions which have been

proposed by Martinelli and co-workers,[70] Armand,[7] Schwarz,[87] Smith and Hoe,[93] Dengler,[28] Anson et al.,[6] Bailey et al.,[10] Cook,[26] Egen et al.,[32] Rodrigues,[83] and Dixon.[30] Lottes, Petrick, and Marchaterre,[67] have summarized all the data that have been obtained up to date at the Argonne National Laboratory. Several possible correlations are discussed and compared with data of other investigators for vertical up-flow of steam-water mixtures. Also, working curves are presented which may be used for the prediction of the density of steam-water mixtures. Besides Schwarz,[87] other German investigators have carried out work on density distribution and pressure drop in two-phase flow; among these can be mentioned Zinzen,[106] Zinzen and Schubert,[107] and Jaroschek and Brandt.[55]

In an effort to explain two-phase flow, the various systems studied were described as possessing a given flow pattern in much the same way as single-phase flow is described as viscous or turbulent. Many different flow patterns and transition regions have been proposed for horizontal, inclined, and vertical pipes, but these proposals have all been similar in many respects.[46] To describe it in another way, two-phase flow can occur in several different geometric shapes. Although most of the work of classifying these flow patterns has been done on two-component, two-phase flow, the trend has been to use the results of these investigations as a comparison when other systems are used. Bergelin and Gazley,[16] Alves,[4] Kosterin,[60] and Krasiakova[61] have studied flow patterns.

There is some variation in the definition of the flow patterns given by different observers. However, for horizontal flow, the most general types of the various geometrical arrangements of liquid and vapor which can exist are:

1. Annular. One component flows in the core of the conduit surrounded by the second phase which flows along the inner perimeter of the conduit. This flow pattern may be attained if both phases move at high rates, although the individual phases do not move at the same velocity.

2. Stratified. The heavier phase flows at the bottom of the conduit and the lighter phase flows above it. The interface is smooth.
3. Fog. This pattern depicts both phases intimately dispersed and flowing essentially at the same speed. The mixture is assumed to be homogeneous.
4. Wavy. This flow pattern is similar to the stratified pattern except that the interface is wavy rather than smooth.
5. Bubble. The lighter phase flows as bubbles concentrated primarily at the top of the conduit.
6. Slug. The heavier phase flows as a continuous phase, while the lighter phase flows in slugs along the top of the conduit.
7. Plug. The heavier and the lighter phases appear to flow alternately; however, the heavier phase may be continuous in some regions.

In addition, Kosterin subclassified plug flow by the amount and type of foam generation, and Krasiakova subclassified annular flow by the concentration of water in the core. Alves has also made some measurements of the amount of water in the gas core. The above flow patterns have been pictorialized by several authors.[4,11,61,36,86] Alves represented his observations by plotting the demarcations between flow patterns on a curve with coordinates of superficial vapor velocity and superficial liquid velocity. Krasiakova represented her observations using superficial vapor velocity and the ratio of superficial vapor to liquid velocity. For comparison, both of these presentations are shown in Figures 1 and 2; Alves' coordinates have been used. It is not surprising that some differences exist between these two representations since they were both arrived at from visual observations and are, therefore, somewhat dependent upon the observer. Attempts have been made to generalize the coordinates for representing the flow patterns [see Baker[11]], but the rational is yet to be proved.

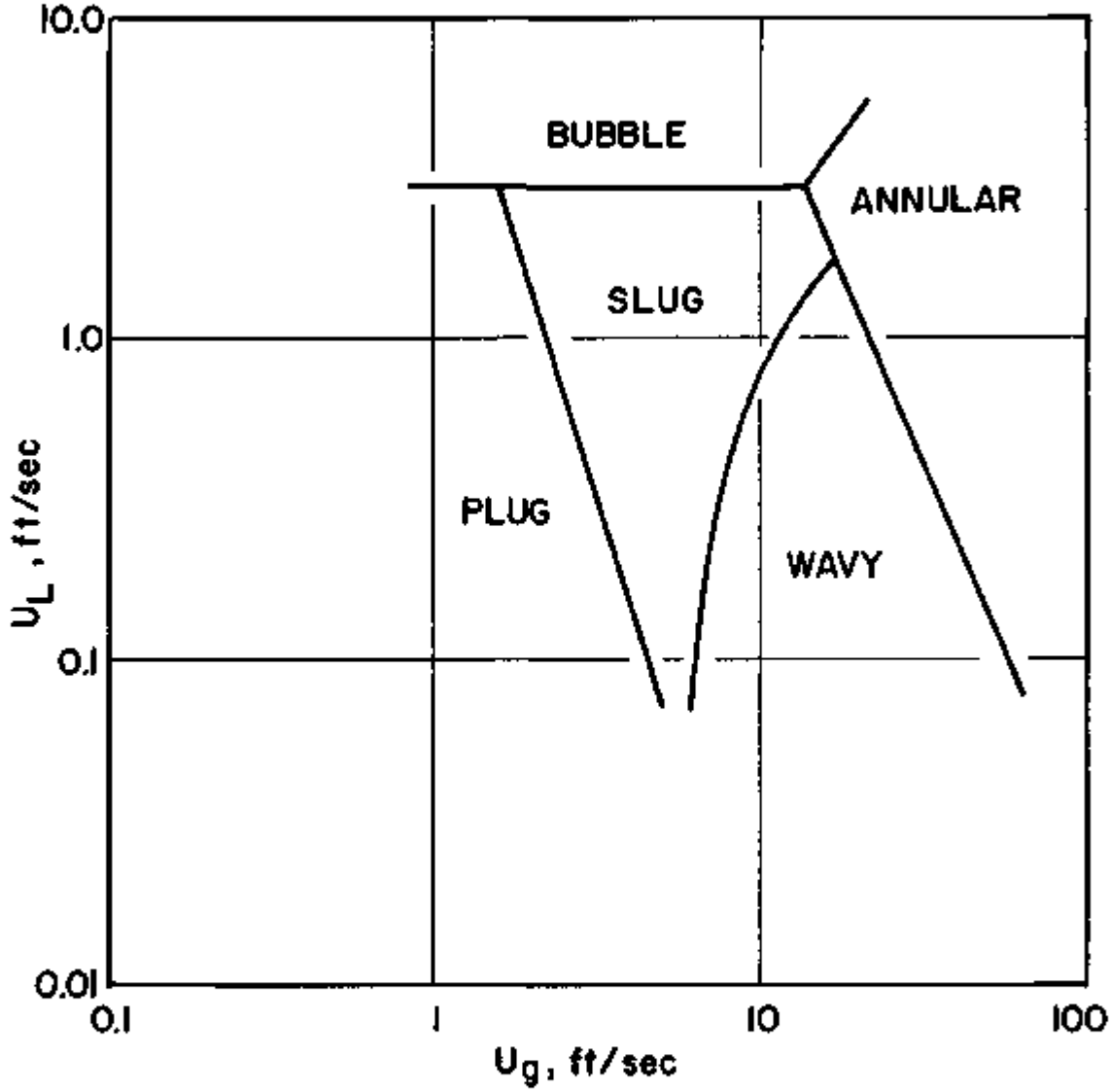

Figure 1. Alves' Limits of Flow Patterns. Coordinates are superficial phase velocities.

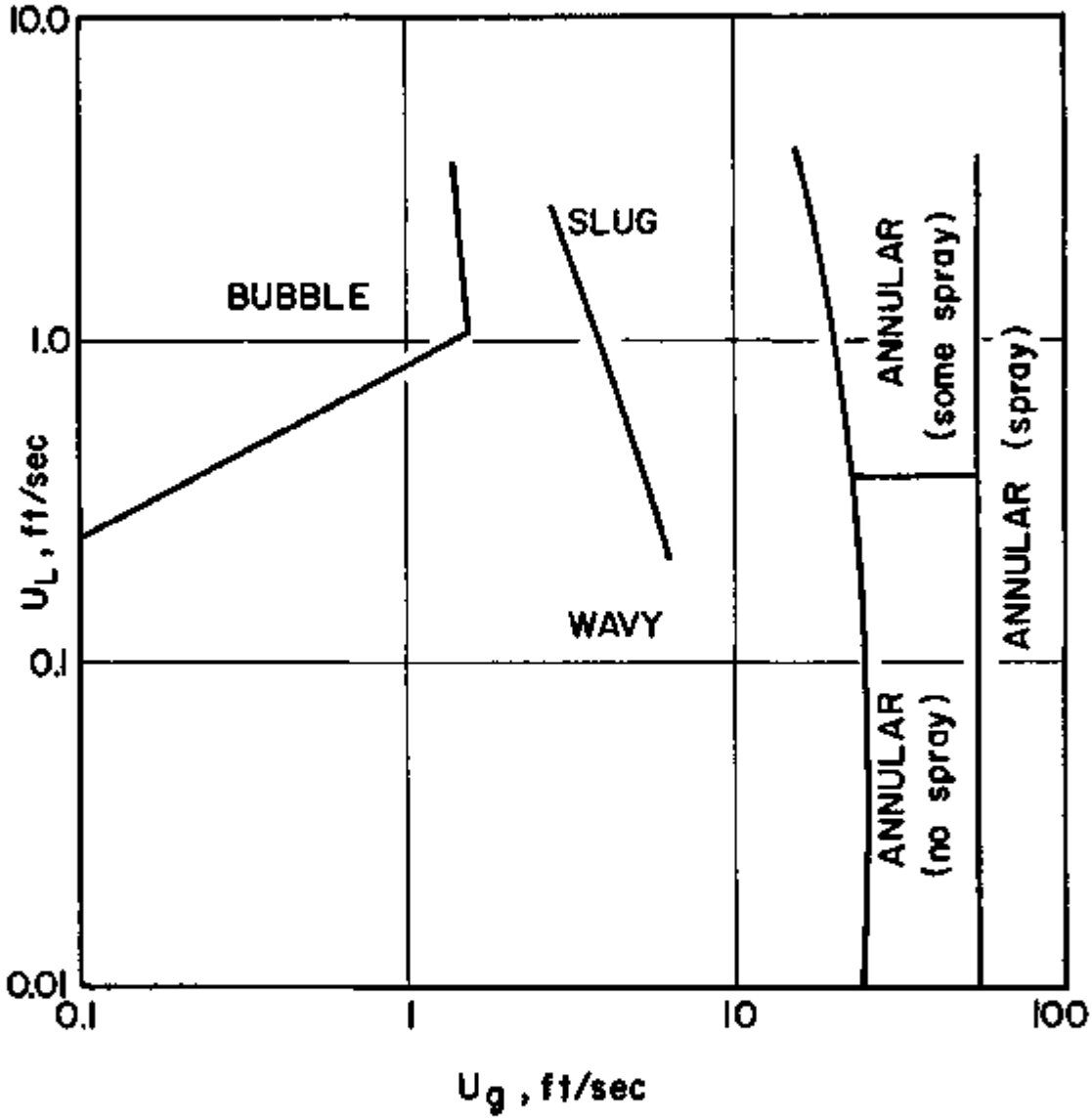

Figure 2. Krasiakova's Limits of Flow Patterns. Coordinates are superficial phase velocities. Subdivisions of bubble flow have been omitted.

Another prominent scheme of classifying two-phase flow was given by Martinelli et al.,[70] who divided the various flows into flow types by considering the superficial Reynolds number of each phase and making an analogy with single-phase flow. For a Reynolds number greater than 2000, the flow type is considered to be turbulent, whereas for a Reynolds number less than 1000 the flow is considered viscous. The region of Reynolds number between 1000 to 2000 is considered as the transition region in which the flow may be either viscous or turbulent, depending on the system and the surroundings.

Although the descriptions are qualitative, the types of flow encountered are important because, to a large extent, they characterize the nature of two-phase flow and, hence, of critical flow. Visual observations and measured effects, however, may not agree in all cases. Since the flow patterns are very important concepts and closely related to the author's theory, they will be discussed in more detail in Chapter V.

2.2. Past Work on Two-phase Pressure Drop

No attempt will be made to cover in detail the literature on two-phase pressure drop and heat transfer. The interested reader is referred to the following literature surveys: Bennett,[15] Collier,[25] Gresham,[39] Isbin,[46] Jacobs,[54] and Masnovi.[73]

Gresham's survey, which includes one hundred and eighty abstracts, gives a very complete coverage of the literature prior to 1953. Collier's, one of the latest, reviews the literature up to the end of 1957.

Because the mathematical models required for theoretical analyses of the problem of two-phase flow are quite complicated, the more successful approaches have been empirical and semi-empirical. The majority of theoretical analyses [e.g., Harvey and Foust[41]] have assumed that the phases are mixed sufficiently to be considered as a homogeneous fluid. The work of Linning[66] is an example of a semi-empirical approach; Linning set up "one-dimensional" models for froth, stratified, and annular

flow configurations, determining unknown parameters experimentally. Lockhart and Martinelli[71] presented a moderately successful correlation for the two-component problem. Martinelli and Nelson[72] adapted the two-component correlation of Lockhart and Martinelli[71] to single-component systems by means of a simple correction to account for changes in the axial component of momentum. The potential advantage of this approach over that of Harvey and Foust is the relative simplicity of the computations. However, Martinelli and Nelson did not possess sufficient experimental data to verify their approach.

One of the most recent works on the prediction of pressure drop in two-phase, single-component fluid flow is that of Isbin et al.[48] They conducted extensive experimental work with steam-water mixtures at qualities ranging from 3 to 98 per cent and at pressures ranging from 25 to 1415 psia. They attempted to correlate their data by use of the Martinelli correlation, but found serious flow-rate and pressure effects. The use of a homogeneous friction-factor model also proved unsuccessful. Therefore, they correlated their data in a restrictive manner which took into account the flow-rate and pressure dependencies.

In spite of the large amount of literature in this area, the information is still inadequate for obtaining accurate and reliable design procedures for two-phase, single-component flow systems.

2.3. Past Work on Critical Flow

Much more is known about critical flow of a single-phase fluid than is known about the two-phase critical flow of fluids. Many text books, such as that of Hall[40] and that of Shapiro,[89] are available which give the theory of single-phase flow.

Most of the research which has been done in the general realm of two-phase flow has concerned either two-phase, two-component systems or two-phase, single-component systems very close to saturation conditions. Most of the work involving the first has been done in the United States,

whereas British investigators have taken the initiative with the latter, by studying the behavior of saturated water or mixtures of liquid water and steam resulting from some kind of an expansion or flashing process.

The field being of such a complexity, it was not surprising to find a variety of possible simplifying assumptions being made by different investigators in an attempt to bring theory close to fact. To date, however, no single design method has yet been proposed that will prove satisfactory, except for a few limiting cases.

The first real attempts at a serious study of two-phase flow were probably those of Sauvage[85] in 1892. According to Isbin,[46] Rateau[80] in 1902 showed the existence of critical flow in the flow of boiling water through nozzles. He obtained this critical condition by dropping the back pressure until the discharge reached a maximum. He also developed a method of calculating the quantity of saturated water discharged through a nozzle based upon isentropic expansion.

Mellanby and Kerr[75] in 1922 studied the flow of wet steam through nozzles. All four nozzles used were of the simple convergent or convergent parallel type. Two of the nozzles were used in conjunction with a search tube so that the tests included pressure measurements as well as flow determinations. Only flow tests were carried out on the other two, as these were not fitted with a search tube. In all cases, flow determinations were made with varying initial superheats at a supply pressure of about 75 psia. The flow curves that these investigators have presented for these four nozzles showed certain variations between themselves, but they all agreed on the two points: (1) that the flow, at and near the initially dry state, was excessive when compared with the theoretical as obtained on the assumption of stable expansion, and (2) that the form of the flow curve over a small range of superheat beyond the initially dry condition was not in agreement with the theoretical assumption of complete supersaturation on any rational basis of expansion losses. Equations were developed in order to estimate the "fractional reversion" (fraction liquid actually present/fraction liquid with no supersaturation) existing in

the nozzles. The fractional reversion was found to be less for the nozzle with central search tube than for the full-bore jet. The difference seems rather unaccountable. From their calculations, it was noticed that there was no indication of reversion before a value of roughly 1½ per cent equivalent wetness was reached.

The work of Stanton[94] in 1926 gave valuable insight into the high-speed flow of air through sharp-edge orifices, convergent nozzles, and convergent-divergent nozzles. This investigator obtained both axial and radial pressure profiles by using both search and Pitot tubes. The most important conclusions derived in this work are as follows: (1) In each of the three characteristic types of orifices which may be used for the discharge of gases from a vessel at constant pressure into a receiver at a pressure appreciably below the critical value (0.527 times the upstream stagnation pressure), the area of the jet diminishes to a minimum value, at which the velocity is that of sound under the conditions existing, and then increases. This minimum section in the case of a free jet is not constant in area or position relative to the plane or throat of the orifice, but depends on the total ratio of expansion. (2) In a jet in which the expansion takes place within solid boundaries, i.e., a diverging nozzle, the minimum section may for all practical purposes be regarded as coincident with the throat of the nozzle for all ratios of expansion. (3) The flow of the fluid up to the minimum section is adiabatic in character.

Goodenough[38] in 1927 said the fact that the speed of the water drops is only a small fraction of the speed of the steam has a decided effect on the discharge of wet steam, for the total friction is comprised of not only the interaction between the fluid and walls, but also of the internal interaction between steam and water particles. Goodenough further showed by calculation that supersaturation would give a net increase in isentropic flow for a given pressure drop. He also pointed out that the surface energy of the droplets formed in such flows could be quite large. Another complication is that any entrained drops (usually larger than those formed by condensation) probably do not cool fast enough during the expansion to

maintain thermal equilibrium with the steam. He points out that all the above could occur simultaneously in a flow process.

Kittredge and Dougherty[58] in 1934 presented an expression for the calculation of critical discharge capacity for steam traps based on the initial and discharge pressures, and the specific volume of the mixture evaluated at the discharge pressure. Their calculated values presented in graphical form are said to be 100 to 200 per cent greater than experimental values through a nozzle.

In 1934, Yellott[105] investigated drop size and supersaturation by studying the flow of low-pressure steam through nozzles similar to those used in turbines. This investigator experimentally verified the existence of supersaturation with the aid of light rays, applications of the laws of optics, and a search tube for nozzles. He found that the condensation occurred between the 3 and 4 per cent moisture lines on a Mollier diagram if an isentropic expansion is assumed.

Rettaliatta[81] in 1936 extended Yellott's work and intended primarily to determine the effect of wall roughness on the flow of steam in nozzles. It was found that wall roughness, causing a retardation of steam flow, made the point of initial condensation occur at a higher pressure and farther downstream than in the smooth-walled nozzle. This caused the Wilson line to occur at the 3.2 per cent moisture line on the Mollier diagram for the rough-walled nozzle, instead of at the 3.7 per cent moisture line as was found for the smooth nozzle. Rettaliatta claimed that this was the result of the increased time of expansion in the case of the rough nozzle.

In 1937, urged by a need for more information on critical flow for the design of cascading drain pipes, Bottomley,[20] experimenting with flow of boiling water through orifices, found that his actual flows based on experimental data were 5 times greater than the predicted values based on computation by the single-phase equilibrium theory. His explanation is that the effects of surface tensions lower the pressure at which the propagation takes place. Because of surface tension, the condition of flow at the

throat is that of unstable equilibrium. Bottomley further cites one experimental test on pipe flow to show that pressure drops and critical outlet pressures are in accordance with his assumption that there is zero relative velocity between phases. Unless the flow form in Bottomley's test was of the frothing type, as a consequence possibly of some additive in the water, his results and conclusions differ radically from those presented here, as will be seen later.

Also, Hodkinson[44] in 1937 noted that his actual flows of boiling water were larger than given by his equilibrium calculations. His evaluations of critical discharge were made at constant entropy and under the assumption of phase equilibrium.

In 1942, Benjamin and Miller[13] reported on the flow of a flashing mixture of water and steam through pipes. They assumed no slip between the two phases and complete approach to thermodynamic equilibrium. They derived an equation for mass velocity which includes a friction term. However, they state that, while friction (i.e., pipe length) will affect the inlet pressure, it will not affect either the critical flow or the critical pressure. The expansion was considered to be isentropic. The equation of continuity and Bernoulli's equation formed the basis for their derivation. A value for "f" or 0.012 was used, and this corresponded to the value measured by Bottomley. Their flow equation is as follows:

$$\left(\frac{W}{A}\right)^2 \left(\frac{1}{2g}\right)\left(\frac{1}{144}\right) = \frac{\int_{P_1}^{P_2} -\rho \; dP}{\ln(\rho_1/\rho_2) + (fL/D)} \quad , \qquad (2.3\text{-}1)$$

where

W = flow, lb_m/sec

A = cross-sectional area, ft^2

g = acceleration of gravity, ft/sec^2

P = pressure, lb_f/ft^2

ρ = density, lb_m/ft^3

f = friction factor, dimensionless

D = diameter of pipe, ft.

Observed and calculated flows and pressures agree rather well. These authors were not certain that the critical velocity and the acoustic velocity were the same.

Woods and Worthington[103] in 1943 discussed in detail boiling in the pile. They were interested both in pressure-drop calculations and also in critical flow. They assumed isentropic expansion in their calculations for critical flow. They also considered no slippage and thermodynamic equilibrium. A method for the computation of pressure drop was outlined which is essentially the Fanning method. Mixture properties were used, and the reciprocal method of averaging was used for viscosities. Small incremental lengths of pipe were taken with the pressure drop being computed over each section.

Stuart and Yarnell[97,98] in 1944 used two orifices in series for their experiment with metastable flow of saturated water as related to surface effect. Their first paper[97] presented a theoretical analysis of the flow of water and steam through two orifices in series over a wide range of pressures and temperatures. Their second paper[98] presented the results of experimental investigations on this subject, with water at an initial pressure of 100 psia and over a range from room temperature to saturation temperature. The principal data sought were the pressures established in the intermediate chamber between the two orifices, and especially the variations of this intermediate pressure with reference to the temperature of water supplied and the type of orifice. One of the most significant facts revealed by these researches is that under certain conditions of flow the fluid assumes a metastable state which greatly influences the characteristics of the process.

Silver and Mitchell[92] in 1945 carried out experiments on convergent-parallel nozzles and developed a theory, based on the assumption of delayed evaporation, to account for the high mass flow rates obtained. The expansion in a nozzle takes place rapidly and the possibility of a metastable state cannot be discounted. It would appear from their description of

the flow form, however, that relative velocity between phases must exist, and that this will exercise an important influence on mass flow. This factor was neglected in the theory developed by Silver and Mitchell. Their experiments and theory correlated well for the nozzle of smaller diameter ($\frac{3}{16}$ in.) but not for that of larger diameter ($\frac{1}{2}$ in.). It also should be mentioned that, though they observed a critical flow effect, they were hampered in their study of this by the fact that a pressure tap located at the throat partially destroyed the metastability and resulted in a reduced flow rate. Therefore, they interpolated between the pressure measured experimentally with the tap and that predicted by their theory to arrive at an estimate of the critical pressure. They noticed a slight increase in mass velocity as the back pressure dropped below the critical, and attempted to explain this by increased heat loss from the nozzle.

Burnell[23] in 1946 was the first investigator to suggest that the peculiarities exhibited in evaporating flow could be accounted for by the existence of relative velocity between the phases. He published conclusive experimental evidence that relative motion was present in the evaporating flow of water. This concept of different velocities later aided subsequent investigators. Burnell worked with both nozzles and pipes. He developed a theory for nozzles similar to that of Bottomley's,[20] but it was somewhat more refined. This approach correlated the observed nozzle flow rates quite well.

However, his flow rates in pipes were 1½ to 2 times those calculated by using a friction factor ($4f = 0.012$) and assuming homogeneous flow. He attempted to measure metastability with a thermocouple and found that none existed, and, hence, explained his higher flow rates by slip.

Silver[91] in 1948 extended the work presented in a previous paper[92] to include a more detailed study of critical flow in nozzles. A theory for the actual amount of vapor which will form was given, together with an analysis of its effect upon the velocity of flow and the

quantity of fluid passed by a nozzle. It was found that, although the system consists of a central core of liquid and an envelope of vapor, the calculated limiting velocity of flow, which was the velocity of pressure propagation in the system, was low. There was a corresponding critical pressure, analogous to that in a gas nozzle. But in contrast to the gas case, both the critical pressure and the limiting velocity itself were functions of the diameter and length of nozzle. Experiments were described which confirmed these theoretical deductions in all respects and which also showed good quantitative agreement with calculated velocities, critical pressures, and amounts of discharge and of evaporation.

In 1949, Tangren, Dodge, and Seifert[99] derived a general expression for the flow process in an idealized mixture. They assumed that a gas-water mixture, when expanded through a de Laval nozzle, acts as a compressible fluid. Their general thermodynamic relations for critical flow of helium-water mixtures through a de Laval nozzle approximated the critical flow expression for perfect gas. Their equations are not directly applicable to a two-phase, single-component flow system with mass transfer.

Allen[3] in 1951 presented a method of designing piping and valves for carrying a flashing mixture of water and steam. He used Bernoulli's equation and the equation of continuity to arrive at a result similar to that of Benjamin and Miller.[13] He, however, assumed isenthalpic expansion to occur, and on that basis he found the specific volume as a function of pressure. He obtained a mathematical expression for the flow rate but did not solve for the maximum value by differentiation. However, by assuming acoustic velocity, he then developed an expression relating inlet pressure, outlet pressure, and flow. He assumed equal velocities for both phases.

In the same year, Bailey[9] reported on experiments relating to the flow of saturated water through orifices and nozzles. He treated the problem on the basis of heat transfer from a metastable case to the surrounding

vapor. He concluded that metastability could exist in both orifices and nozzles, but was more probable in orifices. Flow rates were predicted to within 10 per cent accuracy.

In 1951, the effect of forced circulation on both heat transfer and pressure drop was studied by Schweppe and Foust.[88] They introduced to their electrically heated test section liquid water at its boiling point. They found that the critical flow rate corresponded approximately to the homogeneous theoretical maximum discharge rate. Their values may be erroneous because of the fact that their outlet section of the line was not of uniform cross section and, most of all, their indication of critical exit pressure was based on the pressure tap placed at 5 in. from the end of the pipe, which would not reveal the large kinetic pressure drop as the pipe exit was approached.

In addition, Harvey and Foust[41] the same year studied two-phase flow in evaporator tubes and reported on experiments in which critical flow was realized. They also carried out a mathematical analysis by applying the energy, momentum, and continuity equations to the differential section at the end of a tube, leading to an equation for critical flow. Assumptions made included homogeneous flow, equal phase velocities, equilibrium, perfect gas behavior of water vapor, and pressure drop predictable by Martinelli's correlations. The equations, however, are not of direct application to the present problem.

Linning[66] in 1952 presented an analysis of the adiabatic flow of evaporating fluids in pipes which he supported with experimental data using boiling water. Linning set up "one-dimensional" models for annular, stratified, and froth flow configurations, determining unknown parameters experimentally. Good agreement between his observed critical temperatures (pressures) in a 0.128-in. pipe and those calculated from his equation for annular flow were obtained. Visual observation of the leaving stream confirmed the annular flow postulate.

Pasqua[78] in 1953 discussed the flow of saturated and subcooled liquid Freon-12 through small-diameter orifices, short tubes, and nozzles. Experimental data confirmed the establishment of a metastable state of fluid flow which accounts for the large discrepancies found from a thermal-equilibrium analysis. A method was presented whereby the actual mass flow rate of saturated liquid could be calculated. The analysis was based upon experimental investigations and was restricted to adiabatic conditions. When the theories of Silver and Mitchell[92] or Bailey[9] were applied to saturated Freon-12 flow through nozzles with large length-to-diameter ratios, large discrepancies were found.

In the same year, Cruz[27] reported on the results of his study of critical flow, which represents one of the first nonclassified studies undertaken explicitly to measure critical flows of steam-water mixtures over a wide range of quality. He found that the critical pressure was not sensitive to the manner of initial mixing, to the phase distribution, or to the length of the pipe. He measured pressure gradients throughout his test section while holding inlet quality and flow rate constant. The outlet pressure was varied and critical conditions were taken as the point at which the pressure gradient was no longer affected by a decrease in the pressure of the discharge receiver. His results were correlated by plotting percentage deviation against quality. He also plotted Burnell's data and showed excellent correlation between the two sets of data. This investigator's work will be discussed in more detail later on in this paper, since his results are closely related to the author's.

Stein and co-authors[95] in 1954 studied pressure drop and heat transfer to water in an internally heated annulus. They found maximum mass velocities greater than those predicted by homogeneous flow.

Additional data on the critical flow of steam-water were presented by Moy[77] in 1955. He continued the work of Cruz[27] and extended it to other sizes of pipes and over a greater range of pressures, up to 43 psia.

Moy correlated his data in the same manner as did Cruz. Several analytical models were tried. A modified momentum model based on Linning's approach and making use of slip values from Martinelli's work yielded fair results over the quality range from 10 per cent to 100 per cent, the error increasing to +25 per cent as the quality decreased to 10 per cent. This work will also be discussed in more detail later on in this paper.

A rather comprehensive study of the flow of a flashing mixture of water and steam was given by Haubenreich(42) in 1955. In his experiments he had unsteady flow but, by choosing points carefully, he could approximate steady-state conditions. He assumed that the expansion was at constant enthalpy and, by so doing, was able to calculate values for the friction factor. He found that the friction factor was a function of pressure and pipe diameter, but independent of Reynold's number. He assumed equal velocities for each phase and thermodynamic equilibrium. The use of the "Fanno" line for describing flow conditions along the test section was discussed.

In the same year, a paper by Hoopes(45) considered pressure drop for the flow of steam-water mixtures in an heated annulus. He found no "sonic" jump at the outlet. The flow through the annulus was up to four times as much as would be theoretically calculated from the corresponding acoustic velocity. He believed that the very steep pressure gradient at the outlet may have been interpreted as choking by other investigators. He found the Martinelli-Nelson method to be reasonably satisfactory for predicting pressure drops through small annuli.

In 1958, Agostinelli and Salemann(1) studied the flashing flow of saturated water in fine annular clearances. The ranges of experimental variables were as follows: temperature, 220 to 600°F; inlet pressures, 500 to 3000 psig; diametral clearances, 0.006, 0.009, 0.012, and 0.017 in.; insert shaft lengths, 6 and 10 in.; and flow, 0 to 35 lb_m/min. For all temperatures, clearances, and lengths, critical conditions were observed experimentally. From the test results, plots of mass-flow rate versus

the ratio of exhaust pressure to inlet pressure were made to illustrate graphically the encountered critical flows. For inlet temperatures up to 400°F the critical flows were encountered at back pressures corresponding to the saturation pressure. The critical mass-flow rate at 400°F is slightly in excess of the mass-flow rate corresponding to saturated conditions. For inlet temperatures greater than 400°F, the maximum mass velocity was greater than that corresponding to the saturation pressure. Further, these investigators found that for ordinary engineering computations the critical conditions can be estimated with sufficient accuracy by use of the limits given by the acoustical velocity equation (Homogeneous Flow Model). This could have been assumed initially, since the physical size of the flow section renders separation improbable.

Chisholm[24] in the same year developed by a rather novel approach a relationship which gives good results for the flow of low-quality mixtures through orifices. It agrees with the data of Benjamin and Miller[13] to ±10 per cent.

In 1959, Ishigai and Sekoguchi[53] reported experimental data on the flashing flow of saturated water through horizontal pipes. In this paper, a new correction factor for the friction loss is introduced to satisfy the discrepancies between their experimental data and the homogeneous equilibrium theory, and is determined by experiment. The factor is the ratio of the true coefficient of friction for the flashing flow to the calculated coefficient of friction for a homogeneous flow. An empirical formula for this factor is determined from the experiments from 50 to 120 psia.

Later the same year, Faletti[33] presented one of the most extensive studies carried out on two-phase, one-component critical flow. The flow of steam-water mixtures was studied in concentric annuli having center rods of 0.188- and 0.375-in. OD. Critical throat pressures ranged from 26 to 106 psia, and qualities ranged from 0.1 to 97.5 per cent. The data were correlated by plotting the ratio of the observed mass velocity to the theoretical mass velocity (homogeneous equilibrium theory) versus the quality.

His pressure profiles for runs at critical flow were all characterized by extremely steep pressure gradients near the throat. Faletti also found that the critical throat pressure was sensitive to changes in back pressure when the back pressure was less than the critical pressure. Further, he states that the mass velocity for a system initially at critical conditions was not sensitive to large increases in back pressure. Faletti also found no significant effect of initial mixing and preheating, and states that critical mass velocities in full-bore pipes may not be a strong function of diameter, in agreement with observations made by Cruz and Moy. The work of Faletti will be discussed later on when a presentation of the author's data is given.

From the presented literature survey, one can easily see that a better understanding of the critical-flow phenomenon is needed. Data at higher pressures are needed to check any formulation of a theory. Indeed, it should be quite obvious to the reader after being introduced to the enormous problems existing that the achievement of such a goal would be a contribution of considerable magnitude to the science of high-speed two-phase flow.

CHAPTER III
EXPERIMENTAL EQUIPMENT

3.1. General

The proposed study of the two-phase critical-flow phenomena required the equipment to be sufficiently versatile. Not only is the problem quite new and in the qualitative state, but also in the range of variables explored in this work no unclassified data have been published to the best of the author's knowledge. Hence, the equipment was designed to provide for different ways of mixing the two phases, as well as to allow changes to be readily performed to permit a study of different factors involving piping alterations. A long time was devoted to achieve the best possible operating conditions.

The apparatus, as built on the third floor of the Chemical Engineering Building, University of Minnesota, Minneapolis, Minnesota, and used in this research, is shown schematically in Figure 3. Views of the equipment are shown in Figures 4, 6, 8, 9, 10, 11, 12 and 13.

Emphasis was placed on easy and rapid adjustments to any kind of conditions that might be imposed on the system. This meant that the overall equipment had to undergo several changes and improvements before it could be considered quite satisfactory. Mention will occasionally be made to the things that were learned "the hard way," as their nature bears on the present discussion.

As it now stands, the equipment provides means to prepare and feed to test sections with various geometries, a mixture of steam and cold water, steam and hot water, or hot water alone, where pressure measurements can be taken. It was designed to allow for suitable condensation of the pipe discharges and for a quick application of vacuum to the condenser.

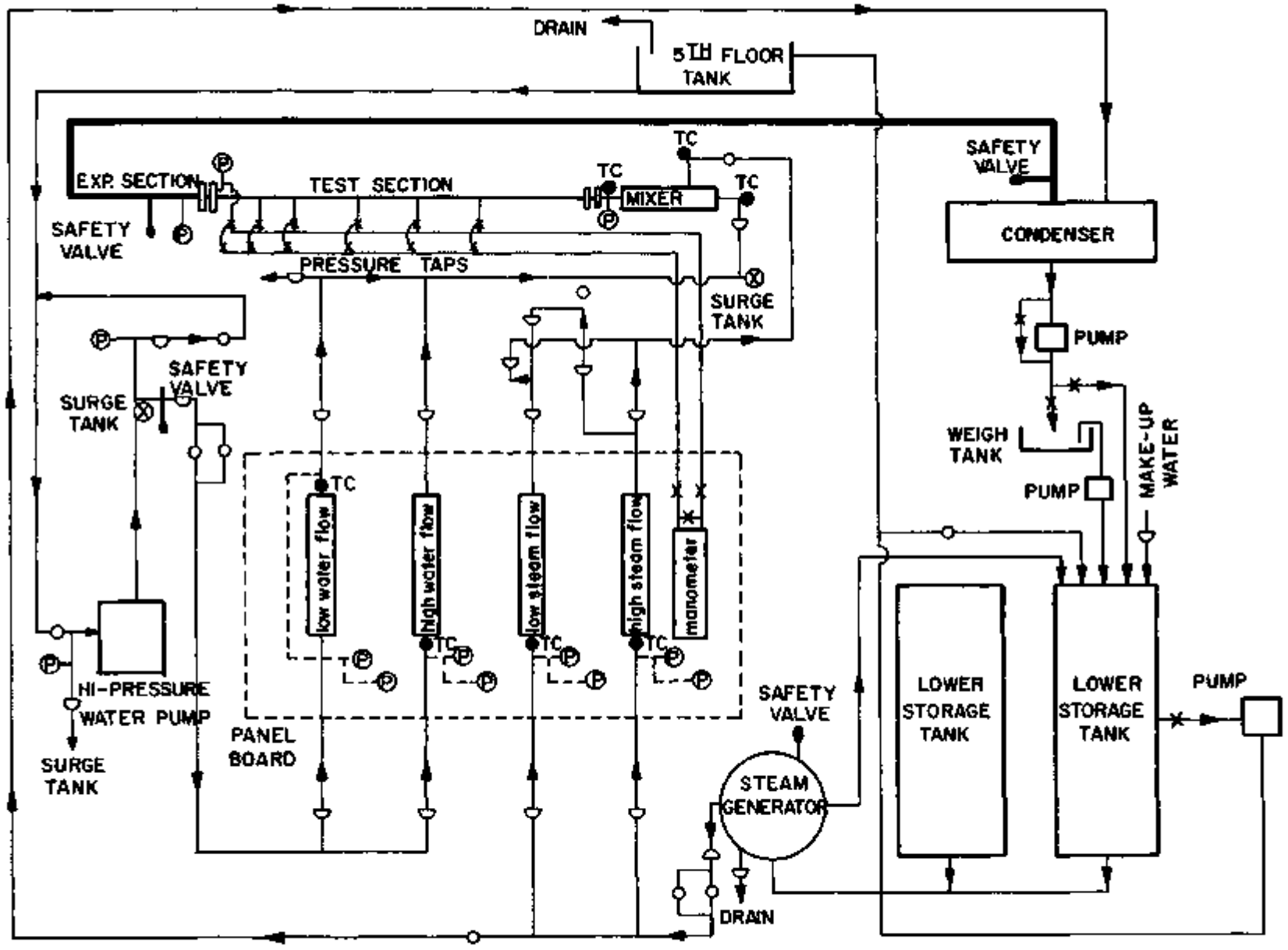

Figure 3. Diagram of the Experimental Equipment

In Figure 3, the conventional symbols are used to designate throttling valves (needle valves were not differentiated from globe or gate valves), check valves, safety valves, strainers, air vents, etc. Pressure stations are indicated by P, and temperature measurements were made at points indicated by T.

The relative complexity of the equipment prompts a consideration of each piece of apparatus. Its description will be broken up into the following main headings:

3.2 Steam supply
3.3 Water supply
3.4 Atmospheric pressure
3.5 Surge tanks
3.6 Dead weight tester
3.7 Mixer
3.8 Test sections
3.9 Condenser
3.10 Piping, valves, and insulation
3.11 Pumps
3.12 Instrumentation

3.2. Steam Supply

A steam boiler was used as the source of superheated steam. The steam generator is a Besler, Model 15, with a capacity of 1500 lb/hr at 900°F and 2000 $lb_f/in.^2$. The steam is generated in a long, continuous tube coiled in the furnace, which is oil fired. More will be said about the steam generator when the operating procedure for the equipment is described. A view of the steam generator is shown in Figure 4.

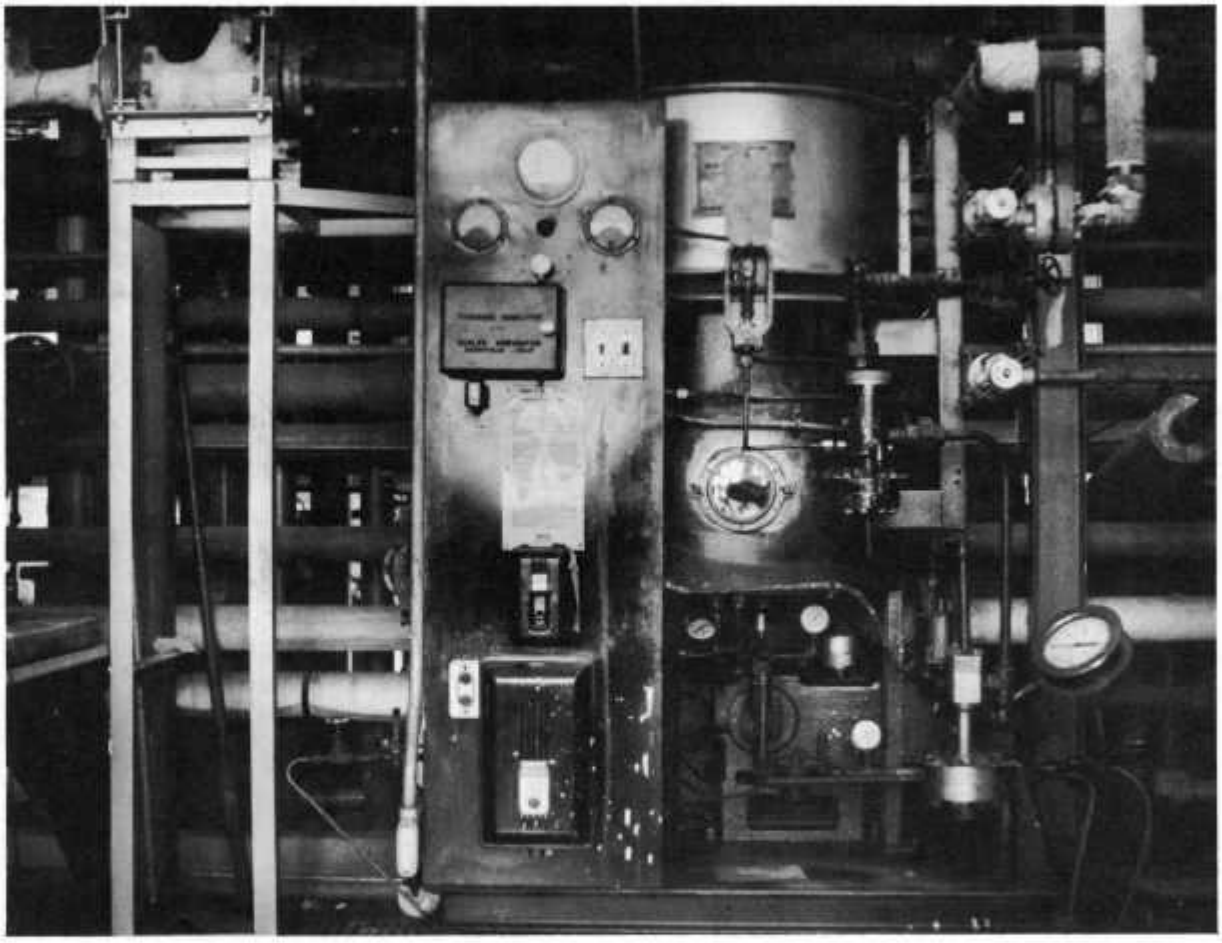

Figure 4. View of the Steam Generator

3.3. Water Supply

A Westinghouse shell-and-tube condenser was used as the source of subcooled water. Steam from the university main steam line and exhaust from the test section were condensed. A Worthington reciprocating vertical triplex water pump, used to deliver the pressurized subcooled water to the test section, had a capacity of 5000 lb/hr at 1750 $lb_f/in.^2$. A Worthington centrifugal pump and a Simer paddle pump were used for the transfer of water from the source condenser to the supply tanks.

3.4. Atmospheric Pressure

In order to establish the existence of critical flow at the end of the test pipe, it was necessary to provide means of reducing the downstream pressure. As critical pressures close to atmospheric were not contemplated, it was not necessary to carry this reduction into the vacuum region; rather, atmospheric pressure was sufficient. This was simply assured by keeping the condenser connecting to the downstream side half empty or less at all times. A Bourdon gauge connected to the downstream section, 4 in. away from the test section, indicated this was true. By this means, vacuum was easily obtained in the condenser, and the duct carrying the discharging fluid from the test pipe to the condenser was designed to reduce the pressure drop between these two points by 2-3 psia for most runs. When the flow rates were extremely high and most of the flow was in the vapor phase, this pressure loss became as high as 5 psia. Calculations indicated a 4-in. pipe was adequate for this purpose.

Since the pressure drop increased with volume of steam flowing, in which case the critical pressure is higher, the fact was of no concern, especially when the lowest critical outlet pressure explored in this work was 40 psia.

3.5. Surge Tanks

An anomalous behavior was observed when the first attempt was made to take pressure-drop data for subcooled water alone flowing through the test section. It was noticed that, for a constant flow rate of water at room temperature, the pressure drop over a section of test section varied markedly with pressure, passing through a maximum and a minimum (a negative reading). This behavior was found to be due to the pressure fluctuations of the water pump, which was of the reciprocating type.

In order to remove these variations, two surge tanks were connected to the system. One was placed at the pump outlet and the other just before the mixer. With these surge tanks in operation there was no effect of fluctuations due to the power pump except above 1300 $lb_f/in.^2$.

The surge tanks were Bendix hydraulic accumulators (made for the hydraulic lines of the brake system of a Douglas DC-6b airplane), having a volume of about one gallon and a maximum operating pressure of 1500 for one and 300 $lb_f/in.^2$ for the other. A bladder containing nitrogen inside the surge tank absorbed the pressure fluctuations.

3.6. Dead Weight Tester

An Ashcroft tester was used to check the Bourdon gauges.

3.7. Mixer

A general way of mixing the liquid and vapor phases had to be developed. The mixing method is in itself a problem, which has not received the attention it deserves in the literature.

The purpose of the mixer was to mix both entering phases so that the discharge, which immediately entered test section I (not test section IV), would be at equilibrium. The unit consisted of a 6-in. piece of heavy duty pipe, of 1.689-in. internal diameter, which was flanged at both ends. Copper

rods, 4 in. long and $\frac{5}{32}$ in. in diameter, were packed into the pipe. These rods were held in place by a $\frac{1}{16}$-in.-thick perforated stainless steel disc on the downstream side and a bronze screen on the upstream side. The superheated steam entered the top of the mixer at right angles to the subcooled water flow, which entered the mixer axially at the upstream end. The idea for mixing was taken from Mosher's work.[76] Indeed, measurements of the pressure and temperature of the resulting two-phase mixture at a point half a foot downstream from the mixer outlet indicated that physical equilibrium had been established within the limits of accuracy of the measurements. The mixer is shown schematically in Figure 5, and a view of the mixing section can be seen in Figure 6.

3.8. Test Section

The steam-water mixture obtained by injection of water into the steam flow was fed to the so-called test section, where pressures were measured and at the outlet of which the critical-flow phenomenon was to be observed.

Four test sections were built, which were designated as test sections I, II, III, and IV.

a) Test section I, TSI.

This test section was cold-drawn, extra heavy, steel, seamless, mechanical tubing with an internal diameter equal to 0.4825 in. and an outside diameter of 0.751 in. Length of the test section was 110 in.

b) Test section II, TSII.

This test section was of same material as test section I, with an internal diameter equal to 0.269 in. and an outside diameter of 0.505 in., and the length equal to 110 in.

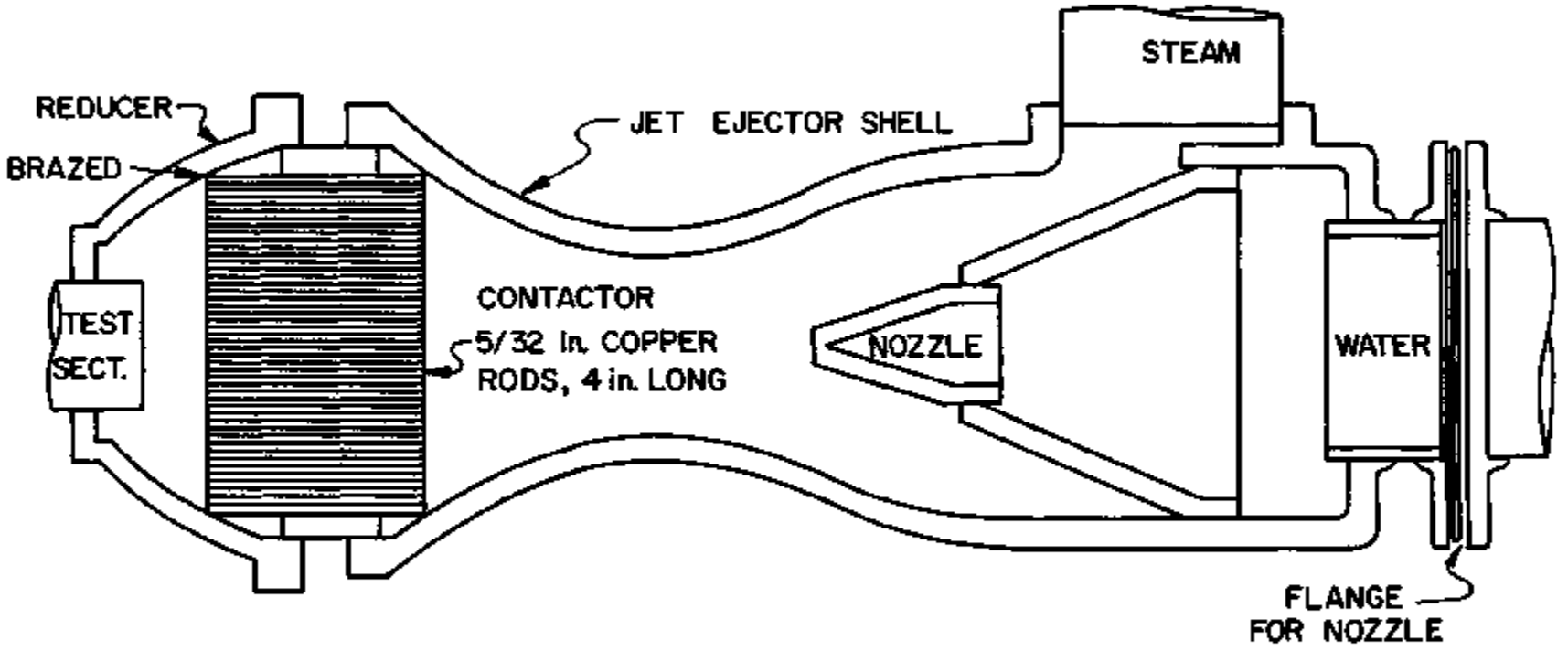

Figure 5. Schematic of the Mixing Section

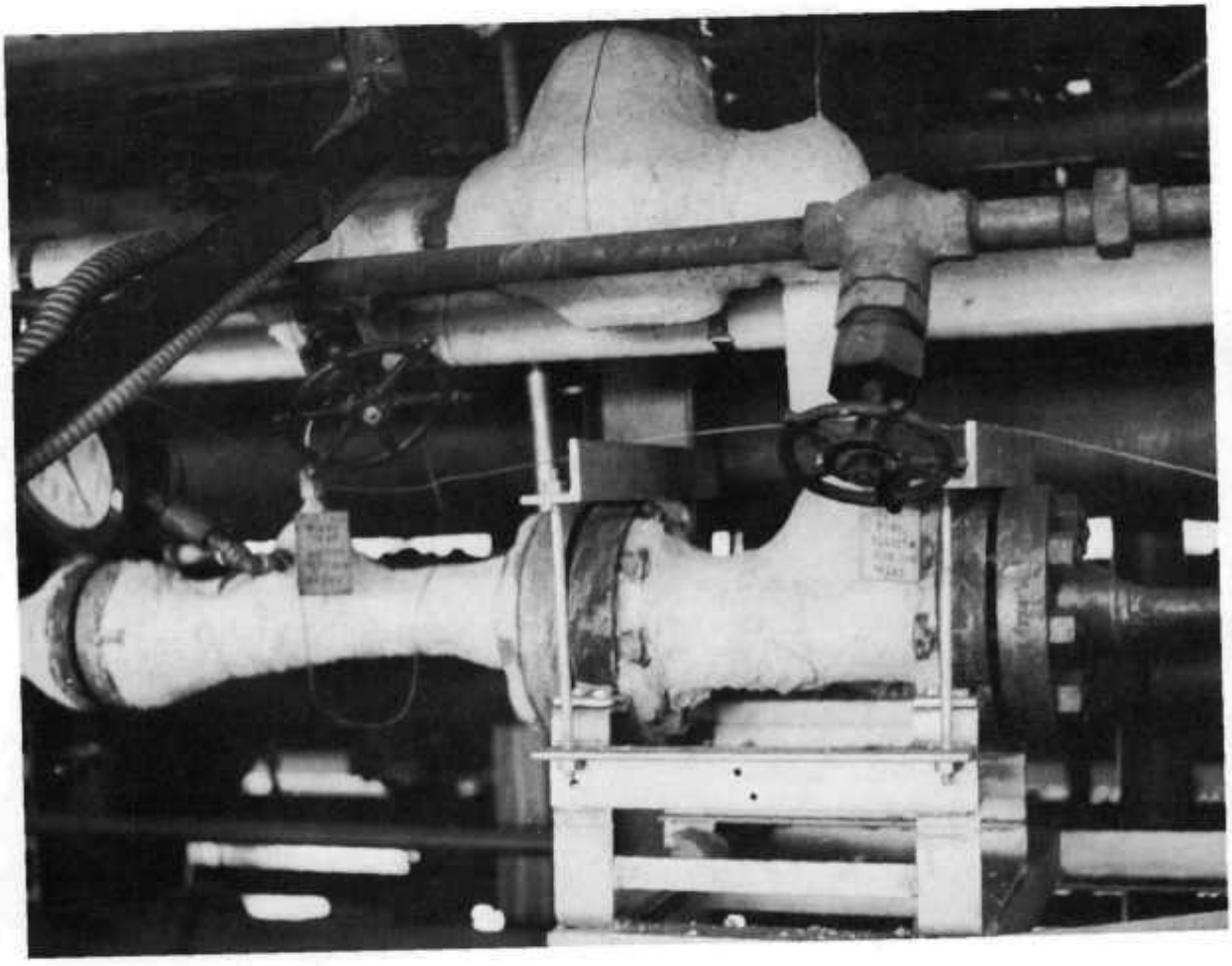

Figure 6. View of the Mixing Section

c) Test section III, TSIII.

This test section consisted of the same material as for the two previous ones, with inside diameter of 0.125 in. and outside diameter equal to 0.253 in., and with a length of 110 in.

d) Test section IV, TSIV.

This test section was identical with test section III except that the length was shorter, being $56\frac{1}{4}$ in.

The outlet end of all four test sections was carefully filed so that a plane and sharp cross section would be obtained. Micrometer measurements of the diameter at the outlet of each pipe, at eight equally spaced points, were made. The diameter at the outlet was taken as the arithmetical mean of that set of values for each pipe.

Six pressure taps were placed on each of the four test sections at the following distances from the pipe outlet: the pressure tap closest to the outlet of the test sections was always placed one diameter length from the outlet. This pressure tap was designated tap I. Pressure taps II, III, IV, V, and VI were placed the following distances from pressure tap I, same for all test sections: 6, 12, 24, 36, and 48 in.

A brief survey of the literature failed to disclose a conclusive report on the best manner of installing pressure taps. Allen and Hooper's suggestions [see Transactions of the ASME, 54, Hyd. 54-1 (1932)] were used as a guide for drilling the tap holes and completing the taps. The sizes of the pressure tap holes for the four test tubes are as follows: Test section I, $\frac{1}{8}$-in. holes; Test section II, $\frac{1}{16}$-in. holes; Test sections III and IV, 0.0465-in. holes.

The holes were drilled through plugged iron fittings previously welded to the pipe side. The size of the plugs was such that a $\frac{1}{4}$-in. length of uniform-diameter hole could be assured. In order to minimize flow

disturbances at the points of pressure measurements, the holes were carefully reamed free of burrs by means of a very soft file, but they were not rounded on the inside pipe surface. The inside of the pipe was sanded with fine emery cloth. The test section was cleaned after the pressure taps were made and at intervals, thereafter, by forcing a cloth soaked in acetone and carbon tetrachloride through the section and rinsing with water. The pressure taps were cleared by running water through them. It should be mentioned that a close-fitting metal dowel was placed inside the section while drilling the pressure tap to minimize burring of the inner surface. The internal surfaces of a test section were checked visually after drilling and filing, and appeared to be perfectly smooth. The pressure taps were then connected to the $\frac{1}{4}$-in. copper manometer lines by means of flared nuts.

The tap closest to the pipe outlet deserved special attention. Although it would be convenient to obtain a pressure measurement as close as possible to the pipe exit, the minimum distance at which the tap could be installed, without the flow being disturbed, was not known, and the rather conservative distance of one diameter length, respectively, for each of the four test sections was adopted. For test sections III and IV, this means that the center of pressure tap I is $\frac{1}{8}$-in. from the pipe exit, for test section II 0.269 in., and for test section I 0.4825 in. As a consequence of this, the last tap had to be contained inside the downstream expansion section. Although the free space between the test pipe and the inside surface of the expansion section was only about $1\frac{1}{2}$ in., this tap was very satisfactorily connected, through the upstream section flange, to the manometer lines. Thus, for all four test sections, the measurement of pressure at tap I was successfully made.

As leaks could easily develop at the connections associated with this tap, without being immediately detected, due to its position, checks were very frequently made of the working condition of this assembly, but fortunately no leaks at any time were discovered.

Figure 7 shows test sections II and IV with their pressure taps and measurements, and in Figures 8 and 9 views are shown of the test sections before and after installation.

3.9. The Condenser

A Westinghouse shell-and-tube condenser of more than the required capacity condensed the discharged fluid from the test section. It received its charge through a 4-in. pipe and the condensate, when operation was at atmospheric pressure, could be pumped out or withdrawn by gravity.

The liquid level in the condenser, which could not be allowed to rise above the point where vacuum was applied, was indicated by a gauge glass. This indicator also helped in establishing the necessary suction head for pumping against higher pressure. A view of the condenser is shown in Figure 10.

3.10. Piping, Valves, and Insulation

Piping was of high-pressure, galvanized iron pipe, except for sections of "black pipe," which were used wherever welding had to be done.

Water lines were not insulated. The steam lines, the mixer, and the test section were insulated with magnesia pipe lagging, which served to minimize the heat losses in the system.

Needle valves were used on the water and steam lines just before and after the rotameters and before the mixer.

3.11. Pumps

A Worthington reciprocating vertical triplex water pump with a capacity of 5000 lb/hr at 1750 $lb_f/in.^2$ was used to deliver the subcooled water to the test section and can be seen in Figure 11. A Worthington centrifugal pump and a Simer paddle pump were used for the transfer of water from the source condenser to the supply tanks.

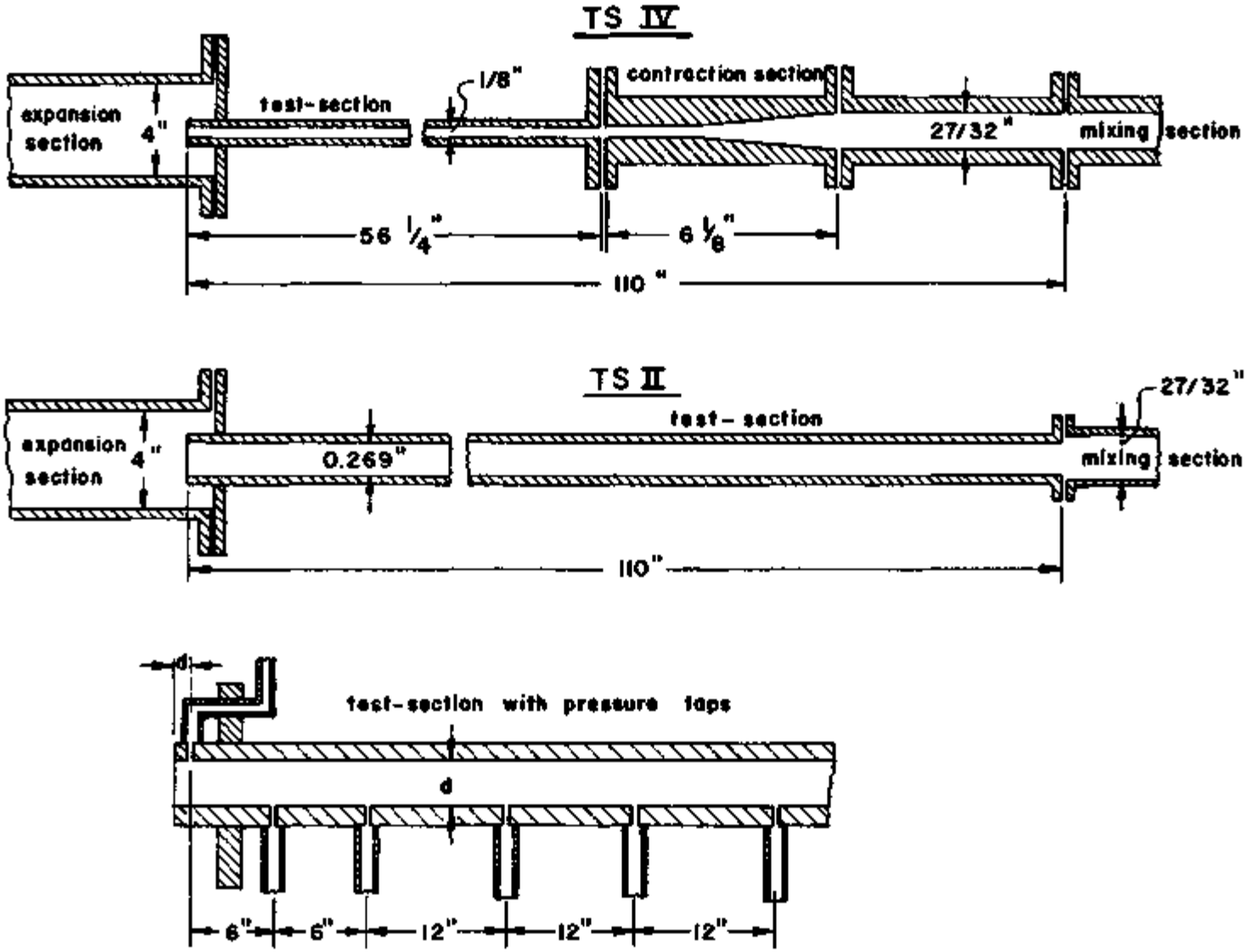

Figure 7. Diagram of the Test Sections

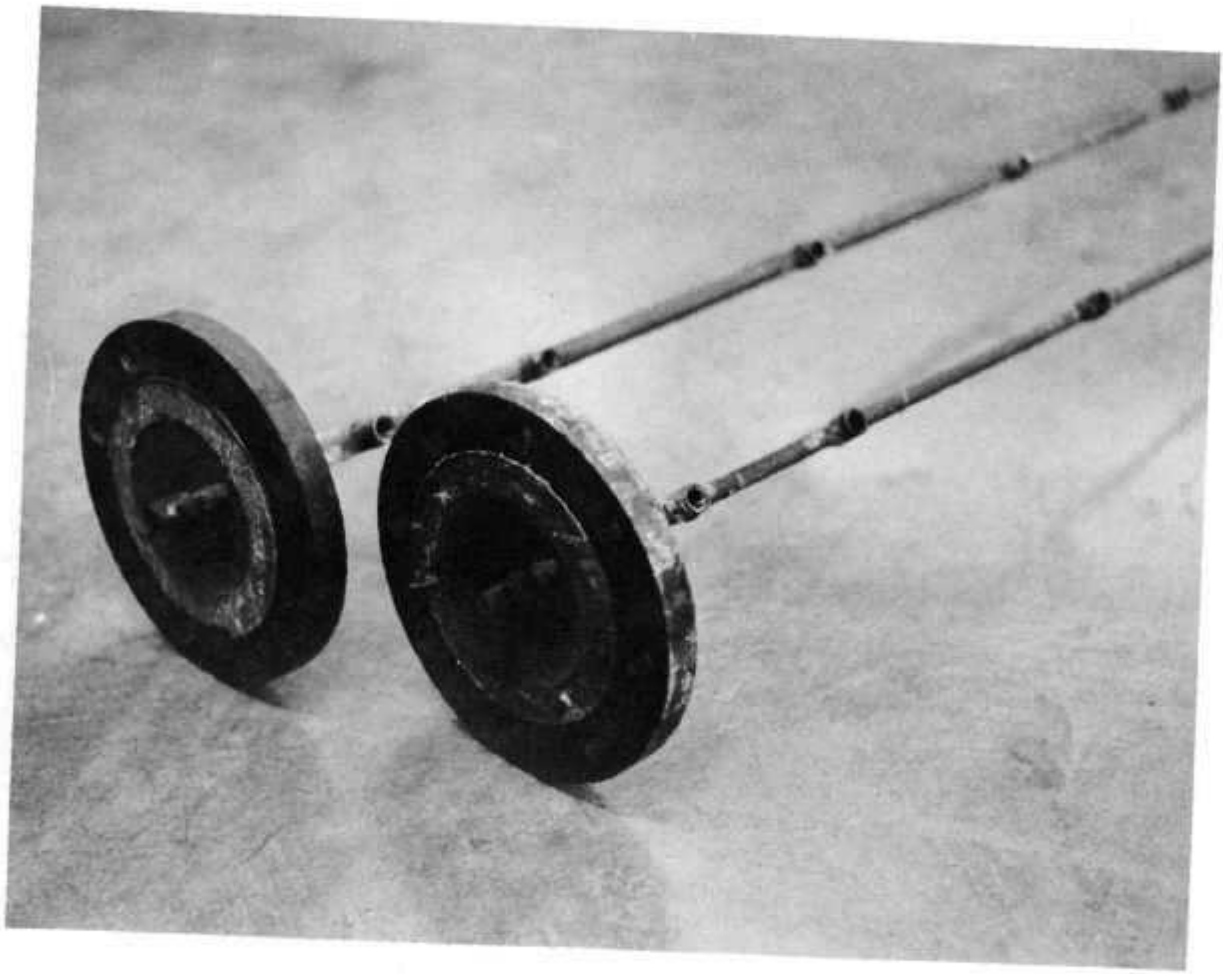

Figure 8. View of the Test Sections before Installation

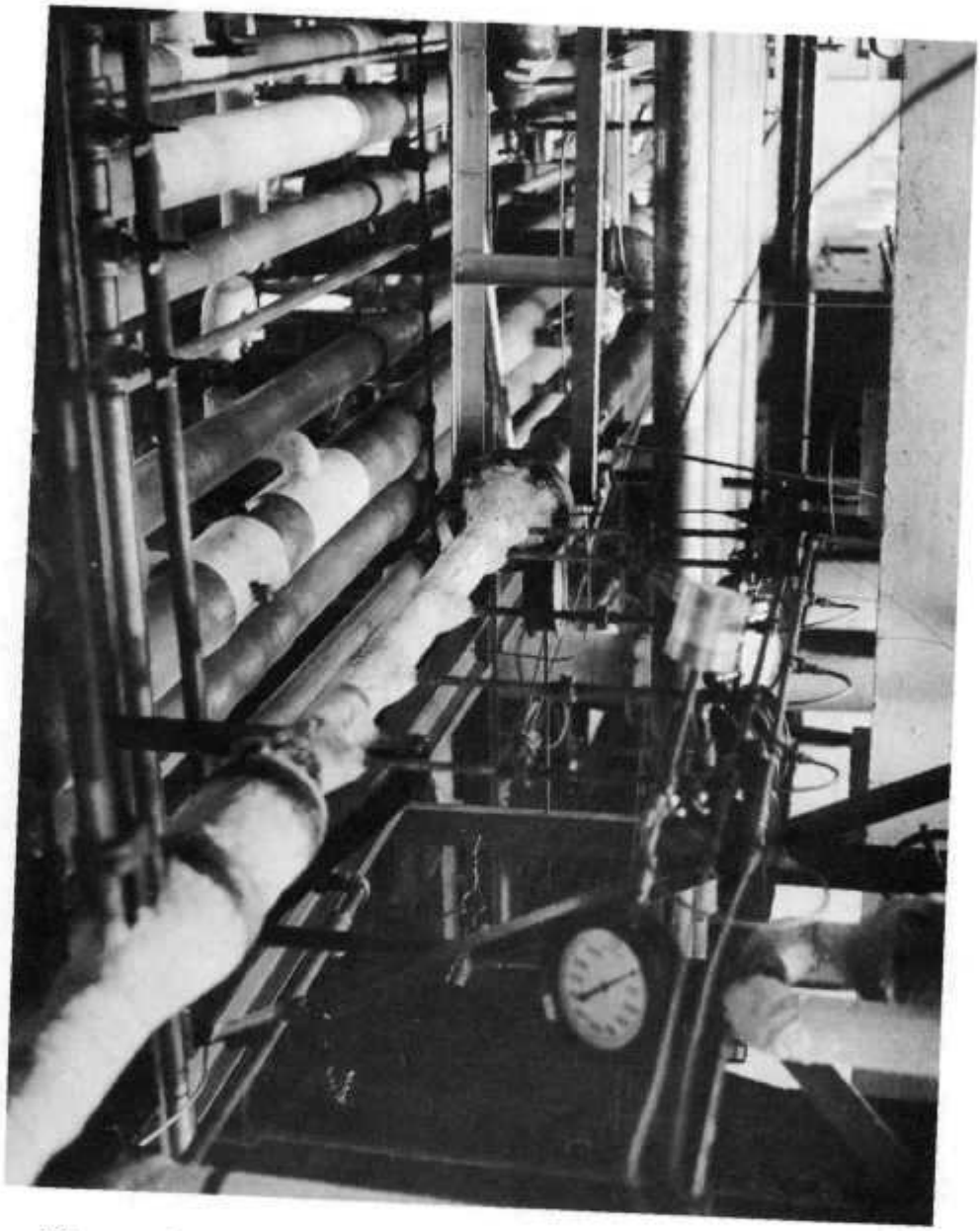

Figure 9. View of the Test Section after Installation

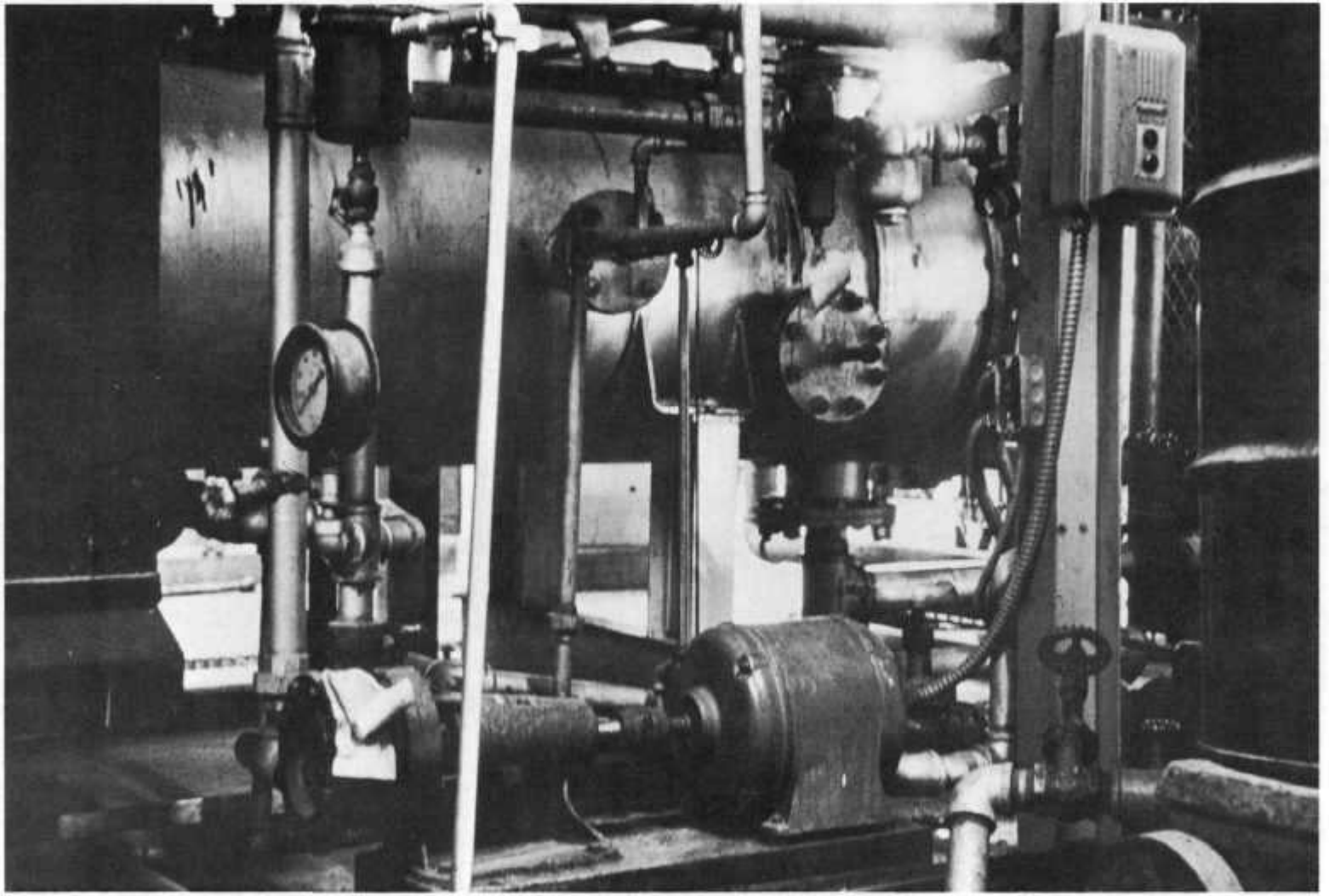

Figure 10. View of the Condenser

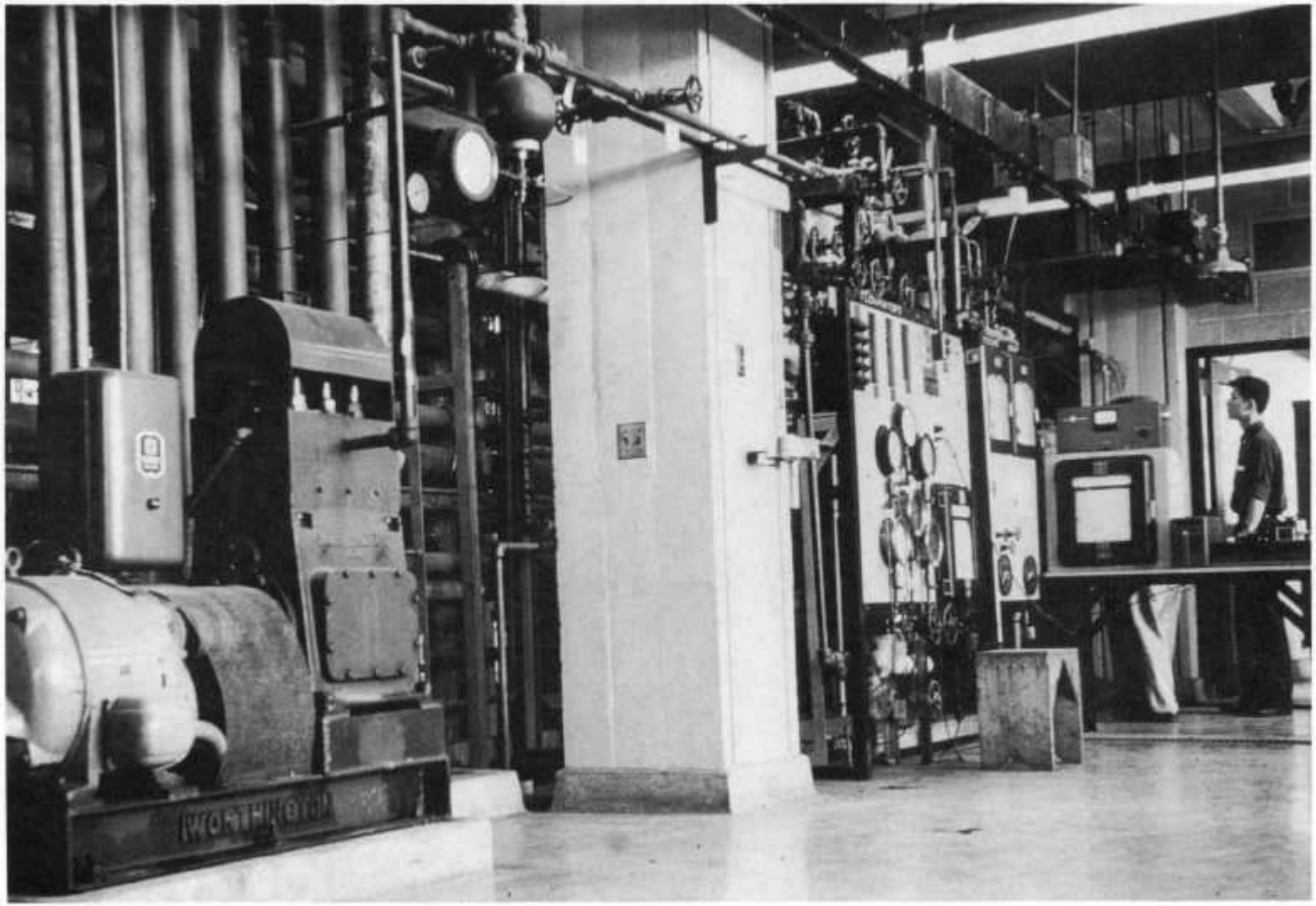

Figure 11. View of the High-pressure Water Pump

3.12. Instrumentation

Instrumentation was designed to supply the following kinds of measurements:

a. flow rates;

b. temperatures; and

c. pressure measurements.

Views of the panel board with instruments and electrical equipment are shown in Figures 12 and 13.

A. Flow Measurements

a) Superheated steam - The steam was measured by means of a rotameter equipped with an extension arm and a magnetic follower. The range of the instrument was from 100 to 1500 lb/hr measured at 600°F and 600 psig.

The steam flowrator was calibrated by weighing the condensate and correcting this rate by a correction factor which corrected for the difference in steam temperature and pressure from that at which the flow rate was designed, namely, 600°F and 600 psig. The correction equation is given by

$$W'_s = W_s \ (v_s/v'_s)^{1/2} \quad , \tag{3.12-1}$$

wherein

W'_s = the true mass rate of steam flow at 600°F and 600 psig, lb_m/hr

W_s = the mass rate of steam flow measured at experimental conditions, lb_m/hr

v_s = specific volume of steam under experimental conditions, ft^3/lb_m

v'_s = specific volume of steam at 600°F and 600 psig, ft^3/lb_m.

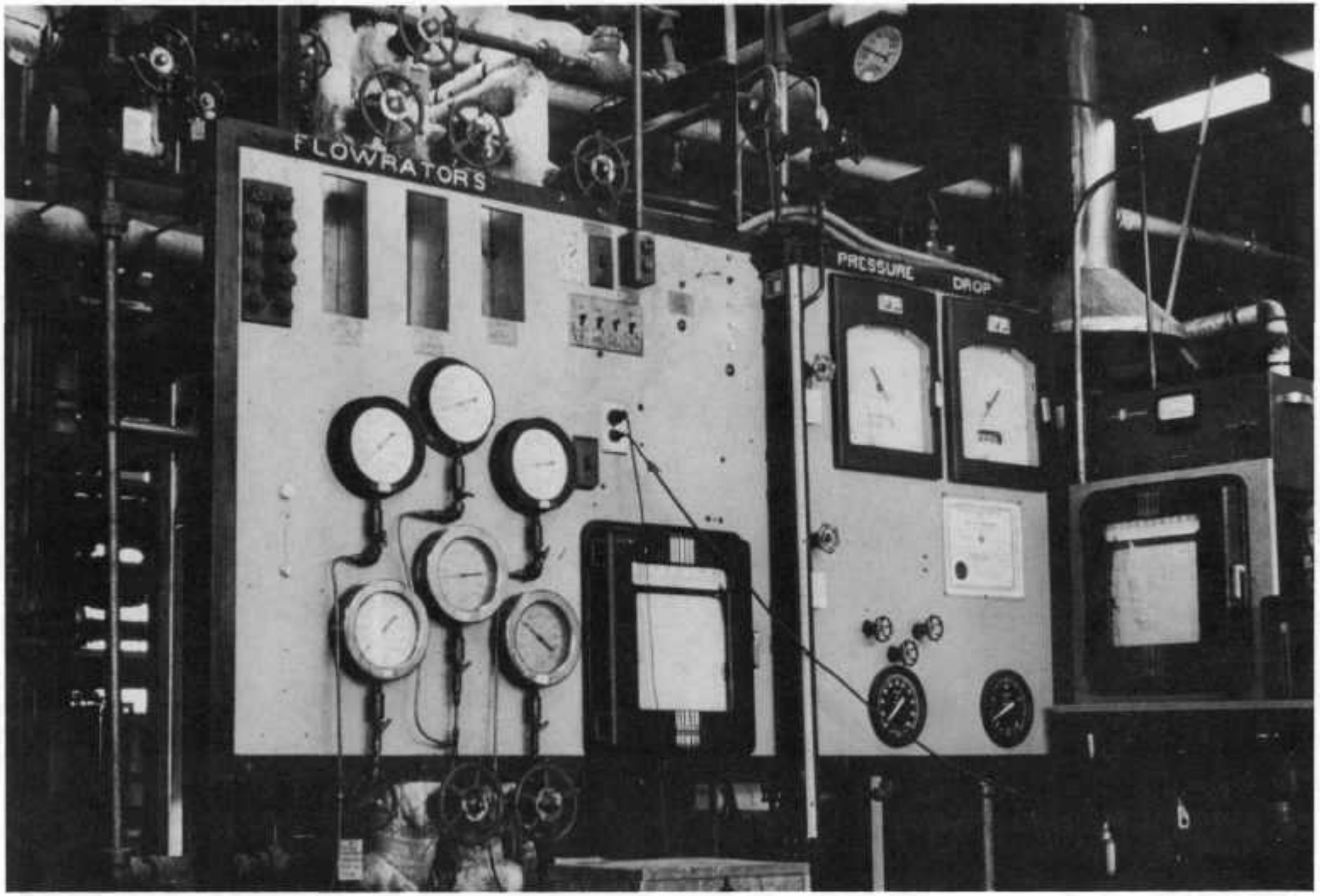

Figure 12. View of the Panel Board

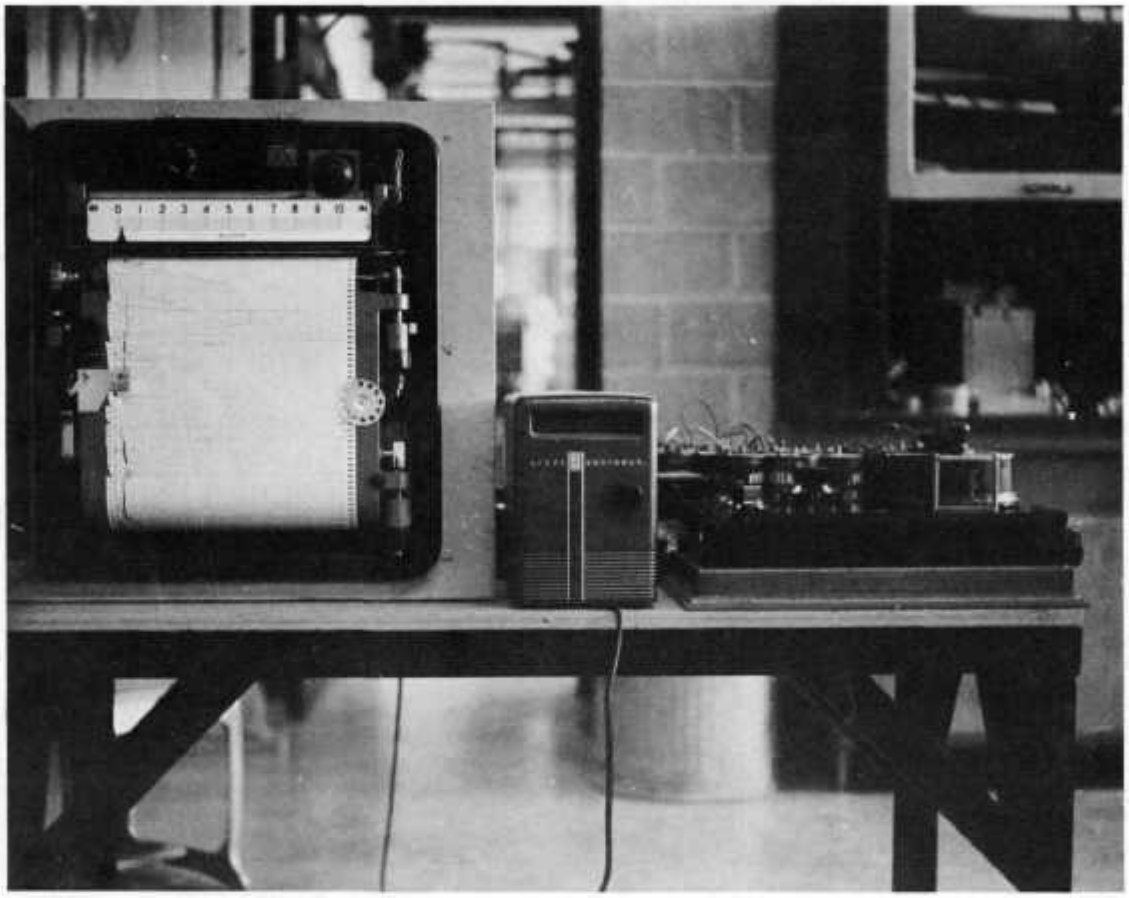

Figure 13. View of the Electrical Equipment

The maximum deviation noted for this flowrator was ± 5 lb_m/hr or a maximum of 3% for the low flow rates. This deviation is well within one-half of the least reading. The least reading being 25 lb_m/hr, the precision of the instrument was taken as ± 12.5 lb_m/hr.

b) Subcooled water - Two rotameters were used, one for the low flow rates and the other for the high flow rates.

The low-flow-rate rotameter was a direct reading Fischer and Porter meter with a 100- to 750-lb_m/hr range. The rotameter for the high flow rates was a Fischer and Porter meter equipped with an extension arm and a magnetic follower. The range of this meter was 500 to 5000 lb_m/hr.

The high-flow water flowrator was calibrated by weighing the effluent in a 55-gal drum. The resulting measured flow rates were an average of 37 lb_m/hr higher than the indicated flow rate. This figure is within the established precision of the instrument of one-half the least reading. The precision of this instrument is taken as ± 25 lb_m/hr.

The low-flow water flowrator was calibrated by the same method as above. Here an average deviation of +10% was found. The coordinates for the calibration curve were:

Flowrator Setting, lb_m/hr	Measured Flow Rate, lb_m/hr
150	137
200	192.5
300	275
400	349
600	555
700	655
750	697

B. Temperature Measurements

All temperatures were measured with iron-constantan thermocouples, silver soldered into mild steel protection tubes of OD equal to 0.125 in. and ID equal to 0.081 in. All thermocouples extended a minimum of 6 in. into the stream being measured and were centered approximately parallel to the flow. All of the thermocouples, except the one measuring the inlet temperature of the test section, were held in place by one-inch pipe plugs to which the protection tubes were soldered. Seven different temperatures of the system in the range from 50 to 700°F were read on a Leeds and Northrup "Speedomax" multipoint recording potentiometer. The "Speedomax" was designed to read off 8 thermocouples automatically.

The iron-constantan thermocouples were calibrated with protection tubes against a similar couple standardized by the Standards Laboratory of the University of Minnesota, Minneapolis, Minnesota. The couples were placed in a steel plug set in a block of insulation. The assembly was heated to a stable and uniform temperature by a surrounding nichrome coil. The calibration showed that each thermocouple was accurate to within $\pm$ 0.02 mv or $\pm$ 0.7°F.

Figure 13 shows the electrical equipment used for measuring the temperatures.

C. Pressure Measurements

The static pressures at the rotameters, right after the mixing section and at the end of the test section, were measured with Bourdon gauges. The differential pressures were measured with, in some cases, a Meriam well-type mercury manometer with a range from 0 to 600 in. of water differential pressure. When the pressure drops became too high, Bourdon gauges were used on each of the six pressure taps, which then gave the static pressures directly.

The Bourdon-tube gauges used to measure the steam and water pressures at the respective flowrators were calibrated with an Ashcroft dead weight tester. The pointer and level mechanism of each gauge was adjusted until perfect calibration was attained. The manufacturer's stated precision for these gauges is ± 10 psi.

The Meriam well-type mercury manometer was assumed to be accurate to within the limits of one-half the least reading. This would make the precision 0.5 in. of water.

The effect of static pressure on the differential pressure readings was studied while pumping water through the system. In the static pressure range from atmospheric to 800 psig, the differential pressure readings varied ± 2 in. of water for essentially the same fluid temperature, flow rate, and pipe length.

A single-phase pressure-drop traverse was taken down the test section to check similarity of the pipe and tap construction. Both superheated steam and liquid water were used.

Consistency of data was checked by repeating two runs which had been run 24 hr before or earlier. In all cases the results were within the range dictated by the precision of the measured variables. Also, usually three, and at least two, trials were taken for each constant setting of the operating variables to assure consistency. In numerous preliminary water and superheated steam runs, single-phase consistency was ascertained.

CHAPTER IV

EXPERIMENTAL PROCEDURE

4.1. Definition of Critical Flow from Experimental Viewpoint

In this work, the term critical throat pressure refers to the pressure existing at the exit plane of the test section (throat) when maximum flow is achieved. Maximum flow is obtained when the downstream or back pressure is sufficiently low such that a change in this pressure will not affect the approximate steady-state upstream axial pressure profile. It shall be pointed out here that, although the pressure profile remains the same before and after a change in back pressure, during the change it is disturbed and becomes quite unstable. Since anomalous behavior has been observed by other investigators,[23,33,77] such as the throat pressure being sensitive to back pressures smaller than the critical pressure, it is important to remember this definition in order to avoid confusion.

4.2. Initial Startup

The experimental procedure varied somewhat depending upon the purpose of the run. Consequently, only a general description of the scheme will be given.

Cooling water and steam from the University mains were allowed to flow into the condenser. The paddle pump, which transferred the condensate from the condenser to the adjacent storage drums, was started. The centrifugal pump, which transferred the liquid to the fifth-floor tank, was started. The two surge tanks were filled to two-thirds running pressure with nitrogen gas. The recording potentiometer was switched on. The rotameter light, the liquid-level indicator light, and the control circuit were switched on. The recording potentiometer was checked by switching out the thermocouples and switching in a known emf.

Ice was placed in the thermocouple cold well. Frequent renewals of the ice supply were made during the day. Time for equilibrium was always allowed before any temperature readings were taken.

4.3. Bleeding the System

The Worthington reciprocating pump and the boiler feed pump were allowed to pump water through the system with the bleed valves open. This was done with the system throttled to about 300 psi and a flow rate of about 3500 lb_m/hr of water. In this manner, the system, including the manometer lines and the differential pressure gauges, was completely purged of air.

4.4. Check of System Using All-liquid Flow

The boiler output water was valved to the drain, and the bleed valves were shut off. The water temperature and flow rate were noted along with the static pressure drop for each increment along the test section. These data allowed a friction factor to be calculated which could be compared to the friction-factor data already established. This comparison gave an indication of the condition of the system, particularly with regard to scaling of the internal pipe surface and to pockets of air within the system.

4.5. Commencing the Flow of Steam

The water flow was valved off and the boiler output was valved back into the test section. The burner control switch on the panel board was switched on, and the snap switch just below it was moved to the "B" (boiler) position. The fuel was then ignited by switching on the burner switch located on the boiler panel board. The differential pressures along the test section were noted. These pressures were controlled by the inlet valve of the test section, the bypass valve for the steam line from the boiler, and the fuel and normalizer valve settings of the boiler.

4.6. Introducing the Water Phase

After the boiler delivery had been stabilized, the Worthington reciprocating pump was switched on simultaneously with moving the snap switch to the "C" (control) position. The pump exit pressure was increased to about two-thirds of the anticipated static pressure for two-phase flow in the inlet test section by closing down on the pump recycle valve. It should be

mentioned here that the mixing process of the high-pressure water and steam streams caused many difficulties. A long time was devoted to this particular problem of the experiment before satisfactory performance of the equipment was achieved.

4.7. Stabilizing the Two-phase Flow

The control variables of steam flow rate, water flow rate, and static pressure of the inlet test section could be varied by adjusting (1) the air-fuel ratio of the boiler, (2) the inlet valve of the test section, and (3) the amount of steam and water recycle. Because of the relative difficulty in setting the inlet superheated steam flow rate, this variable was first established and then the inlet water flow rate was changed. In this manner the quality of the two-phase mixture could be varied from 0 to 100 per cent.

4.8. Making a Run

After the preliminary preparations were completed, the flow rates and temperatures were set in such a manner that the pressure at the exit of the test section (the throat pressure) and the stagnation enthalpy were at the desired value. As total flow rate, stagnation enthalpy, and throat pressure were all interrelated, this meant that some trial-and-error valve setting was necessary. In the meantime, the pressure in the downstream receiver (the back pressure) was kept at atmospheric or lower at all times. With some practice this operation did not pose any particular difficulty and required anywhere from 45 to 60 min.

The time interval preceding the taking of data for any particular run varied somewhat. It was sometimes as long as 5 to 6 hr, but never shorter than $1\frac{1}{2}$ hr for the first run in any operating day. Duration of a run was estimated at 2 hr, although the actual recording of the essential data usually took only about 0.5 hr.

It should be mentioned here that, because of the randomly varying steam pressure in the boiler and occasionally cycling inherent in the system, conditions were not as steady as desired. Pressures might vary by several psi.

The steam boiler sometimes was hard to operate at steady pressure. Consequently, whenever possible, the data were taken in a rapid manner to take advantage of short spells of steady behavior. In spite of the obvious shortcomings of this procedure, rather good results were obtained because of the short time required for the system to reach steady state. The heat balances were all quite good, and, likewise, whenever material balances were made, good results were obtained. The measurements which probably suffered the most were the upstream pressures in the test section, since these were not taken in the same manner. This was not true for the pressure tap next to the throat, which was recorded simultaneously with the flow rates and the temperatures. The throat pressure was also observed over a period of time to get a better perception of the pressure fluctuations.

When the temperatures, pressures, and flowrates appeared stable, data were recorded as shown on the data sheet (see Table I). After the

Table I

TWO-PHASE CRITICAL DISCHARGE DATA SHEET

(Corrected Values)

Run No: TSII-42
Date : March 17-1960
Time : 2 hours

Water Flowmeter: Small
Steam Flowmeter: Large

Pressure Readings

Position	psia
Steam Boiler	1350
Steam Flowmeter	350
Water Flowmeter	595
Outlet Mixing-Section	280
Pressure Tap 6	173
Pressure Tap 5	159
Pressure Tap 4	123
Pressure Tap 3	99
Pressure Tap 2	85
Pressure Tap 1	56
Back Pressure	15

Flow Rates

Phase	lbs/hr
Steam	322
Water	595.5

Temperature Readings

Position	°F
Steam Boiler	645.0
Steam Flowmeter	583.3
Water Flowmeter	98.0
Steam Inlet Mixing-Section	513.3
Water Inlet Mixing-Section	98.0
Outlet Mixing-Section	410.0

Remarks: Pressure fluctuations at Steam Boiler ± 15 psia
Pressure fluctuations at Steam Flowmeter ± 2 psia
Pressure fluctuations at Pressure Tap 6 ± 5 psia

above data were taken, all the data were then rechecked to see if any gross error in reading had been made. Quite often two complete sets of data were taken in order to get an idea of the random change in system conditions.

One must remember that the procedure was not always the same, but varied depending upon what was thought to be advantageous. However, care was taken to always follow good practice, so that errors were kept to a minimum.

4.9. Organization of the Runs

Intuition would indicate that there would be a certain minimum length and diameter of test section at which the critical flow rates and pressures might be affected because of lack of time to reach the flow patterns, slip and metastability, etc. On the other hand, increased length and diameter, by increasing the pressure drop prior to the throat, reduces the maximum critical pressure that can be obtained. Consequently, the writer followed the plan of action given below.

The first test section built, TSI, was a 0.4825-in.-ID steel pipe. Its purpose was to give some idea of the pressure gradient along the pipe. Since the highest outlet critical pressure that could be obtained with this test section was 60 psi, it was decided to go to pipe of smaller size, without taking any complete critical two-phase flow runs on test section I.

The next test section, TSII, was a 0.269-in.-ID steel pipe with a length of 110 in., the same as TSI. With this test section 90 complete two-phase critical flow runs were taken, with qualities from 10 to 70%, and critical pressures from 40 to 140 psia. All of these runs were considered to be very good. Excellent pressure profiles were obtained and are shown in Figures 25 and 26, Chapter VI.

The third test section, TSIII, with 0.125-in.-ID and a length of 110 in., was built with the goal in mind to obtain still higher outlet critical pressures. However, the $\frac{1}{8}$-in. test section connected directly to the 1-in.-ID mixing section, as had been done previously for TSI and TSII,

caused serious pressure fluctuations at the inlet of the test section. These pressure fluctuations were transmitted down toward the throat of the pipe and made it impossible to obtain any reliable pressure profiles on this test section.

After a careful balance of the factors involved, the test section was shortened to 56-$\frac{1}{4}$ in. and was built and connected to the mixing section as shown in Figure 7, Chapter III. This was test section 4, TSIV. The effect of length was checked by making some low-pressure runs with this shorter test section. With this change in the design, 56 two-phase critical flow runs were obtained with qualities from 1 to 50% and pressures from 80 to 360 psia. Again, excellent pressure profiles were obtained and are shown in Figures 27 and 28, Chapter VI.

Summing it up, 146 two-phase critical flow runs were tabulated with the following ranges of the variables:

Table II

RANGE OF EXPERIMENTAL VARIABLES

Pipe	Number of Runs	P, psia	G, $lb_m/sec\text{-}ft^2$	Quality, %
TSII	90	40-140	500-1300	10-70
TSIV	56	80-360	1400-4300	1-50

CHAPTER V

THEORY OF TWO-PHASE CRITICAL FLOW

Previous Theory of Critical Flow

5.1. General

Although the theory concerning critical discharges of single-phase flow, in particular of gases, is well known, the direct opposite is true for two-phase mixtures. This is the result of phenomena such as the relative velocity between phases, changes of phase caused by the pressure gradient, and the possibility of lack of thermodynamic equilibrium. Before discussing these phenomena, it would be well worth while to describe the critical flow of a single-phase compressible fluid.

In fact, it still remains to be determined whether such a phenomena occurs for two-phase flow with the same implications that it carries for single-phase flow.

As Hall points out,[40] it is more significant to consider a maximum discharge from the viewpoint of propagation of pressure impulses than from the viewpoint of acoustics, as one is quite independent from the other. Sound is just one example of the much wider realm of moving pressure gradients. It appears logical, then, because sonic two-phase flow may be in doubt, to approach the problem from the viewpoint of maximum flows by first investigating the critical velocities of gases, secondly, extending that concept to a homogeneous mixture, and, thirdly, to a heterogeneous mixture.

5.2. Single-phase Flow

If one imagines a flow system, such as a pipe attached to a constant-pressure source on one end and to a large receiver on the other, one knows that, when the downstream pressure is reduced below that of the upstream

end, flow begins and a pressure gradient is set up in the pipe. When steady state is reached, the force on the fluid from this pressure gradient is exactly balanced by frictional and inertial forces, and, therefore, the flow stabilizes. If the upstream pressure and thermodynamic state of the fluid are kept constant, further drop in the downstream pressure will result in an increased flow rate until a maximum flow rate is obtained. When this flow rate is reached, further reduction of the receiver pressure will no longer affect the flow rate. For a single-phase mixture, the pressures in the pipe are also invariant. A derivation of the equation giving this maximum or critical flow rate follows.

The criterion adopted for critical flow of a compressible fluid through a pipe is

$$\left(\frac{\partial G}{\partial P_e}\right)_s = 0 \qquad (5.2\text{-}1)$$

at constant upstream pressure P_1 and with f, the friction factor, equal to zero. Here, P_e is the exit pressure and the partial designation is used to indicate constant entropy.

In general, for steady-state turbulent flow, the mechanical energy balance can be written (see Ref. 31, page 312) as

$$\frac{g}{g_c}\, dz + dF + \frac{u}{g_c}\, du + v\, dP = dW_0 \quad . \qquad (5.2\text{-}2)$$

When there is no friction, mechanical work, or head to be considered, this becomes

$$\frac{u}{g_c}\, du + v\, dP = 0 \quad . \qquad (5.2\text{-}3)$$

Now, differentiating the continuity equation $Gv = u$ with respect to P, one obtains

$$\frac{du}{dP} = v\,\frac{dG}{dP} + G\,\frac{dv}{dP} \quad , \qquad (5.2\text{-}4)$$

and, since $dG/dP = 0$,

$$\frac{du}{dP} = G_{max} \frac{dv}{dP} \quad . \tag{5.2-5}$$

Substitution of this into the flow equation yields

$$v + \frac{uG_{max}}{g_c} \frac{dv}{dP} = 0 \tag{5.2-6}$$

or, since $u = Gv$,

$$v + \frac{G_{max}^2}{g_c} v \frac{dv}{dP} = 0 \quad . \tag{5.2-7}$$

Rearranging,

$$G_{max}^2 = g_c \left(- \frac{dP}{dv}\right) \quad , \tag{5.2-8}$$

where G_{max} is the maximum mass velocity, and P and v the pressure and specific volume, respectively, at the exit end of the discharging line.

If the magnitude of the pressure change (propagated through and by the fluid) is considered negligible, so that no heat transfer or fluid friction result from the temperature and pressure gradients developed, as is found with flow of gases, the direct action of impulse is then both adiabatic and isentropic.

It is interesting to note that for a single-phase medium the equation giving the critical velocity is identical with the equation for the velocity of sound in the same medium. For a single phase, it can be said, with reasonable safety, that the maximum flow and critical pressure are reached when the velocity of the stream is equal to that of a rarefaction wave in the same medium. Because of this, the downstream pressure can no longer be transmitted up into the pipe; therefore, the downstream conditions no longer affect the conditions in the pipe. For a perfect gas, then, an equation such as

$$u_{max}^2 = g_c KPv \quad , \tag{5.2-9}$$

where u, P, and v are, respectively, the velocity, pressure, and specific volume at the pipe outlet, g_c the conversion constant, and K defined by the relationship $K = c_p/c_v$, can be used to calculate critical velocities.

In the case of steam, calculations can be performed very conveniently by using the steam tables.

5.3. Two-phase, One-component Flow

A simple way to extend these concepts to the critical flow of steam-water mixtures is to assume that the mixture is perfectly homogeneous.

As defined, homogeneous two-phase flow involves an intimate mixture of steam, as the vapor phase, in equilibrium with water droplets, as the liquid phase.

The procedure in the past has been to adopt the simpler assumptions of thermodynamic equilibrium and equal phase velocities. When these limitations could not be justified (marked differences were found between theoretical and observed values), different phase velocities were ascribed to each phase or a transient state was considered. Very little attention has been devoted to the case in which equilibrium is not present nor do the two phases flow with the same velocities. When one considers the complexities involved in such a situation, it becomes obvious why this has been so.

5.4. Homogeneous Two-phase Flow ("Homogeneous Flow Model").

If, with the assumption of reversible, adiabatic flow, equal phase velocities and additive specific volumes are postulated, the mixture can be given the same theoretical treatment which applies to single-phase flow.

The specific volume for two-phase homogeneous flow is defined as follows:

$$v = v_l (1-x) + v_g x \quad , \qquad (5.4\text{-}1)$$

where v_l, v_g, and x are, respectively, the specific volumes of liquid and gas, and weight fraction of vapor in the mixture. Differentiation of the specific volume of the mixture with respect to pressure P at constant entropy yields:

$$\left(\frac{dv}{dP}\right)_{sm} = x\left(\frac{dv_g}{dP}\right)_{sm} + (v_g - v_l)\left(\frac{dx}{dP}\right)_{sm} + (1-x)\left(\frac{dv_l}{dP}\right)_{sm} \quad . \qquad (5.4\text{-}2)$$

Inserting this in the equation for maximum single-phase flow (6.2-8),

$$G_{max} = \left[\frac{-g_c}{x(dv_g/dP)_{sm} + (v_g - v_l)(dx/dP)_{sm} + (1-x)(dv_l/dP)_{sm}}\right]^{1/2} . \qquad (5.4\text{-}3)$$

If the assumptions were correct, a chart prepared for any desired range of conditions with total outlet pressure plotted versus maximum mass velocity with critical quality as parameter would be of obvious value. Such a plot was prepared for pressures from atmospheric to the critical pressure and is shown in Figure 14. Because the method of calculating is important and subject to different possible interpretations in a few points, the computing procedure is explained in Appendix C.

5.5. Complications of Two-phase Flow.

The flow of a two-phase, single-component mixture is much more complicated than the "Homogeneous Model" would indicate. It would be wise to spend some time discussing the phenomena which complicate the problem. These are: (1) change of phase, boiling or condensation, (2) slip or relative velocity between the phases, (3) flow pattern, and (4) possible occurrence of metastability. The first of these occurs because of the existence of the pressure drop which propels the fluid. In general, for an isentropic expansion, the exit quality (per cent steam by weight) tends to increase for lower values of initial quality and to decrease for the higher values. When initially saturated water undergoes an isentropic expansion, the volume increase for a given pressure change is

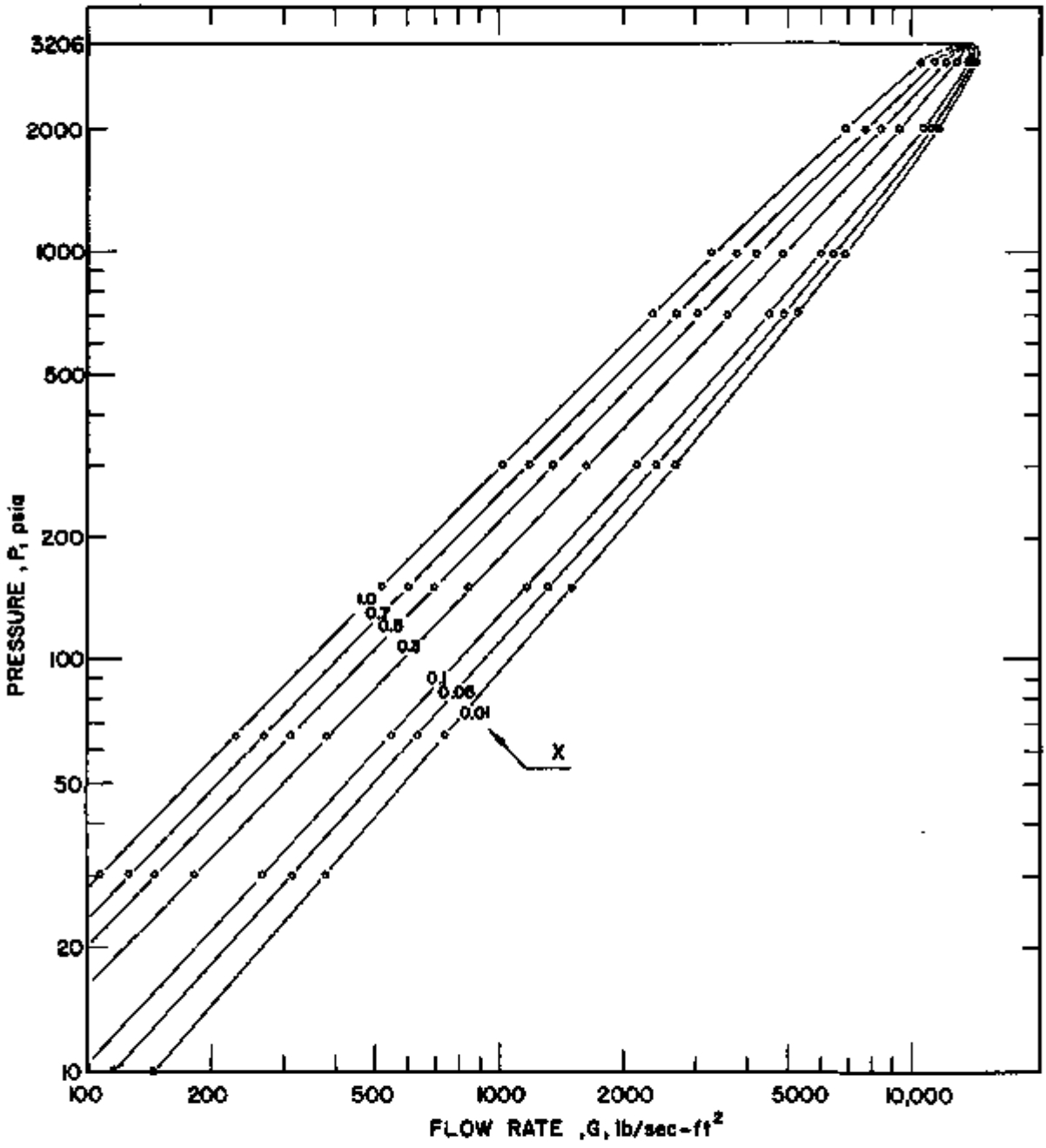

Figure 14. Prediction of Critical Flow Rate from Homogeneous Flow Model

extremely large. If no slip is assumed, this leads to rather low values of the maximum or critical velocity.

However, this has been found not to be the case. Much higher mass velocities have been observed. This statement has been verified for low pressures.[23,27,33,66,77] Some investigators[23,47,66] have explained at least qualitatively the discrepancies of observed data and theory by the existence of slip and the possible lack of thermodynamic equilibrium.

Slip occurs mainly because the vapor phase is less dense than the liquid phase and, therefore, is much more easily accelerated by the forces arising from the pressure gradient. Friction between the phases and entrainment of the liquid in the form of droplets (and froths) tend to decrease the relative velocities between the phases. Slip reduces the momentum and kinetic energy associated with a given mass velocity. Therefore, a greater flow rate may result from a given pressure drop.

The ability to predict accurately the steam volume fractions in boiling systems is a prerequisite for a competent evaluation of the performance characteristics of such systems. This is especially true in boiling water reactors where the nuclear aspects are intimately interrelated to the two-phase flow characteristics of the system. The reactor recirculation rate, coolant and moderator densities, core neutron kinetics, and reactor stability are all dependent upon the steam volume fraction or the slip ratio.

The significance of these terms is dependent upon the flow pattern. Thus, with unsteady flow patterns, such as the plug and slug type, the liquid holdup at any cross section fluctuates with time and is only a constant over a considerable tube length. Alternatively, in annular flow, the liquid holdup remains constant provided other conditions are constant and is the true fraction of cross-sectional area occupied by liquid at that point.

Turbulent cocurrent flow of a liquid and a gaseous phase through a pipe or channel is characterized by several regimes. If the volumetric rate of flow of the gas is much greater than that of the liquid, the gas will flow as a continuous phase. The liquid in this case will be either a continuous or a dispersed phase, depending upon the mass velocities, the pipe diameter, and the orientation of the flow axis. In horizontal flow at relatively low mass velocities, the liquid flows along the bottom of the pipe (stratified flow). This is certainly not the case for critical two-phase flow. If the mass velocities are increased, keeping the ratio of the volumetric flow rates constant, the interface becomes quite wavy, and eventually a portion of the liquid is entrained as droplets in the gas. If the gas mass velocity only is increased, the liquid tends to spread out into an annular film over the walls of the pipe (annular flow). This last example is more likely to be the true physical picture of two-phase critical flow and will be discussed in more detail later on.

Metastability, the lack of thermodynamic equilibrium, has been shown to exist in orifices and nozzles,[9,75,78,97,98] though its existence in pipes has not been proven. With a saturated liquid, metastability can occur because of the delay in initiation of boiling as the fluid flows into a region of pressure less than its saturation pressure. This delay can occur either because of the lack of nuclei or because of the short time of expansion or both. In the case of saturated steam, which is cooling during an isentropic expansion, the situation is quite complex. Here nuclei are needed; the more subcooling which occurs, the smaller the size of nuclei which will suffice. Both the time rate of expansion and mechanical disturbances are also important. This type of metastability can result in "condensation shock," an irreversible phenomenon in which a cloud of fine water droplets form, giving rise to a sudden, almost instantaneous, pressure rise.

A third type of metastability occurs because of the increase in vapor pressure of curved surfaces. This type is not really a true metastability and renders thermodynamic data, such as those found in the steam tables, somewhat inapplicable to flow regions where the water phase exists partially or entirely in the form of fine drops.

As mentioned earlier, the lack of thermodynamic equilibrium has been shown to exist in orifices and nozzles, though its existence in pipes has not been proven. The author strongly believes that the lack of equilibrium is not a major problem, and, indeed, the equilibrium conditions are believed to be satisfied in straight tubes. This statement is verified by Burnell,[23] who obtained critical flow data with pipes of small bore, which Moy[77] compared with his own critical flow data and were found in good agreement. Moy's data are compared with the author's data in Chapter VI. Not only did Burnell recognize the probability of each of the phases flowing at different velocities but, by actual pressure-temperature checks, he was able to determine that equilibrium was attained. However, where one has a sudden change in the pressure gradient, as in orifices or nozzles,the failure to attain equilibrium is understandable.

Thermodynamic instability, metastability, or nonthermodynamic equilibrium between phases has been suggested as a second cause for the actual critical flow rate exceeding that predicted by the homogeneous flow model. Stuart and Yarnell[98] first observed this phenomenon during steam-water experiments with orifices. Their explanation was that surface tension increased the effective pressure and thus retarded bubble formation. Due to its character, the effects of metastability are exceedingly difficult to include in an empirical or analytical expression. For this reason, it is generally omitted and thermodynamic equilibrium is assumed. Fortunately, it is generally accepted that metastable conditions exist only in orifices or short lengths of pipes and that in critical flow studies in relatively long sections of pipe its effects can be safely ignored.

Later on in this work it will be shown that the assumption of thermodynamic equilibrium in a straight pipe flow appears to be valid and that the differences between experimental data and the only theoretical model developed before this work, the "Homogeneous Model," is mainly due to slip between the phases. Other semi-empirical models have been developed,[47,66] but have been dependent upon slip data. Since slip data have not been determined for high velocity ranges, as is the case for critical two-phase flow, the authors of these semi-empirical models have used slip correlations for low velocity ranges.[7,67,71] These models have not achieved significant recognition.

As one can see, any attempt to attack this problem completely analytically will be dependent upon the derivation of a theoretical expression for the slip ratio or void fraction under critical flow conditions.

In the second part of this theoretical discussion of two-phase critical flow, the author's proposed model and theory for predicting critical flow conditions will be presented.

The Author's Theory of Two-phase Critical Flow

5.6. General

The simultaneous flow of two phases in a pipe renders possible the occurrence of a variety of flow mechanisms, and it is necessary to consider these qualitatively before developing the appropriate theory. As mentioned in Chapter II of this work, this feature of two-phase flow has received considerable attention by American investigators, notably by Martinelli and others[70] and by Bergelin and Gazley.[16] In Great Britain, Lewis and Robertson[65] have described the forms of flow occurring in a heated vertical tube passing evaporating water. Russian contributions have been made by Shugaev and Sorokin,[90] Kosterin,[60] and Krasiakova.[61] A number of attempts have been made to predict

flow patterns by plotting one function of the properties of a system against another and assigning flow pattern types to various areas. Both Alves[4] and Krasiakova[61] (see Chapter II of this work) have presented such plots where the functions were simply superficial gas velocity versus superficial liquid velocity. The forms of their regional plots are similar. Baker[11] obtained a similar type of regional graph but employed empirical dimensional functions of the properties of the systems as coordinates.

When the vapor-phase flow rate is continually being increased in a tube from inlet to outlet due to heat transfer or flashing of a saturated liquid, then the flow patterns will be similar to those stated by the above investigators with the difference that there may be a continuous transition from one flow pattern to another consistent with increasing vapor and decreasing liquid flow rates. Thus, several flow patterns may be observed in one length of pipe under particular conditions. Observations of fluids boiling in vertical tubes indicate that the flow patterns may not be so clearly defined, which is obviously due to the agitation induced by continuous formation of vapor bubbles whenever heat is transferred to a predominantly liquid phase. Flow patterns reported have been mainly those for boiling liquids in vertical tubes. Authors who have made such studies include Barbet,[12] Kirschbaun, Kranz, and Starck,[57] Badger et al.,[8,22,26] and Dengler.[28] Looking at Figure 1 and 2, presented in Chapter II of this work, and having in mind the failure of the "Homogeneous Flow Model," it seems obvious to explore an annular flow pattern in setting up a mathematical model for explaining the two-phase critical-flow phenomenon. It appears evident from the literature that, when the superficial phase velocities are high enough, an annular flow pattern is established for the flowing two-phase system. Since the superficial velocities under critical flow conditions are higher than the limits for initiation of separated flow, it becomes a logical choice of the flow pattern for the mathematical treatment of two-phase critical flow.

To assume a homogeneous flow pattern where the velocities of vapor and liquid are identical, as presented in part I of this theoretical discussion, will be shown, in Chapter VI, not to be valid, as has been the case in previous work on the subject matter. Other flow patterns, including the dispersion of some of the liquid in the vapor phase, could be considered but would complicate a mathematical analysis of this problem beyond resolution.

5.7. Development of the Equation of Motion Describing the Two-phase, One-component System in a Pipe

When saturated water flows through a tube, evaporation may occur and produce a two-phase mixture of vapor and liquid to flow through the tube. Inasmuch as the vapor is much more voluminous (at pressures less than the critical value) than the liquid from which it was formed, a marked acceleration of the mixture will occur during evaporation. The force for acceleration and overcoming frictional resistances produces the pressure gradient. The pressure is assumed to be uniform at a cross section of the tube. The result is that very different velocities exist in the tube, with the vapor portions always having a higher velocity than the liquid portions. This type of flow is called slip flow in that slippage occurs between the vapor and liquid phases. Although a general description of slip flow is clear-cut, a specific description of how the liquid and vapor become arranged in a tube, and an exact mathematical expression for pressure drop, phase velocities, and critical flow conditions have not yet been developed. In the following pages the author presents how this has been done in an effective way, based on the following physical model.

The flow model assumed is annular flow, i.e., one component flows in the core (gas phase) of the conduit surrounded by the second phase (liquid) which flows along the inner perimeter of the conduit. Physical pictures of annular flow are shown in Figures 15 and 16.

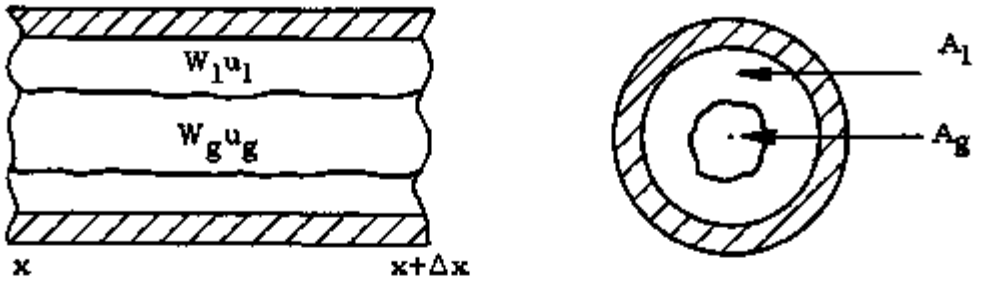

Figure 15. Physical Pictures of Annular Flow

The velocity profiles for the two-phase annular flow model might look like those seen in Figure 16.

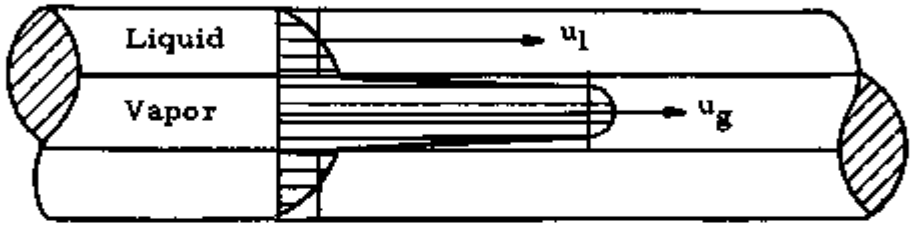

Figure 16. Velocity Profiles for Two-phase Annular Flow

The analysis is restricted to the one-dimensional, steady flow of real fluids. The assumptions of one-dimensional flow is strictly applicable to cases where the velocity of the fluid is uniform over the entire cross section of flow. The analysis is therefore valid only for an ideal case, but in practice an average velocity may be used for a variety of velocity profiles and the problem considered ideal. Hence, average velocities are used for the vapor and liquid phase in the continuity, momentum, and energy equations.

When a momentum balance is formed for the vapor phase, and forces acting in the direction of flow are made positive, it may be shown that

$$\underset{(a)}{-(P+\Delta P)(A_g+\Delta A_g)} + PA_g + \underset{(b)}{\left(P+\frac{\Delta P}{2}\right)\Delta A_g} - \Delta F_{fg}$$

$$\underset{(c)}{-\frac{(u_g+\Delta u_g)(W_g+\Delta W_g)}{g_c}} + \underset{(d)}{\frac{u_g W_g}{g_c}} + \underset{(e)}{\frac{u_l \Delta W_g}{g_c}} = 0 \quad , \qquad (5.7\text{-}1)$$

or, in the limit as $\Delta x \to 0$,

$$-d(PA_g) + PdA_g - dF_{fg} - \frac{d(u_g W_g)}{g_c} + \frac{u_l dW_g}{g_c} = 0 \quad , \tag{5.7-2}$$

where the terms in Eq. (5.7-1) denoted by letters under them represent:

(a) total static force applied to vapor over the length Δx;

(b) friction force applied to vapor over the length Δx;

(c) momentum of vapor leaving the section Δx;

(d) momentum of vapor entering the section Δx;

(e) entering momentum of fluid entering section Δx as liquid and leaving as vapor, i.e., momentum change of liquid evaporated in section Δx (note that $-\Delta W_l = \Delta W_g$).

In this equation,

A_g = cross-sectional area of the vapor phase, ft^2

P = static pressure, lb_f/ft^2

F_{fg} = friction force in the vapor phase, lb_f

W_g = weight of vapor flowing, lb_m/sec

u_g = linear vapor velocity, ft/sec

u_l = linear liquid velocity, ft/sec

g_c = conversion factor, $lb_m\text{-}ft/lb_f\text{-}sec^2$.

When account is taken of a loss of momentum from the liquid phase by mass transfer to the vapor phase, the momentum balance of liquid phase yields

$$\underset{(a)}{-(P+\Delta P)(A_l+\Delta A_l)} + PA_l + \underset{(b)}{\left(P+\frac{\Delta P}{2}\right)\Delta A_l - \Delta F_{fl}}$$

$$\underset{(c)}{-\frac{(u_l+\Delta u_l)(W_l+\Delta W_l)}{g_c}} + \underset{(d)}{\frac{u_l W_l}{g_c}} + \underset{(e)}{\frac{u_l \Delta W_l}{g_c}} = 0 \quad , \tag{5.7-3}$$

or, in the limit as $\Delta x \to 0$,

$$-d(PA_l) + PdA_l - dF_{fl} - \frac{d(u_l W_l)}{g_c} + \frac{u_l dW_l}{g_c} = 0 \quad , \tag{5.7-4}$$

The nomenclature is the same as in the vapor-phase momentum balance except that the subscript l refers to the liquid phase. The momentum balance for the entire fluid is obtained by adding the separate momentum balance Eqs. (5.7-2) and (5.7-4):

$$-[dF_{fg} + dF_{fl}] - [d(PA_g) + d(PA_l)] - [d(u_g W_g) + d(u_l W_l)] = 0 \quad . \quad (5.7\text{-}5)$$

But, since

$$dA_l = -dA_g \quad , \quad \text{and} \quad dW_l = -dW_g \quad , \quad (5.7\text{-}6)$$

Eq. (5.7-5) reduces to

$$-A\,dP - (dF_{fg} + dF_{fl}) - \frac{1}{g_c} d(u_g W_g + u_l W_l) = 0 \quad , \quad (5.7\text{-}7)$$

(f) (g) (h)

wherein

(f) total static force applied to fluid over the length dx;

(g) total friction force applied to fluid over the length dx;

(h) total momentum change of fluid over the length dx, and

$A = A_g + A_l$ = total cross-sectional area of tube.

The term (g) will be rewritten as $dF_{fg} + dF_{fl} = dF_2$. Then Eq. (5.7-7) can be rewritten in the form

$$-A\frac{dP}{dx} - \frac{1}{g_c}\frac{d}{dx}(W_l u_l + W_g u_g) - \frac{dF_2}{dx} = 0 \quad . \quad (5.7\text{-}8)$$

The equations of continuity for a two-phase flow system, as in Figures 15 and 16, when a normal section of the flow at any stage in the evaporating expansion of a fluid through a horizontal pipe is considered, can be written as follows:

$$u_g = Gx/\alpha_g \rho_g \quad (5.7\text{-}9)$$

$$u_l = G(1-x)/(1-\alpha_g)\rho_l \quad (5.7\text{-}10)$$

$$W_g = xGA \quad (5.7\text{-}11)$$

$$W_l = (1-x)GA \quad (5.7\text{-}12)$$

Substituting the continuity equations into the equation of motion, (5.7-8), one gets

$$\frac{1}{g_c}\frac{d}{dx}(\alpha_l\rho_l\bar{u}_l^2 + \alpha_g\rho_g\bar{u}_g^2) + \frac{dP}{dx} + \frac{dF_z}{dx} = 0 \quad . \tag{5.7-13}$$

In order to make a more detailed accounting for the rate of momentum gain by viscous transfer, assume that the total friction can be expressed in the following manner:

$$dF = \frac{fG^2Av}{2g_cD}\,dL \quad , \tag{5.7-14}$$

wherein

f represents the two-phase friction coefficient, dimensionless
v is a specific volume assigned to the two-phase mixture, ft^3/lb_m
G is the flow rate, $lb_m/sec\text{-}ft^2$
D is internal diameter of the conduit, ft.

The next problem is to determine the specific volume v of the two-phase mixture. What function is v with respect to the system variables such as quality, void fraction, and pressure? For homogeneous two-phase flow, the specific volume has been defined in the following way:

$$v = v_l(1-x) + v_g x \quad , \tag{5.7-15}$$

which obviously cannot be used here, since this includes no slippage. A list of applications of the homogeneous flow model, which implies Eq. (5.7-15), is given below:

(a) analysis of natural circulation loops
Haywood,[43] Lewis and Robertson,[65] Markson et al.,[69] Silver,[91] Schwarz.[87]

(b) flow of flashing water
Benjamin and Miller,[13,14] Allen,[3] Bottomley,[20] Bridge,[21] Burnell,[23] Ishigai and Sekoguchi.[53]

(c) flow of flashing refrigerants
Marcy,[68] Bolstad and Jordan.[19]

(d) vaporization of mixture in horizontal tubes
McAdams, Woods, and Heroman.[74]

(e) flow of gas-oil mixtures
Dittus and Hildebrand.[29]

(f) flow of gas-oil mixtures
Uren et al.,[101] Versluys.[102]

(g) air-water (emulsion) flow
Shugaev and Sorokin.[90]

(h) forced circulation boiling
Isbin et al.,[48] Jens and Leppert,[56] Koel,[59] Stein et al.[95]

(i) burnout studies in two-phase flow
Isbin et al.,[51] Fauske.[34]

Earlier investigators have defined the specific volume for slip flow (annular flow) as follows:

$$v = \frac{1}{\rho_l(1-\alpha_g) + \rho_g\alpha_g} \quad , \tag{5.7-16}$$

where

$\alpha_g = A_g/A$, void fraction
ρ, density, lb_m/ft^3.

To utilize this definition of the two-phase specific volume would not be in agreement with Eq. (5.7-14). The form of Eq. (5.7-14) may be considered to be a restriction imposed upon the evaluation of the specific volume of the mixture. This assumption implies that the specific volume v which, through proper mathematical interpretation, can describe the rate of momentum by convection, must be identical with v in Eq. (5.7-14).

The following mathematical procedure and a physical comparison of two-phase and single-phase flow suggest a suitable definition for the specific volume v. As will be seen later, the definition appears to be justified.

Substituting Eqs. (5.7-14), (5.7-9), (5.7-10), (5.7-11), and (5.7-12) into Eq. (5.7-8), one gets

$$\frac{G^2}{g_c}\left\{d\left[\frac{x^2 v_g}{\alpha_g}+\frac{(1-x)^2 v_l}{1-\alpha_g}\right]+\frac{f v dl}{2D}\right\}+dP=0 \quad . \tag{5.7-17}$$

The equation of motion for one phase only flowing through a conduit is

$$\frac{G^2}{g_c}\left[dv'+\frac{f'v'dl}{2D}\right]+dP'=0 \quad , \tag{5.7-18}$$

wherein the symbols designate the same as used under two-phase flow, the superscript indicating one-phase system.

Since Eq. (5.7-17) represents the motion of the total fluid (both phases), it seems reasonable to compare this equation with Eq. (5.7-18), which describes the motion of total fluid also (one phase). One should particularly note that the specific volume v' occurs both in the acceleration and friction terms. Therefore, by equating similar terms in Eqs. (5.7-17) and (5.7-18) one can draw the following conclusion: the definition of the specific volume v for two-phase flow utilizing Eq. (5.7-14) is

$$v=\frac{x^2 v_g}{\alpha_g}+\frac{(1-x)^2 v_l}{1-\alpha_g} \quad . \tag{5.7-19}$$

This is a very significant result for:

1) In this fashion v is not only a function of void fraction and pressure, as defined by earlier investigators, but also of quality x.
2) With v defined in this fashion it is possible to solve the system and obtain analytical solutions for void fractions, and hence for critical flow, as will be seen later.
3) As defined here, calculated values of v will lie between calculated values as defined by Eqs. (5.7-15) and (5.7-16), which, indeed, are two extreme definitions of the specific volume of the two-phase mixture. Table III shows this.

Table III

TABLE OF THE SPECIFIC VOLUMES AS DEFINED BY EQS. (5.7-15) (5.7-16), AND BY THE AUTHOR, EQ. (5.7-19), USING VOID FRACTION AS DERIVED IN THIS WORK

	x, %	From Eq. (5.7-15) $V_{Homogeneous}$, ft^3/lb	From Eq. (5.7-16) $V_{annular}$, ft^3/lb	From Eq. (5.7-19) V_{Fauske}, ft^3/lb
P=40 psia	10	1.0652	0.0640	0.1953
	20	2.1133	0.1220	0.5667
	40	4.2095	0.2025	1.8895
	80	8.4018	1.4762	6.8552
P=100 psia	10	0.4592	0.0486	0.1092
	20	0.9006	0.0865	0.2784
	40	1.7834	0.1963	0.8501
	80	3.5491	0.9079	2.9269
P=500 psia	10	0.1105	0.03416	0.04957
	20	0.2013	0.05160	0.09298
	40	0.3829	0.10006	0.22042
	80	0.7462	0.3540	0.6378
P=1000 psia	10	0.0640	0.03170	0.03961
	20	0.1064	0.04370	0.06304
	40	0.1912	0.07790	0.12617
	80	0.3608	0.21990	0.3174

In Figure 17, the specific volume of the two-phase mixture as defined by Eq. (5.7-19) is plotted versus quality x, with pressure P as a parameter for a pressure range from atmospheric to the critical point, namely, 3206 psia. If Eq. (5.7-19) is substituted into Eq. (5.7-17), the general differential equation describing the fluid motion of the two-phase system becomes

$$\frac{G^2}{g_c}\left\{d\left[\frac{x^2 v_g}{\alpha_g}+\frac{(1-x)^2 v_l}{1-\alpha_g}\right]+\left[\frac{x^2 v_g}{\alpha_g}+\frac{(1-x)^2 v_l}{1-\alpha_g}\right]\frac{f}{2D}\,dL\right\}+dP=0 \quad . \tag{5.7-20}$$

This momentum equation must be solved in such a way that the solution may not only give the relations among the pressure drop, the mass flow rate, and other factors, but also be applicable without discrepancy to the critical flow.

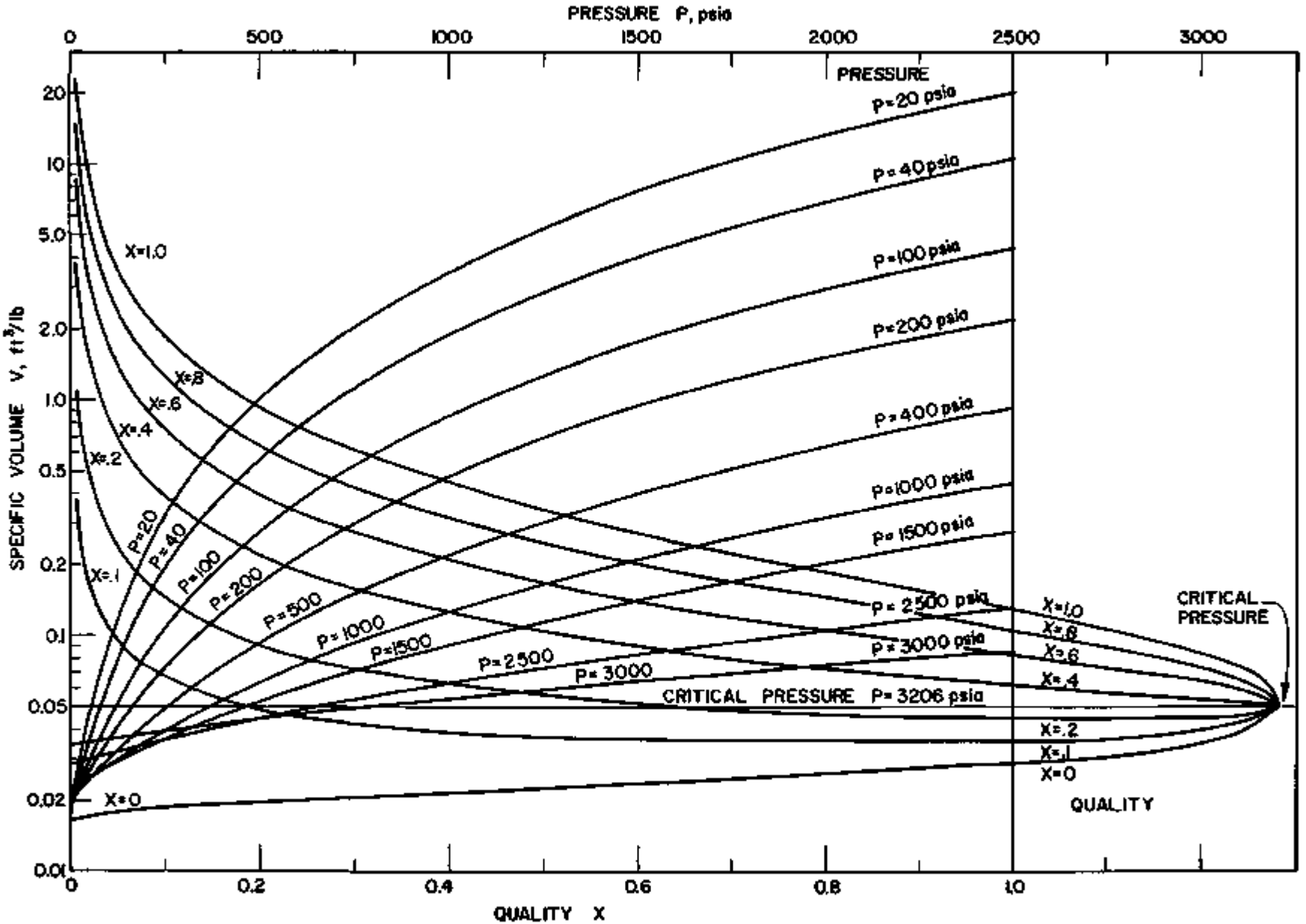

Figure 17. Theoretical Prediction of the Specific Volume for Critical Flow

5.8. Definitions Used for Critical Two-phase Flow.

1. The flow is called the critical flow when flow rate no longer increases with increasing pressure difference, i.e., when

$$\frac{dG}{dP} = 0 \quad . \tag{5.8-1}$$

This definition of critical flow is the basic one and has been used by most investigators in this field.

2. At conditions of critical flow, the pressure gradient along the pipe proceeding to the exit has an absolute, finite maximum possible value for a given flow rate and quality. In mathematical form,

$$\left|\frac{dP}{dL}\right|_{G,x} \approx \left|\frac{\Delta P}{\Delta L}\right|_{G,x} = \left\{\text{maximum}\right\}_{\text{Finite}} \quad . \tag{5.8-2}$$

The reasoning for saying that $|dP/dL|_{G,x}$ has a finite maximum value can be interpreted from Figure 18. There can be no doubt that the pressure gradient approaches a maximum value as one proceeds towards the outlet of the pipe, if one compares lines I and III in Figure 18. The specific volume of the mixture increases with decreasing system pressure and the frictional and momentum pressure drops per unit length increase.

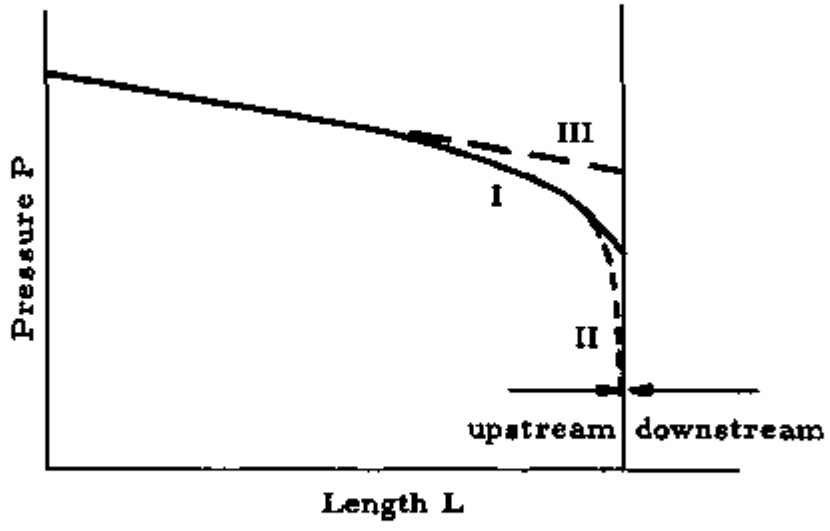

Figure 18. Pressure Profiles for Two-phase Flow

Line I represents a typical pressure profile for a given flow rate G and a quality x, these corresponding to critical flow. Line III corresponds to a typical pressure profile for ordinary two-phase flow in which critical conditions do not exist. Pressure profile III would be obtained if one had a throttling valve at the exit of the pipe and no free expansion could take place.

That $\left|dP/dL\right|_{G,x}$ for critical flow is finite is the next question to be considered. If line II should represent the critical pressure profile, indeed $\left|dP/dL\right|_{G,x}$ would be infinite. However, line I has been verified experimentally in this work, and data will be presented in Chapter VI. Cruz,[27] Moy,[77] and Faletti[33] also verified the finite maximum pressure gradient by an examination of the pressure profiles. Definition number 2 has been postulated by the author and, as far as is known, has not been applied to any previous mathematical treatment of two-phase critical flow.

5.9. Derivation of Slip Ratio and Void Fraction for Critical Two-phase Flow.

The slip ratio k is defined as the ratio of the average vapor velocity to the average liquid velocity.

Combination of the equations of continuity (5.7-9) and (5.7-10) and solution for the void fraction α_g gives

$$\alpha_g = \left(\frac{1-x}{x}\,\frac{v_l}{v_g}\,k+1\right)^{-1} \quad , \tag{5.9-1}$$

wherein k is defined as above.

Substituting into Eq. (5.7-19) for α_g the expression in Eq. (5.9-1), the specific volume v becomes a function of slip ratio as follows:

$$v = \frac{[(1-x)v_l k + xv_g][1+x(k-1)]}{k} \quad . \tag{5.9-2}$$

Dividing through by dL in Eq. (5.7-20) and using the expression for v in Eq. (5.9-2), we obtain the equation of motion as

$$\frac{G^2}{g_c}\left[\frac{d}{dL}\left\{\frac{[(1-x)v_l k + xv_g][1+x(k-1)]}{k}\right\} + \left\{\frac{[(1-x)v_l k + xv_g][1+x(k-1)]}{k}\right\}\frac{f}{2D}\right]$$

$$+\frac{dP}{dL} = 0 \quad . \tag{5.9-3}$$

From the second definition of critical two-phase flow, Eq. (5.8-2), it should be clear from Eq. (5.9-3) that also the sum of the acceleration and friction terms should possess a maximum value for a given flow rate G and quality x corresponding to critical-flow conditions, as one proceeds down the pipe toward the outlet.

In a two-phase flow system in a conduit, the pressure drop per length is in high degree dependent upon the flow pattern obtained in the system. Since the void fraction or slip ratio related in Eq. (5.9-1) is restricted to the flow pattern, in this case separated flow, it seems reasonable to maximize the sum of acceleration and friction terms with respect to the void fraction or slip ratio, so that this can satisfy the maximum pressure drop. This is logical since the slip ratio k is the only system variable that apparently is not fixed by the definition Eq. (5.8-2). The void fraction or the slip ratio is, in other words, one extra degree of freedom in the two-phase flow system. Hence, k or α_g is a tool by which a maximum pressure gradient $|dP/dL|$ can be achieved both physically as well as mathematically as long as free expansion can take place in a two-phase flow system where a sufficient pressure difference $(P_{th}-P_b)$ exists.

As a direct result from what has been stated above, the following relation can be written:

$$\frac{\partial}{\partial k}\left\{\frac{G^2}{g_c}\left[\frac{d}{dL}\left\{\frac{[(1-x)v_l k + xv_g][1+x(k-1)]}{k}\right\} + \left\{\frac{[(1-x)v_l k + xv_g][1+x(k-1)]}{k}\right\}\frac{f}{2D}\right]\right\} = 0 \quad . \tag{5.9-4}$$

Carrying out the partial differentiation with respect to the system variable k and interchanging derivatives, we find that Eq. (5.9-4) reduces to

$$\frac{G^2}{g_c}\left[\frac{d}{dL}\left(\frac{\partial v}{\partial k}\right)+\frac{f}{2D}\left(\frac{\partial v}{\partial k}\right)+\frac{v}{2D}\left(\frac{\partial f}{\partial k}\right)\right]=0 \quad , \tag{5.9-5}$$

wherein

$$v=\frac{[(1-x)v_l k+xv_g][1+x(k-1)]}{k} .$$

as before. Further,

$$\frac{\partial v}{\partial k}=(x-x^2)\left(v_l-\frac{v_g}{k^2}\right) \quad . \tag{5.9-6}$$

Substituting for $\partial v/\partial k$ into Eq. (5.9-5),

$$\frac{G^2}{g_c}\left[\frac{d}{dL}\left\{(x-x^2)\left(v_l-\frac{v_g}{k^2}\right)\right\}+\frac{f}{2D}\left\{(x-x^2)\left(v_l-\frac{v_g}{k^2}\right)\right\}+\frac{v}{2D}\left(\frac{\partial f}{\partial k}\right)\right]=0 \; . \tag{5.9-7}$$

A number of interpretations of the maximization process are feasible, at least from a mathematical point of view. The reader should have in mind that the functional relationship of the two-phase friction factor is not known with respect to the various parameters involved. Hence, if analytical solutions are hoped to be achieved, one is restricted to the following interpretations of Eq. (5.9-5):

(a) Isentropic flow:

If a parallelism to single-phase critical-flow theory is adapted, where the friction factor is set equal to zero (isentropic flow), there is only one possible solution that satisfies Eq. (5.9-5):

$$\frac{\partial v}{\partial k}=0 \quad . \tag{5.9-8}$$

As one can see, this procedure requires no particular definition of the specific volume of the two-phase mixture [see Eqs. (5.7-14) and (5.7-19)]. However, due to the adopted model, different phase velocities involve irreversibilities which are, naturally, incompatible with isentropy.

(b) Nonisentropic flow:

If nonisentropic flow, where f is not zero, is considered, the problem of not knowing the functional relationship between f and k becomes apparent. Therefore, in order to satisfy Eq. (5.9-5) and to obtain a closed solution for k, one is restricted to the following:

$$\frac{\partial v}{\partial k} = 0 \tag{5.9-9}$$

$$\frac{\partial f}{\partial k} = 0 \quad . \tag{5.9-10}$$

This particular solution is made possible due to the adoption of the specific volume v as defined by Eq. (5.7-19). If Eqs. (5.9-9) and (5.9-10) are satisfied, so is Eq. (5.9-5). Hence, from Eq. (5.9-6) one can get the restriction on the slip ratio k:

$$\frac{\partial v}{\partial k} = (x-x^2)\left(v_l - \frac{v_g}{k^2}\right) = 0 \quad . \tag{5.9-11}$$

Equation (5.9-11) is automatically satisfied for x = 0 and x = 1, respectively all water and all steam. Hence, in these two limiting cases no slip can occur and the value of k is taken as 1. As a direct result from Eq. (5.9-11) and what has been stated above,

$$\begin{aligned} &k = (v_g/v_l)^{1/2} = f(P) \text{ for } 0 < x < 1 \quad ; \\ &k = 1 \text{ for } x = 0 \text{ and } x = 1 \quad . \end{aligned} \tag{5.9-12}$$

So, with k given by Eq. (5.9-12) and $\partial f/\partial k = 0$, the second definition of critical two-phase flow, Eq. (5.8-2), is indeed satisfied. There are two ways to interpret the mathematical meaning of $\partial f/\partial k = 0$ for nonisentropic flow. In the first one, f remains constant for varying k. In the second, f goes through a maximum or minimum at which $k = (v_g/v_l)^{1/2}$. Although the first interpretation seems rather unjustified, the second certainly would compensate for $\partial v/\partial k = 0$ in the momentum equation. That this is so was checked by integrating the momentum Eq. (5.7-20) and solving for

the average friction factor f_m. If experimental data are used and different values of slip ratio k are tried, a graph similar to Figure 19 may be obtained. As one can see from Figure 19, f_m goes through a maximum, this point corresponding approximately to $k = (v_g/v_l)^{1/2}$. The reader should be aware that the model adopted is strictly applicable only at the exit, where the critical phenomenon occurs. However, in obtaining graph 19, the model was extrapolated upstream in the steepest part of the curve of pressure versus length, where critical flow is almost fully developed. Therefore, from this comparison of experimental data, the maximization process of the sum of acceleration and friction terms can be said to have been justified for nonisentropic flow. The procedure for integrating the momentum equation will be shown later, and a numerical example for obtaining Figure 19 is shown in Appendix G.

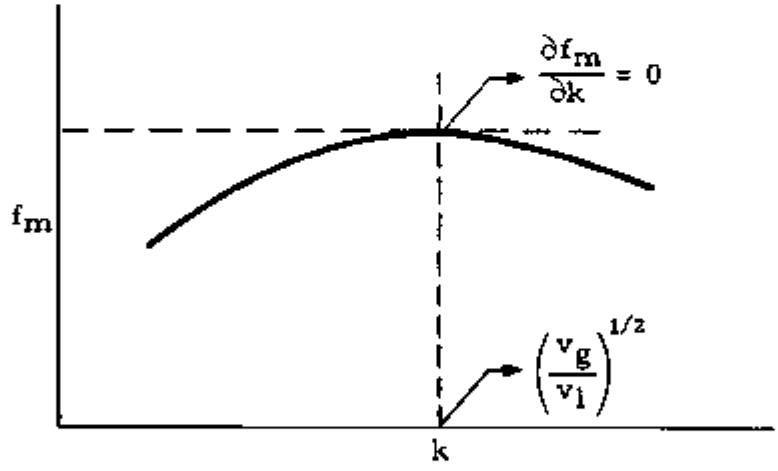

Figure 19. Two-phase Friction Factor Plotted Versus Slip Ratio

As in the manner carried out above, by taking into account a new definition of critical flow, a very significant result is obtained regarding the slip ratio. By use of the obtained result in Eq. (5.9-1), the void fraction becomes

$$\alpha_g = \left[\frac{1-x}{x}\left(\frac{v_l}{v_g}\right)^{1/2} + 1\right]^{-1} \quad . \tag{5.9-13}$$

Equations (5.9-9) and (5.9-10) can, of course, be written as

$$\frac{\partial v}{\partial \alpha_g} = 0 \qquad (5.9\text{-}14)$$

and

$$\frac{\partial f}{\partial \alpha_g} = 0 \quad , \qquad (5.9\text{-}15)$$

and will yield the same result as obtained in (5.9-13).

As a result of this, slip ratio and void fraction can be determined for critical flow by specifying pressure and quality of the two-phase system. As will be seen later, when pressure and quality are specified, the flow rate is automatically fixed, since these three variables are interrelated. (This is only true for critical flow.) Hence, the following can be postulated:

$$\alpha_g = f^{I}(x,P,G) = f^{II}(x,P) = f^{III}(x,G) = f^{IV}(G,P) \quad . \qquad (5.9\text{-}16)$$

5.10. Discussion of Void Fraction and Slip Ratio

To check if the limits of Eq. (5.9-13), which predicts the void fraction, are right, the following restriction must be satisfied:

1) for $x = 0$, $\alpha_g = 0$ (no gas phase);
2) for $x = 1$, $\alpha_g = 1$ (all gas phase).

These two restrictions are certainly satisfied by an examination of Eq. (5.9-13).

As can be seen from Eq. (5.9-12), there is no quality effect on the slip ratio, which at first may puzzle the reader. Marchaterre and Petrick,[67] however, verify this to some extent. From their experimental results one can conclude that the effect of quality on the slip ratio decreases with the pressure for the range of variables used at Argonne National Laboratory. The quality effect on the slip ratio also appears to diminish with increasing mass velocity. This has been observed for recent data obtained in the range of higher mass velocity. Since the

superficial velocity is extremely high under critical-flow conditions, up to 100 times higher than the usual investigations, it seems reasonable that the slip ratio is indeed independent of quality.

Further, as the superficial velocity increases, the slip ratio decreases. This is also in accordance with the theoretical expression for slip ratio, for if mass velocity is increasing under critical flow for a constant quality, the pressure must increase and, therefore, the slip ratio is decreasing.

As expected, the slip ratio decreases with increasing pressure, and this is certainly fulfilled by Eq. (5.9-12).

As a final conclusion from what has been stated above, the theoretically developed expression for slip ratio has the same trends and indications that have been found by other investigators in experiments at low-velocity ranges.

Although the theoretical expression for the slip ratio as developed by the author has the same trends, it should be mentioned that the slip ratio is markedly greater than previously determined slip ratios for low-velocity ranges. It should also be pointed out that Eq. (5.9-12) only holds for two-phase systems under critical-flow conditions. Figure 20 shows how void fraction α_g varies with quality x, with pressure P as a parameter, calculated from Eq. (5.9-13). Figure 21 presents the slip ratio, k, as a function of pressure.

5.11. Derivation Leading to a Theoretical Evaluation of the Critical Flow Rate

Integrating the equation of motion, Eq. (5.7-20), in the interval from P_0 to P, one gets

$$\int_{P_0}^{P} \frac{1}{v}\, dP + \frac{G^2}{g_c}\left[\ln \frac{v}{v_0} + \frac{f_m L}{2D}\right] = 0 \quad , \qquad (5.11\text{-}1)$$

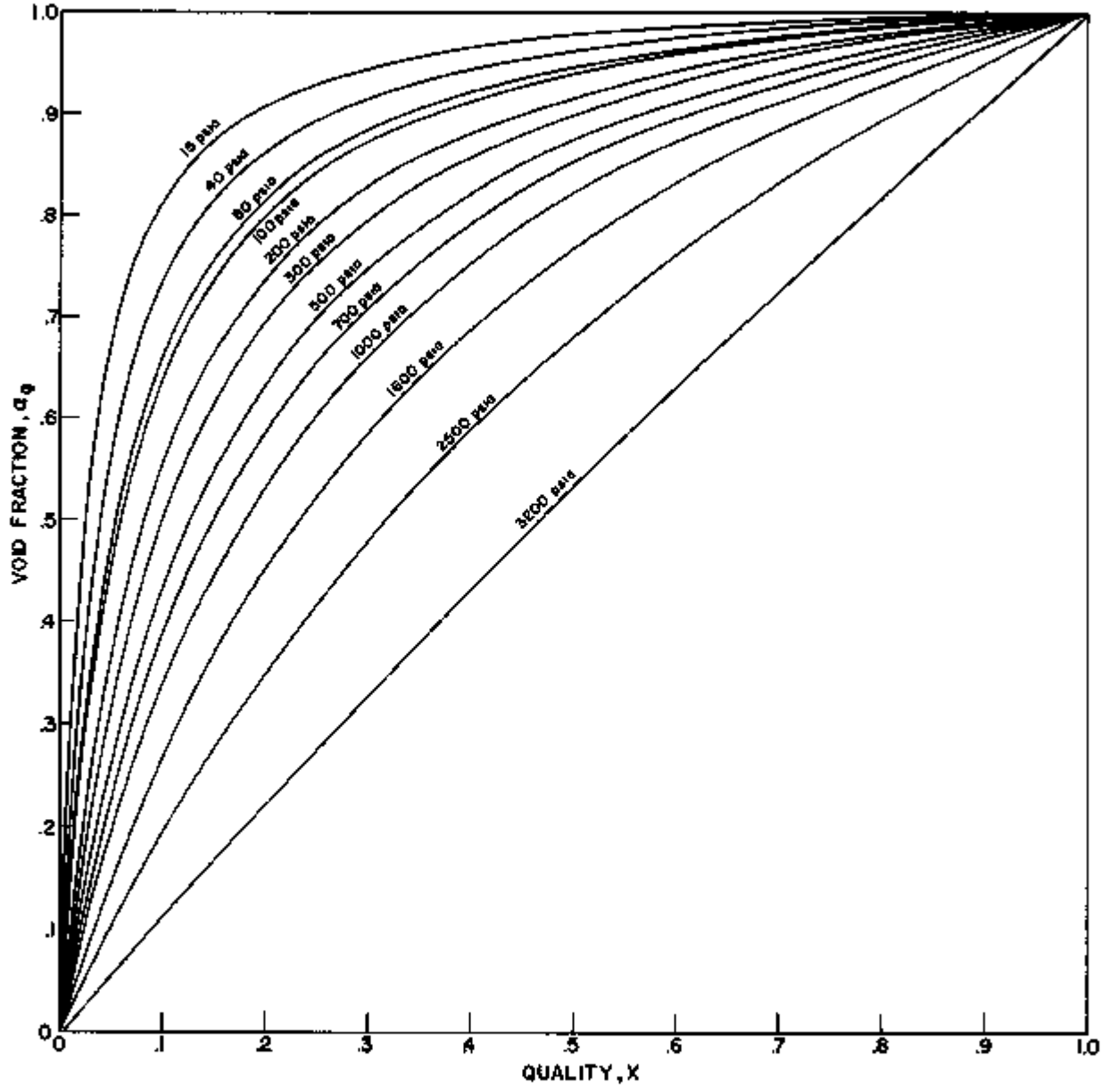

Figure 20. Theoretical Prediction of Void Fraction for Critical Flow

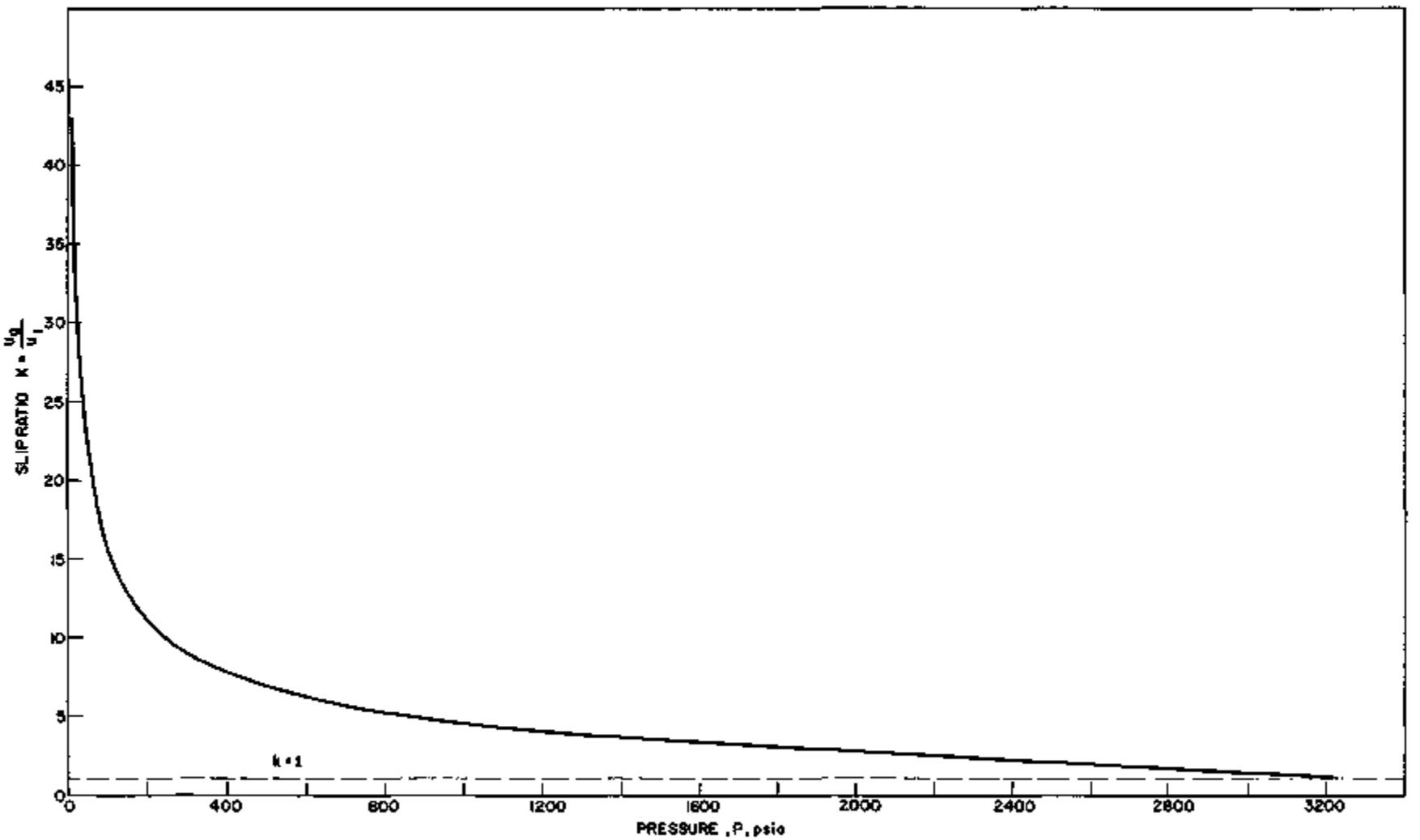

Figure 21. Theoretical Prediction of Slip Ratio for Critical Flow

wherein v_0 is the specific volume of the two-phase mixture at P_0 as defined by Eq. (5.9-2), and v is the specific volume as defined for v_0 at any pressure P, and

$$f_m = \int_{P_0}^{P} f \frac{d(1/L)}{dP} dP \quad . \tag{5.11-2}$$

Equation (5.11-2) gives the two-phase friction factor for the friction loss over the range from P_0 to P with length L. Here $P_0 - P$ is taken to be relatively small as compared with P.

The flow is called the critical flow when the flow rate no longer increases with increasing pressure differences. This is the basic definition of critical flow mentioned before in Eq. (5.8-1).

Carrying out the differentiation of Eq. (5.11-1) with respect to P and using Eq. (5.8-1), one gets the following relation:

$$\frac{1}{v}\left[\ln \frac{v}{v_0} + \frac{f_m L}{2D}\right] - \left[\frac{d \ln v}{dP} + \frac{L}{2D} \frac{df_m}{dP}\right] \int_{P_0}^{P} \frac{1}{v} dP = 0 \quad . \tag{5.11-3}$$

Combining Eq. (5.11-1) with (5.11-3) and solving for the critical flow rate G_{crit}, one gets the following:

$$G_{crit} = \left[\frac{-g_c}{v[d \ln v/dP + L/2D \, df_m/dP]}\right]^{1/2} \quad . \tag{5.11-4}$$

Furthermore, at critical-flow conditions for a given G and x, one can write

$$\left(\frac{df_m}{dP}\right)_{G_{crit}, x_{crit}} = \frac{\partial f_m}{\partial k} \frac{dk}{dP} \quad . \tag{5.11-5}$$

But, since $\partial f_m / \partial k = 0$, it follows that

$$\frac{df_m}{dP} = 0 \quad . \tag{5.11-6}$$

Application of the definition of specific volume v and use of Eq. (5.11-6), leads to the following equation for the critical flow rate:

$$G_{crit} = \left[\frac{g_c}{d/dP\,[\{(1-x)v_l k + xv_g\}\ \{1+x(k-1)\}/k]}\right]^{1/2} \quad . \qquad (5.11\text{-}7)$$

The dependent variables v_l, v_g, x, and k have to be differentiated with respect to the independent variable, namely, the pressure P. If this is carried out, the final expression for determining G_{crit} theoretically becomes

$$G_{crit} = \left[\frac{-g_c k}{\{(1-x+kx)x\}\,dv_g/dP + \{v_g(1+2kx-2x)+v_l(2xk-2k-2xk^2+k^2)\}\,dk/dP + \{k[1+x(k-2)-x^2(k-1)]\}\,dv_l/dP}\right]^{1/2} \qquad (5.11\text{-}8)$$

wherein the slip ratio k is given by Eq. (5.9-12).

Since the specific volume of liquid changes very slowly with pressure, the term including dv_l/dP can be neglected for pressures up to 400 psia. A numerical example showing the error by doing so is shown in Appendix D.

Thus, by specifying the outlet pressure and quality, the critical two-phase flow rate can be calculated from Eq. (5.11-8). At this point, a decision has to be made as to whether the evaluation of the partial derivatives in Eq. (5.11-8) should be carried out under isenthalpic or isentropic conditions. For adiabatic flow, such as in the flow of flashing mixtures of steam and water, both isentropic and isenthalpic conditions have been assumed by earlier investigators to evaluate v in the integral $\int dP/v$, where v is defined by Eq. (5.4-1). If the kinetic energy or potential term is significant, the isenthalpic condition is not correct; and with frictional losses present, the isentropic assumption is also in error. In many cases, very little difference is found between the use of isenthalpic and isentropic expansions for flashing steam-water mixtures. Bridge[21] has evaluated the integral $\int dP/v$ for isenthalpic expansions for initial saturation pressure up to 600 psia. Allen[3] derived analytical

expressions for the isenthalpic expansion. As for the only theoretical model presented of the problem considered in this work previous to the author's, the so-called "Homogeneous Flow Model," the evaluation of the partial derivatives $\partial x/\partial P$, $\partial v_g/\partial P$, and $\partial v_l/\partial P$ were carried out under isentropic conditions. This is in accordance with the model, since the friction factor in the momentum equation is set equal to zero. In 1959, Ishigai and Sekoguchi[53] published a paper on the flashing flow of saturated water through horizontal pipes. In this paper, a new correction factor for friction loss is introduced to satisfy the before-mentioned discrepancy between the "Homogeneous Flow Model" and observed data, and is determined by experiment. The only difference between the "Homogeneous Flow Model" as discussed earlier in this work and the above-mentioned semi-empirical model is that the first neglects friction and the second takes it into account. However, Ishigai and Sekoguchi contradict themselves, as their evaluation of dv/dP is carried out under isentropic conditions. Since the friction term is included in the momentum equation, this cannot be considered to be a reversible process.

In this work, isenthalpic conditions are adopted for evaluation of dv/dP in Eq. (5.11-7), in accordance with nonisentropic flow (see Section 5.9). The existence of different phase velocities, which is the case in the writer's theory, implies that two-phase critical or maximum mass velocities are not isentropic mass velocities as is the case in single-phase flow. Different phase velocities involve irreversibilities which are, naturally, incompatible with isentropy. Furthermore, the kinetic energy and potential terms for the flashing flow of water-steam mixtures are in most cases negligible compared with the total enthalpy of the flowing fluid in the pipe. Hence, the adoption of isenthalpic rather than isentropic conditions seems more adequate. The procedure for evaluation of the derivatives in Eq. (5.11-8) is as follows.

Calculation of dx/dP

The derivative dx/dP is approximated by $\Delta x/\Delta P$ determined at constant mixture enthalpy. For a given pressure P and quality x, one has

$$H_m = h_f + x h_{fg} \tag{5.11-9}$$

or

$$\frac{dx}{dP} = -\frac{1}{h_{fg}}\left(\frac{dh_f}{dP} + x\,\frac{dh_{fg}}{dP}\right) \quad , \tag{5.11-10}$$

wherein

H_m is total enthalpy of the mixture, Btu/lb_m

h_f is enthalpy of saturated liquid at pressure P, Btu/lb_m

h_{fg} is the change in enthalpy in going from the liquid to the vapor state, Btu/lb_m.

An approximate value for dx/dP is, then,

$$\frac{dx}{dP} \approx \frac{\Delta x}{\Delta P} = -\frac{1}{h_{fg}}\left(\frac{\Delta h_f}{\Delta P} + x\,\frac{\Delta h_{fg}}{\Delta P}\right) \quad , \tag{5.11-11}$$

where h_{fg} Δh_f, and Δh_{fg} can be found from steam tables.

Calculation of dv_g/dP

The derivative dv_g/dP can be approximately represented by $\Delta v_g/\Delta P$ evaluated at constant mixture enthalpy. Actually, v_g is the specific volume of the saturated vapor and is a function of pressure; hence,

$$\frac{dv_g}{dP} \approx \frac{\Delta v_g}{\Delta P} \quad , \tag{5.11-12}$$

where Δv_g can be found in steam tables.

Calculation of dv_l/dP

The value of dv_l/dP is approximated by $\Delta v_l/\Delta P$ determined at constant mixture enthalpy and is determined in the same fashion as dv_g/dP.

The use of steam tables implies that we may assume a plane interface between phases, which is not necessarily the case in high-speed pipe flow. In the case of liquid drops suspended in the vapor, the interface area is indeed greatly increased, and surface tension effects should be considered. However, if the suspended liquid drops are of the order 4×10^{-7} in. in diameter, the heat of vaporization is increased by only approximately one Btu/lb_m. If liquid droplets should occur in the vapor phase, it is assumed that they are of sufficient size to eliminate the need of surface tension corrections.

A complete numerical example of calculating the critical flow rate from Eq. (5.11-8) is shown in Appendix D.

It should be pointed out here that, insofar as the author knows, Eq. (5.11-8) represents the first complete theoretical solution for predicting the two-phase critical flow rate, taking into account slip between phases without the use of any experimental correlations. This contribution was made possible mainly due to an analysis leading to new definitions of the specific volume of the two-phase mixture and for critical two-phase flow. From these concepts, a theoretical expression for void fraction α_g can be obtained. In Figure 22 the critical flow rate G as calculated from Eq. (5.11-8) is plotted versus the critical discharge pressure and quality, respectively, with quality and pressure as parameters. The quality range is from 1 to 100% and pressures from atmospheric up to the critical pressure, namely, 3206 psia. This chart is calculated for steam-water mixtures.

As mentioned before, Eq. (5.11-8) gives the critical discharge flow rate for two-phase, one-component flow.

For two-phase, two-component flow with no mass transfer, $dx/dP = 0$ and Eq. (5.11-8) reduces to the following:

$$G_{crit} = \left[\frac{-g_c k}{\{(1 - x + kx)x)\,(dv_g/dP) + (k[1 + x(k - 2) - x^2\,(k - 1)])\,(dv_l/dP)} \right]^{1/2} \qquad (5.11\text{-}13)$$

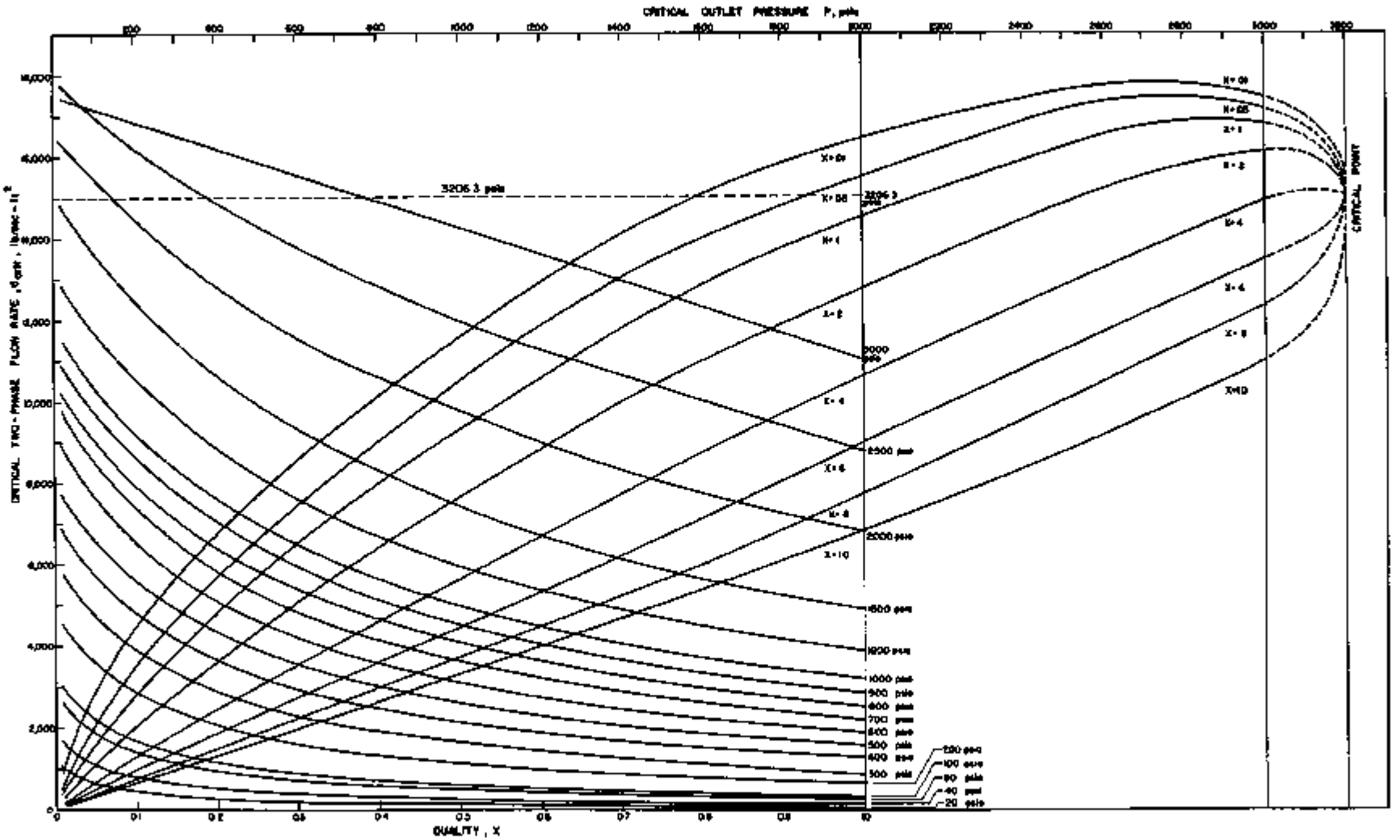

Figure 22. Theoretical Predictions of Critical Flow Rates

Typical two-phase, two-component systems are air-water and oil-gas mixtures.

5.12. Derivation Leading to Evaluation of the Two-phase Friction Coefficient for Critical Flow

Solving Eq. (5.11-1) for the average friction factor f_m, one gets

$$f_m = - \frac{2D}{L} \left[\frac{g_c}{G^2} \int_{P_0}^{P} \frac{1}{v} \, dP + \log \frac{v}{v_0} \right] \quad . \tag{5.12-1}$$

To be able to calculate f_m from Eq. (5.12-1), one would have to be able to evaluate the integral $\int_{P_0}^{P} (1/v) \, dP$.

Evaluation of $\int_{P_0}^{P} (1/v) \, dP$

If the expression (5.9-2) for specific volume is inserted, the integral becomes

$$I = \int_{P_0}^{P} \frac{k}{x \left\{ [(1-x)/x] \, v_l k + v_g \right\} [1 + x(k-1)]} \, dP \quad . \tag{5.12-2}$$

The most sensitive variable, by far, in Eq. (5.12-2) is the specific volume of gas, v_g. For a short interval P_0 to P, ($P_0 - P$ is relatively small compared to P), the mean values for the variables k, x, and v_l are reasonable approximations.

If thermodynamic equilibrium is assumed between the liquid and vapor phases, the specific volume of the gas phase becomes a function of pressure alone. Therefore, the following empirical relation between specific volume and pressure can be used:

$$v_g = aP^{-n} \quad , \tag{5.12-3}$$

wherein a and n are constant for all practical pressures and can be evaluated from the steam tables. If the above approximations are applied, the integral to be evaluated takes the following form:

$$I = \left[\frac{k}{x\,[1+x(k-1)]}\right]_{mean} \frac{1}{a} \int_{P_0}^{P} \frac{P^n}{1+(\Gamma/a)\,P^n}\,dP \quad , \qquad (5.12\text{-}4)$$

wherein

$$\Gamma = \frac{1-x}{x} v_1 k \quad .$$

The integral in Eq. (5.12-4) cannot be solved analytically, but if

$$\left|\frac{\Gamma}{a} P^n\right| < 1 \quad , \qquad (5.12\text{-}5)$$

one can expand this integral in a series as follows:

$$I = \left[\frac{k}{x\,[1+x(k-1)]}\right]_{mean} \left| \frac{P^{n+1}}{a} \sum_{m=0}^{\infty} \frac{[-(\Gamma/a)P^n]^m}{n(m+1)+1} \right|_{P_0}^{P} \quad . \qquad (5.12\text{-}6)$$

In most practical cases Eq. (5.12-5) is satisfied, and, therefore, since the series converge, only 3 to 4 terms are needed. Further, since it is an alternating series, the error is always less than the next neglected term, so one can easily control the error involved. The complete equation for calculating the friction factor then becomes

$$f_m = -\frac{2D}{L}\left\{\frac{g_c}{G^2}\left[\frac{k}{x[1+x(k-1)]}\right]_{mean}\left| \frac{P^{n+1}}{a} \sum_{m=0}^{\infty} \frac{[-(\Gamma/a)P^n]^m}{n(m+1)+1} \right|_{P_0}^{P} + \log\frac{v}{v_0}\right\} , \qquad (5.12\text{-}7)$$

where v and k are given by Eq. (5.9-2) and (5.9-12), respectively. Equation (5.12-7) was applied in the extremely steep portion of the curve of pressure versus length for several runs with various conditions where curves like the one in Figure 19 were obtained.

5.13. Outline of the Procedure for Calculating the Mixture Quality at Any Point Along the Test Section from Experimental Data.

The quality of the steam at a point in the system is determined by using a total energy balance.

The following assumptions are made:

1. no heat input;
2. no change of potential energy;
3. system at thermodynamic equilibrium; and
4. phase velocities represented by average linear velocities. Considering Figure 23 below:

Total energy in at 1 = total energy out at 2.

This can be written:

$$W_s H_s + W_{sL} h_{sL} + \frac{W_s u_s^2}{2g_c J} + \frac{W_{sL} u_{sL}^2}{2g_c J} = (W_s + W_{sL})(h_l + x h_{fg}) + (KE)_{TP} + Q_{Loss} \quad ; (5.13\text{-}1)$$

here Q_{Loss} represents all the energy losses.

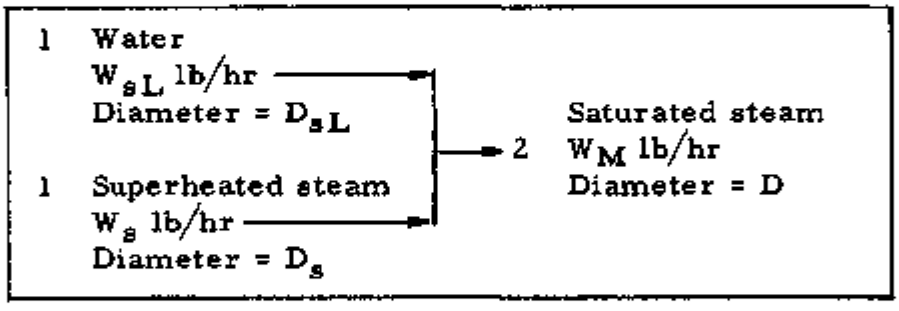

Figure 23. Simple Flow Diagram of the Two-phase Flow Loop

If Eq. (5.13-1) is solved for the quality x, there is obtained

$$x = \frac{W_s H_s + W_{sL} h_{sL} + (W_s u_s^2/2g_c J) + (W_{sL} u_{sL}^2/2g_c J) - (KE)_{TP} - Q_{Loss} - W_m h_l}{W_m h_{fg}} , \quad (5.13\text{-}2)$$

wherein

$$W_m = W_s + W_{sL} = W_g + W_l \quad .$$

In general, for turbulent flow

$$(KE)_{TP} = \frac{x W_m u_g^2}{2g_c J} + \frac{(1-x) W_m u_l^2}{2g_c J} \quad (5.13\text{-}3)$$

$$= \frac{W_m}{2g_c J} \left[x u_g^2 + (1-x) u_l^2 \right] \quad . \quad (5.13\text{-}4)$$

For homogeneous flow,

$$u_g = u_l = u_m \quad . \tag{5.13-5}$$

Inserting Eq. (5.13-5) into Eq. (5.13-4), one gets

$$(KE)_{TP,Homogeneous} = \frac{W_m u_m^2}{2g_c J}\left[x+(1-x)\right] = \frac{W_m u_m^2}{2g_c J} \quad . \tag{5.13-6}$$

Now,

$$u_m = Gv_m \quad ,$$

where

$$v_m = xv_g + (1-x)v_l \quad .$$

Thus,

$$(KE)_{TP,Homogeneous} = \frac{W_m G^2 v_m^2}{2g_c J} = \frac{W_m^3 v_m^2}{2g_c J A^2} \quad . \tag{5.13-7}$$

For annular flow, the equations of continuity are

$$u_g = xGv_g/\alpha_g \quad ; \tag{5.13-8}$$

$$u_l = \frac{(1-x)Gv_l}{1-\alpha_g} \quad , \tag{5.13-9}$$

wherein α_g is given by Eq. (5.9-1). If these velocity expressions are inserted in Eq. (5.13-4),

$$(KE)_{TP,Ann} = \frac{W_m}{2g_c J}\left\{x\left(\frac{xW_m v_g}{A\alpha_g}\right)^2 + (1-x)\left[\frac{(1-x)W_m v_l}{A(1-\alpha_g)}\right]^2\right\} \tag{5.13-10}$$

$$= \frac{W_m^3}{2g_c J A^2}\left[\frac{x^3 v_g^2}{\alpha_g^2} + \frac{(1-x)^3 v_l^2}{(1-\alpha_g)^2}\right] \quad . \tag{5.13-11}$$

If Eq. (5.13-11) is put into Eq. (5.13-2) and one lets $A = \pi D^2/4$, there results

$$x = x_0 + c \quad , \tag{5.13-12}$$

wherein

$$x_0 = \frac{W_s H_s + W_{sL} h_{sL} - Q_{Loss} - W_m h_l}{W_m h_{fg}} \qquad (5.13\text{-}13)$$

$$c = \frac{8}{\pi^2 g_c J W_m h_{fg}} \left\{ \frac{W_s^3 v_s^2}{D_s^4} + \frac{W_{sL}^3 v_{sL}^2}{D_{sL}^4} - \frac{W_m^3}{D^4} \left[\frac{x^3 v_g^2}{\alpha_g^2} + \frac{(1-x)^3 v_l^2}{(1-\alpha_g)^2} \right] \right\} . \qquad (5.13\text{-}14)$$

The term x_0 can be thought of as an approximation to the true quality and the term c as the kinetic energy correction factor.

To calculate the quality from the Eq. (5.13-12), an iteration procedure is used which converges quite rapidly. First, the quality x is approximated by x_0, from Eq. (5.13-13). Having a first estimate of x, then c, the two-phase kinetic-energy correction factor, is approximated by Eq. (5.13-14). This procedure is repeated until the quality x becomes constant. This usually requires at the most 2 to 3 evaluations of the correction factor c.

From the above procedure the qualities along the test sections were calculated from the experimental data obtained in this work. Equation (5.13-7) was adopted rather than Eq. (5.13-11) for the kinetic-energy term, and the error introduced is negligible. In Appendix F an example calculation is carried out, showing the quality calculated by both ways. For all experimental results reported, the quality noted is based upon the evaluation using Eqs. (5.13-2) and (5.13-7).

5.14. Absolute Average Velocities for the Two Phases at Critical Flow Conditions.

The absolute average phase velocities can be calculated from the continuity Eqs. (5.7-9) and (5.7-10):

$$u_g = xGv_g/\alpha_g \quad ; \qquad (5.14\text{-}1)$$

$$u_l = \frac{(1-x)Gv_l}{1-\alpha_g} \quad . \qquad (5.14\text{-}2)$$

The following scheme represents the procedure:

1. Choose P and x.
2. Calculate the slip ratio k from Eq. (5.9-12).
3. Calculate critical flow rate G from Eq. (5.11-8)
4. Calculate void fraction α_g from Eq. (5.9-13).
5. Calculate the absolute velocities from Eqs. (5.14-1) and (5.14-2).

As will be discussed in Chapter VII, the absolute velocities calculated from this theory are far below sonic velocities, except when the quality approaches 1.0. In Figure 24, the linear vapor velocity is plotted versus quality, with pressure P as parameter. Figure 24 shows that no true sonic choking occurs for two-phase critical flow. When the quality approaches 1.0, Eq. (5.11-8) converges to the solution for one-phase critical flow, for which sonic flow does occur.

Putting x = 1.0 in Eq. (5.11-8), there is obtained

$$G = \left[\frac{-g_c k}{k\{(dv_g/dP) + 2v_g\,[1-(1/k)]\,(dx/dP)\}}\right]^{1/2} . \qquad (5.14\text{-}3)$$

But at quality equal to 1.0 (only vapor phase), no slip exists. In this case, k is taken as 1 from Eq. (5.9-12), and Eq. (5.14-3) reduces to

$$G = \left[\frac{-g_c}{dv_g/dP}\right]^{1/2} , \qquad (5.14\text{-}4)$$

which is exactly the solution for one-phase critical flow in which the discharge velocity of the gas is equal to the velocity of sound in that medium.

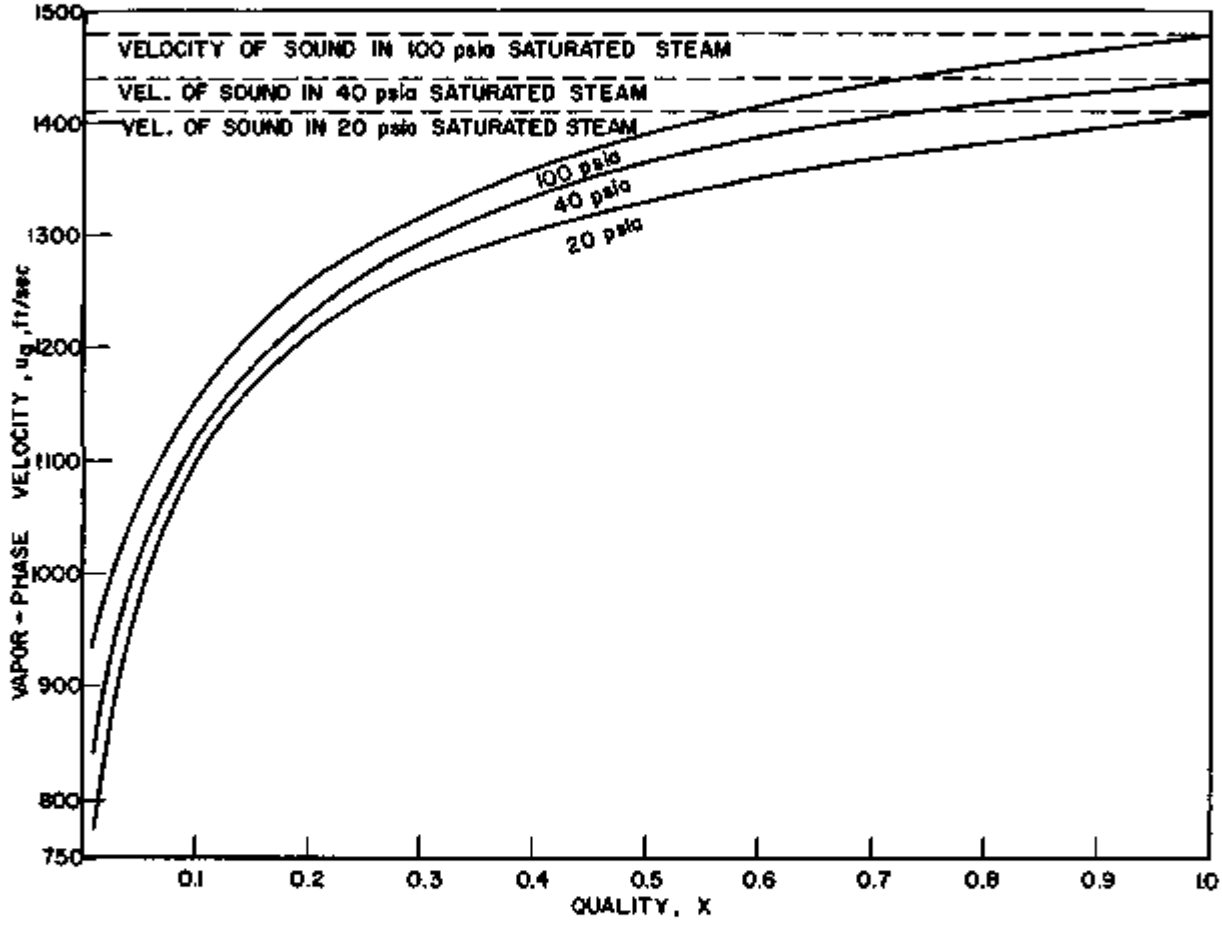

Figure 24. Theoretical Prediction of the Vapor-phase Velocity Compared with the Velocity of Sound

CHAPTER VI

ANALYSIS OF CRITICAL TWO-PHASE FLOW DATA; COMPARISON WITH THE DEVELOPED THEORY, INCLUDING PREVIOUS MAJOR INVESTIGATIONS

6.1. Treatment of Data

Thermocouple potentials, read in millivolts, were converted to degrees Fahrenheit by the use of calibration charts.

Pressure readings were converted from cm Hg, in. Hg, and psig to psia. The pressure measurements taken along the test section at critical-flow conditions were plotted against length in order to determine, by extrapolation, the value of the critical pressure.

Steam and water flow rates were converted into usable units with the aid of calibration charts, and corrected for temperature and pressure whenever necessary.

Computations involved in determining the critical mass velocity, critical pressure, total energy of the two-phase mixture, and exit quality from these data are illustrated by the sample calculations based on run (TSII-42), the corrected data for which appear on page 50 and are shown in Appendix F.

6.2. Pressure Profiles

Pressure profiles were drawn from pressure measurements obtained with the taps on the wall of the test section. This was done for every run, in order to obtain the critical throat pressure by extrapolating the pressure curve obtained, from pressure tap I to the exit of the pipe. Representative profiles obtained with TSII and TSIV are shown in graphs 25 through 28. The upstream pressures taken from wall taps are tabulated in Appendix B for all critical two-phase runs made in this work, with back pressure subcritical.

The extrapolation method employed in this work was used by earlier investigators, among them Isbin, Cruz, and Moy.[47] They studied

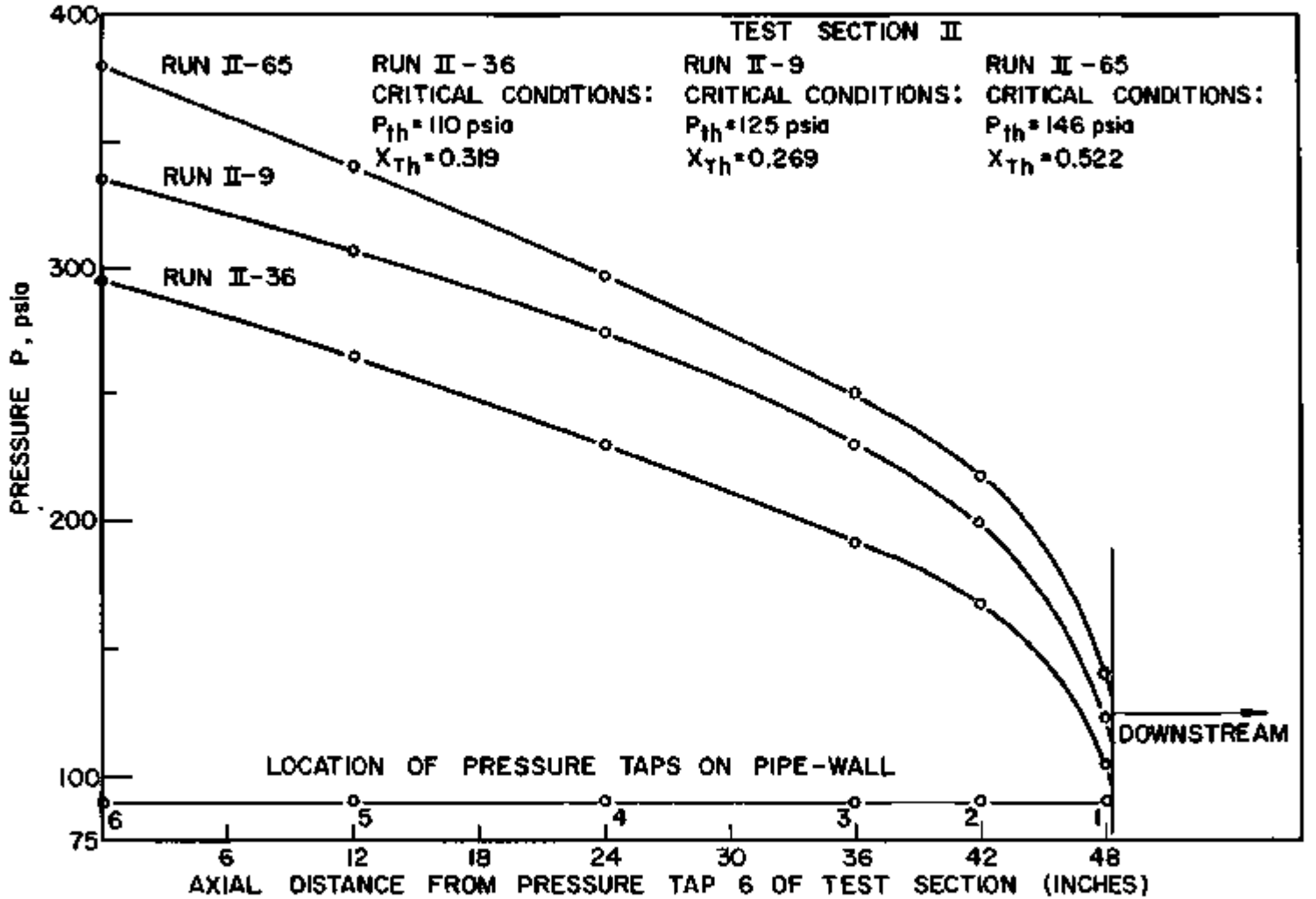

Figure 25. Experimental Pressure Profiles

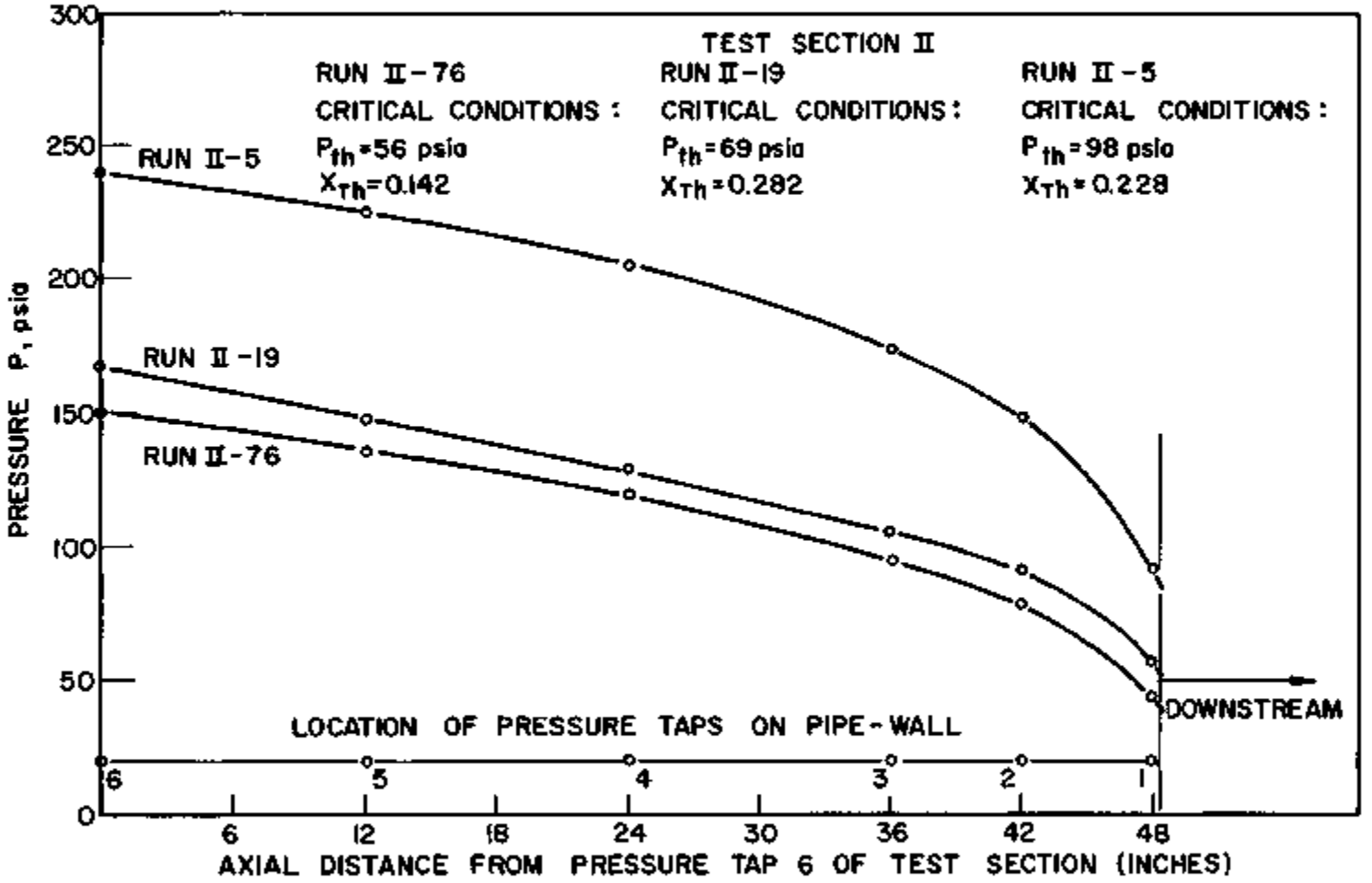

Figure 26. Experimental Pressure Profiles

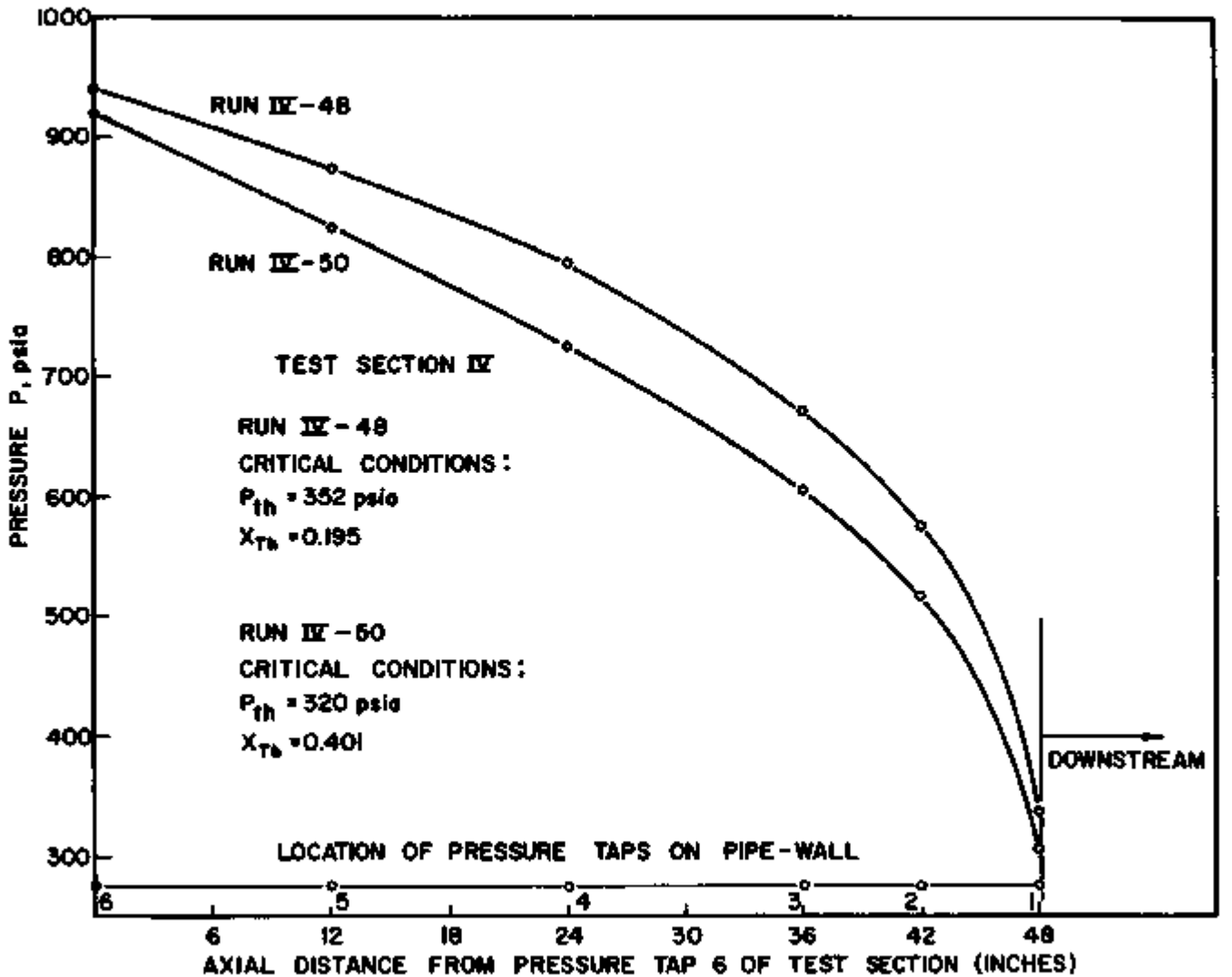

Figure 27. Experimental Pressure Profiles

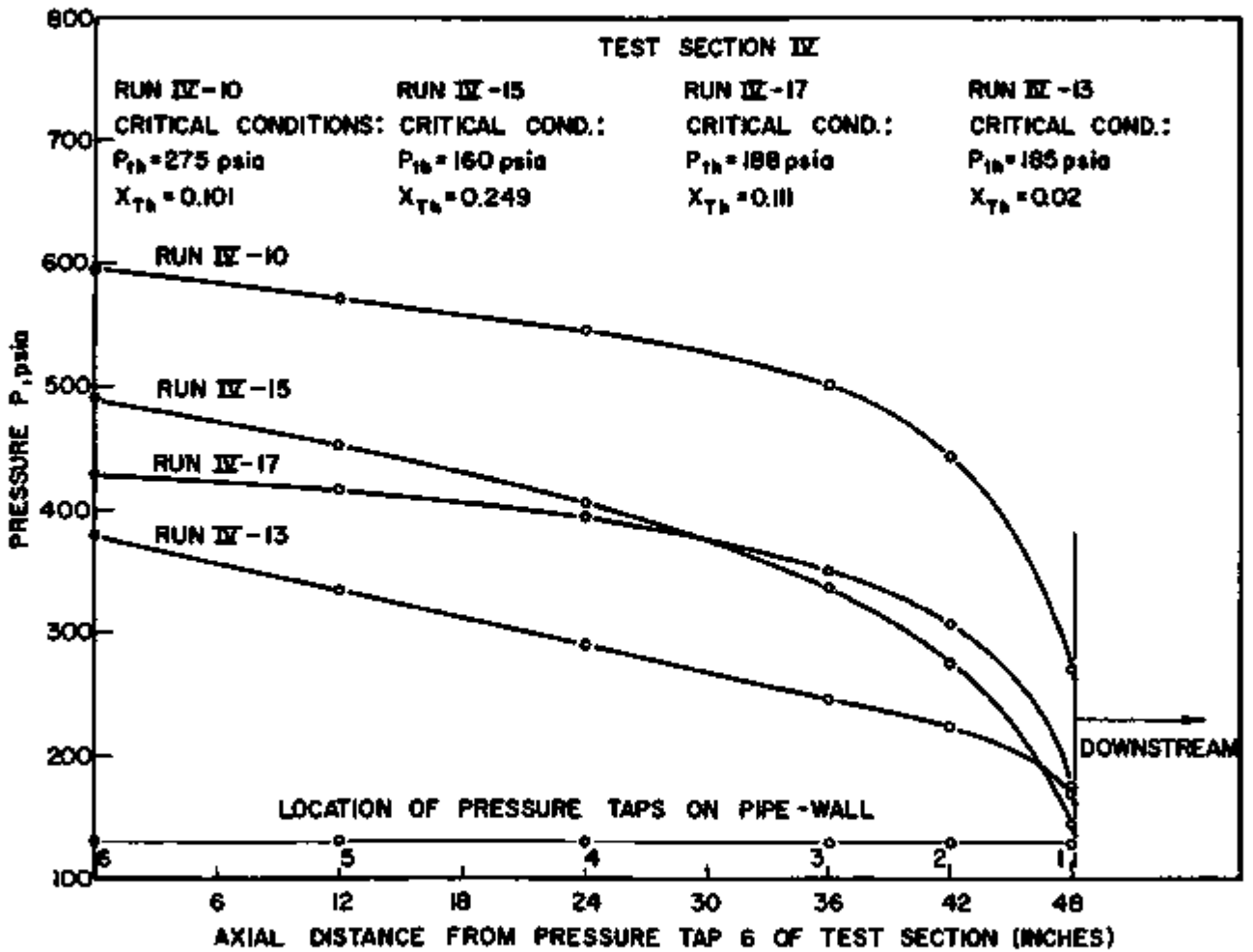

Figure 28. Experimental Pressure Profiles

the critical phenomenon in pipes ranging from one-quarter- to one-inch nominal pipe size. In addition, a one- by three-quarter-inch annulus and a three-quarter- by one-quarter-inch annulus were studied.

Faletti[33] measured critical flow of steam-water mixtures in concentric annuli having center rods of 0.188- and 0.375-in. OD. These rods ran the entire length of the 0.574-in.-ID test section and extended beyond the throat (exit plane). Pressure taps on the walls of the test section and on the center rods (one of which could be moved axially) permitted a study of the pressure profiles both upstream and downstream of the throat; in this way Faletti could measure the critical pressure at the exit plane, and an extrapolation method was not necessary. Further, he stated that an extrapolation method, such as the one used by Isbin, Cruz, and Moy, could be in serious error, since the observation was made that the pressure profiles dropped off sharply $\frac{10}{32}$ in. upstream from the throat. The inside diameter of Cruz's[27] test section was 1.0419 in., and his last pressure tap was $1\frac{3}{32}$ in. from the exit plane of the test tube. This distance corresponds to 0.3 equivalent diameter with respect to Faletti's observation. As for Moy,[77] his smallest test section had an ID of 0.3743 in., with the last pressure tap $\frac{1}{2}$ in. from the exit of the pipe. This distance corresponds to 0.63 equivalent diameter. For the two test sections used in this work, the distance of $\frac{10}{32}$ in. corresponds to 1.25 equivalent diameters for TSII and 2.5 equivalent diameters for TSIV. The taps for these two test sections are within one diameter from the exit and should be close enough to the exit to observe any sharp drop in the pressure gradient. Indeed, by looking at the pressure profiles shown in graphs 25 through 28, the sharp drop in pressure gradient is accountable in every run.

The method used by Faletti, with a probe extended beyond the throat (exit plane), is not free from errors, inasmuch as serious disturbances at the exit might be induced by the extended probe in the region of critical flow. It should be mentioned here that the method of probing from the exit end was examined by Isbin and Cruz in preliminary runs of their research. The

method was discarded in favor of the extrapolation method, because of observed flow disturbances caused by the probe. The pressure profiles obtained in this work are believed to be of high accuracy, since the flow disturbances were minimized, and the sharp drop of the pressure gradient close to the exit plane of the test pipe as stated by Faletti has, indeed, been observed in this research by the extrapolation method without using a probe.

A study of the profiles given in graphical form shows that both the steepness and the shape of the profile upstream of the throat were a function of quality. As a general trend, the steepness of the pressure gradient along the pipe seems to increase with increasing quality. This can best be seen in graph 28 by comparison of Run IV-17 with Run IV-15, for which the pressure profiles cross each other. However, this work is devoted to the details of the critical phenomenon which occurs at the exit plane of the pipe, rather than to the characteristics of pressure drop upstream.

As for the second criteria of critical two-phase flow postulated by the author,

$$\left|\frac{dP}{dl}\right|_{G,x} = \{\text{Maximum}\}_{\text{finite}} \qquad (6.2\text{-}1)$$

can be verified by looking at the pressure profiles in graphs 25 through 28. From an analysis of these graphs, it appears to be correct to state that $\left|\frac{dP}{dl}\right|$ is finite. Furthermore, the increasing steepness in the pressure profile as one approaches the exit of the tube indicates simply that the pressure gradient approaches a finite maximum value. This value is determined by the flow rate G and quality x corresponding to the critical-flow conditions.

6.3. Graphical Presentation of the Data

All data have been plotted in Figures 29 through 42.

In these plots, the ordinate gives the critical outlet discharge pressure, and the abscissa represents the critical two-phase flow rate. Hence, the data are gathered in 14 groups, each graph showing the quality x as a

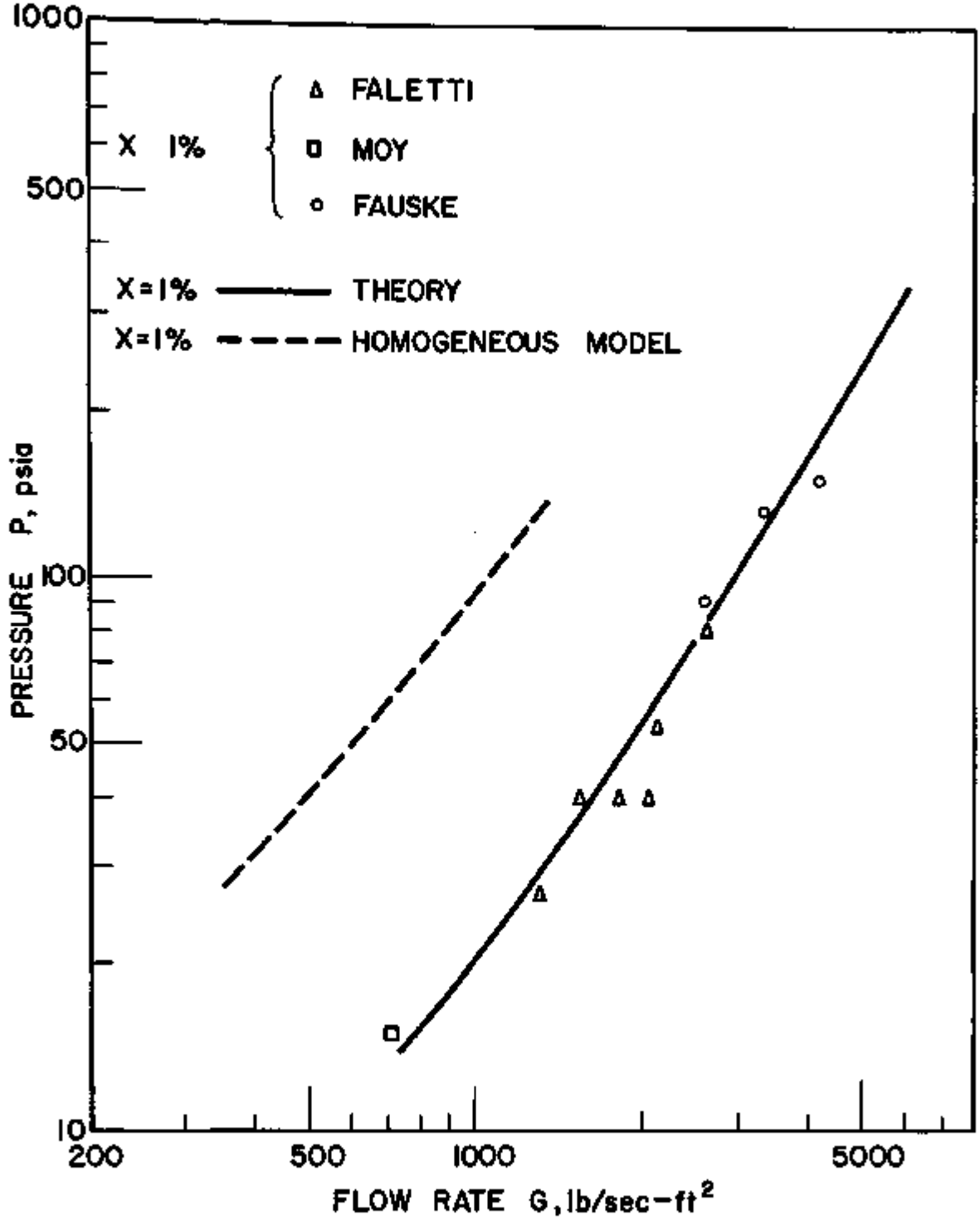

Figure 29. Comparison between the Data and the Author's Theory

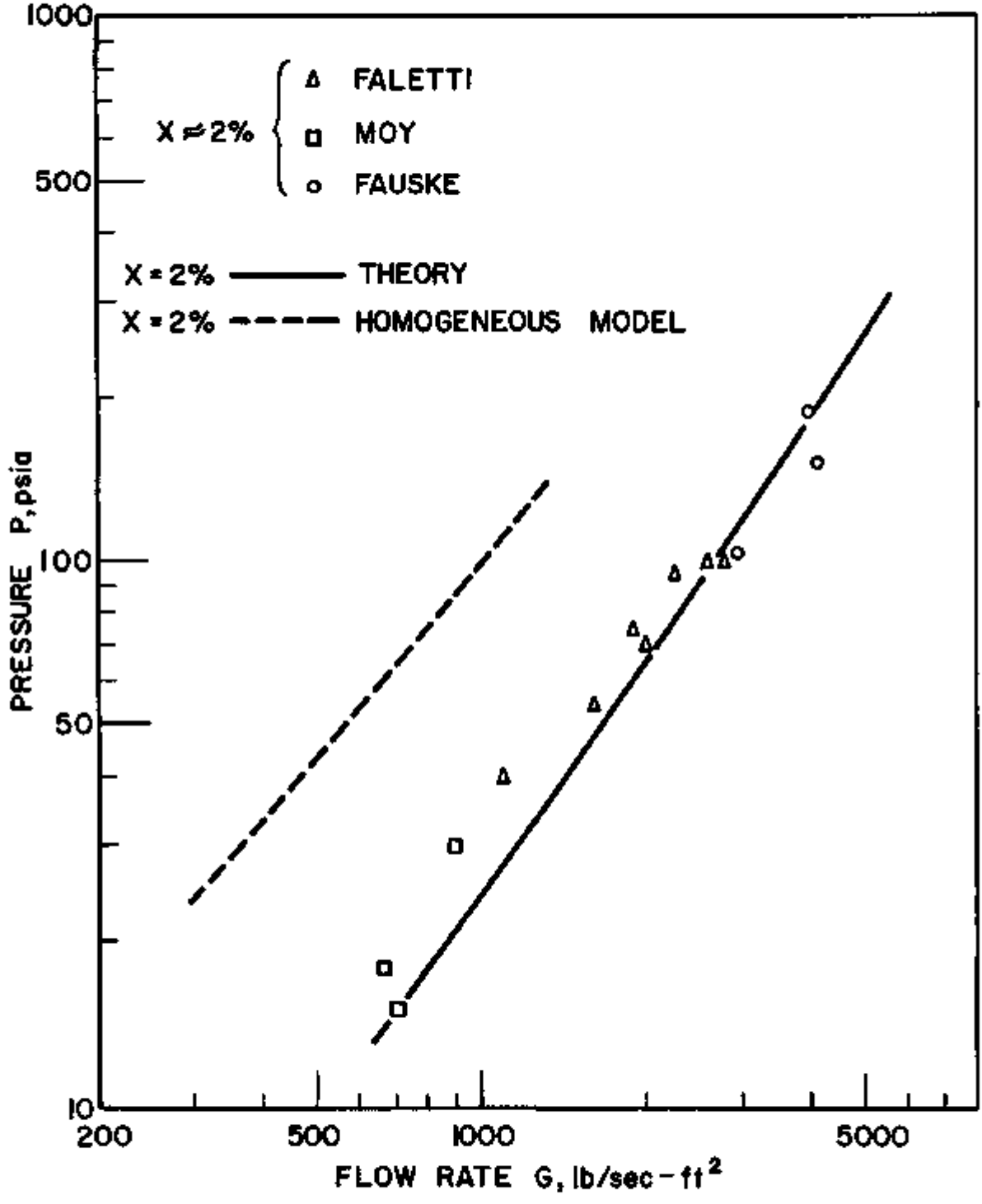

Figure 30. Comparison between the Data and the Author's Theory

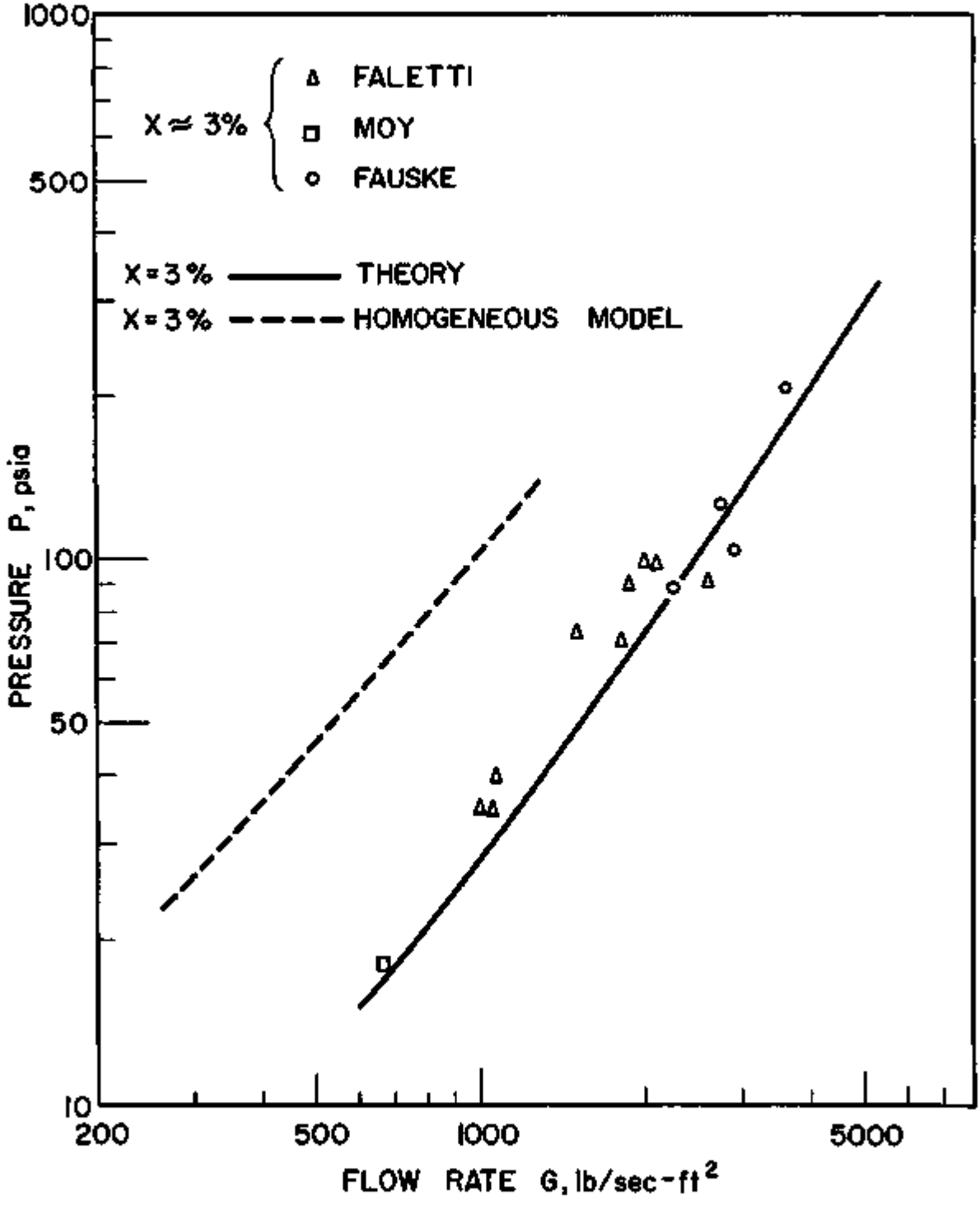

Figure 31. Comparison between the Data and the Author's Theory

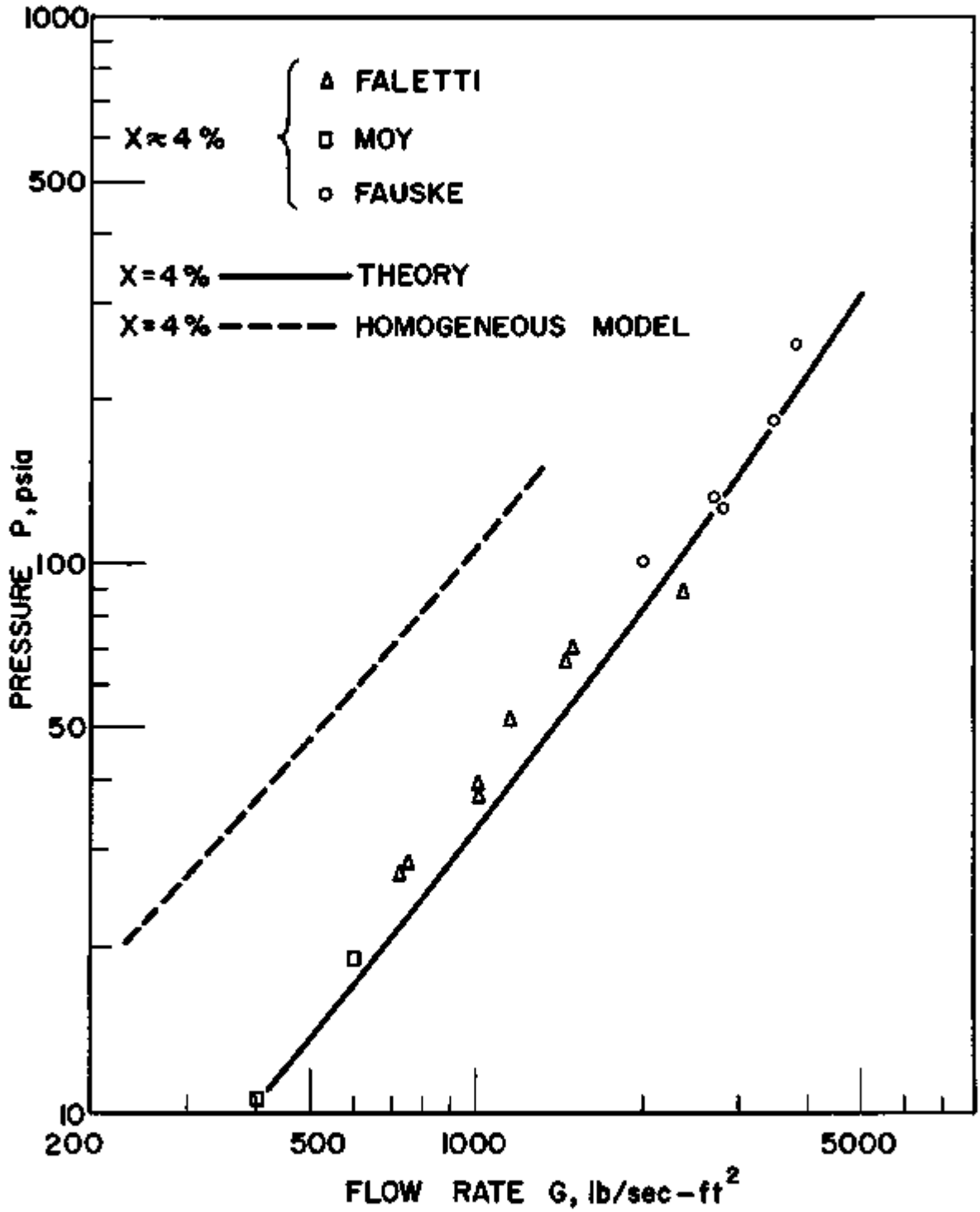

Figure 32. Comparison between the Data and the Author's Theory

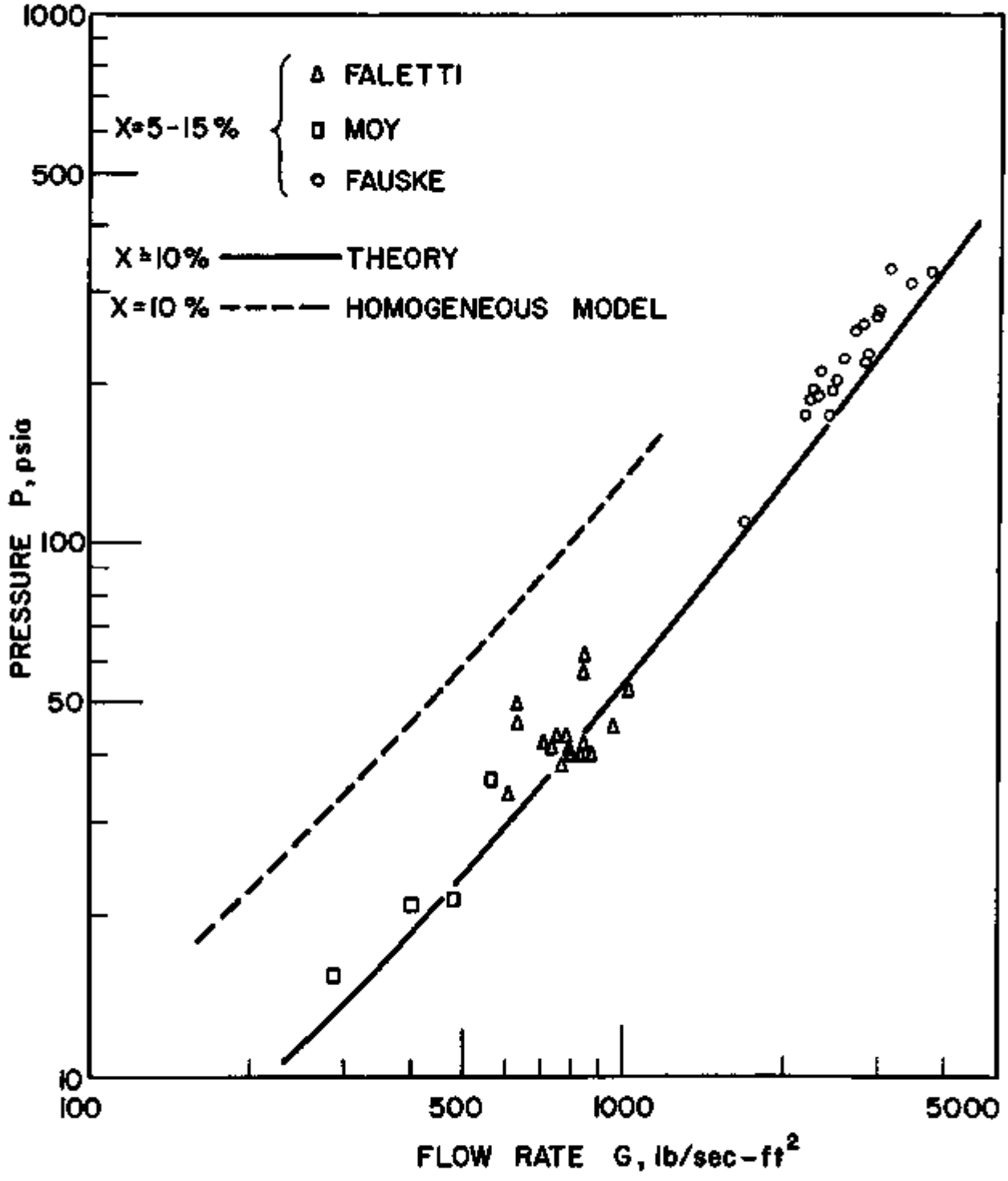

Figure 33. Comparison between the Data and the Author's Theory

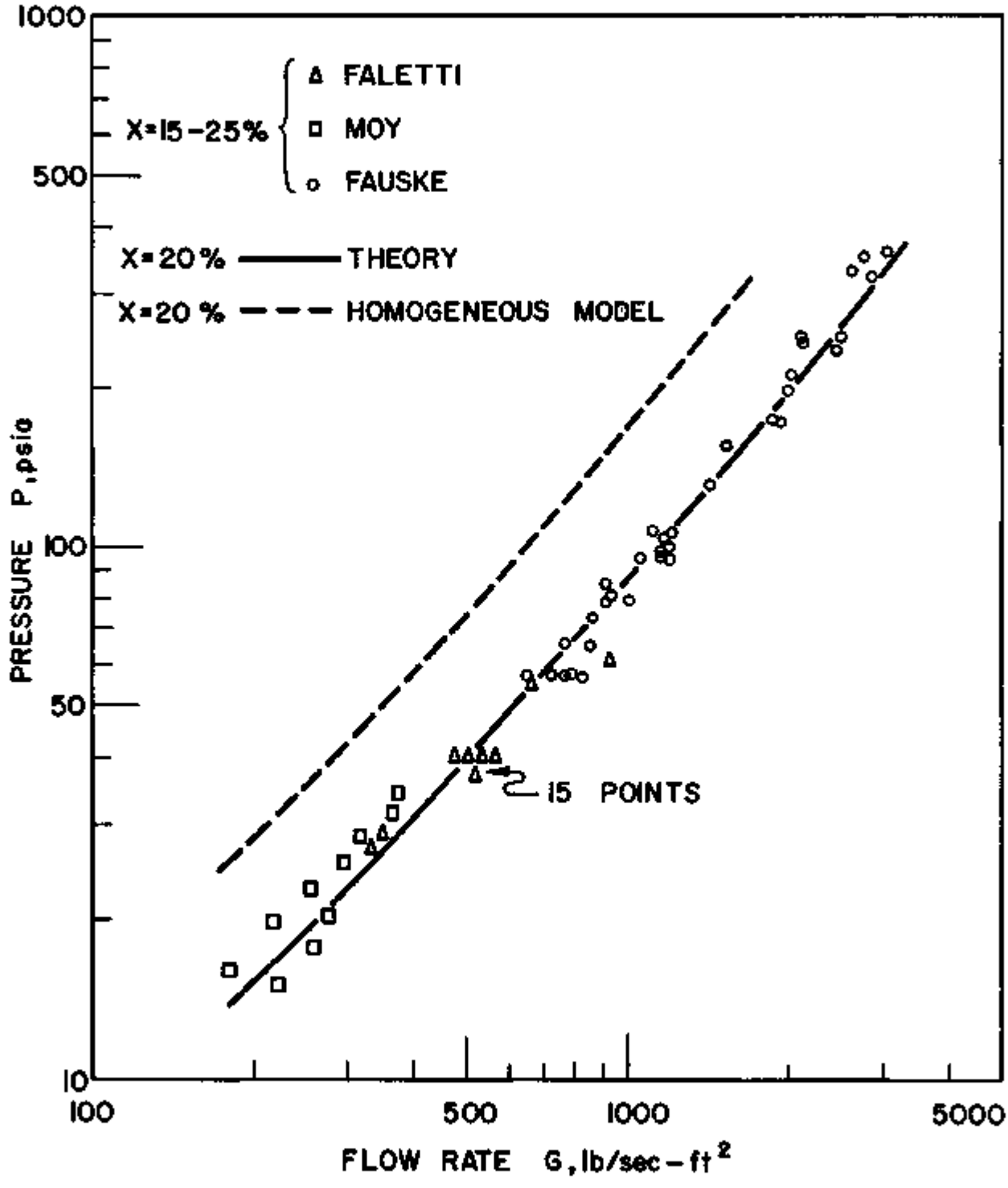

Figure 34. Comparison between the Data and the Author's Theory

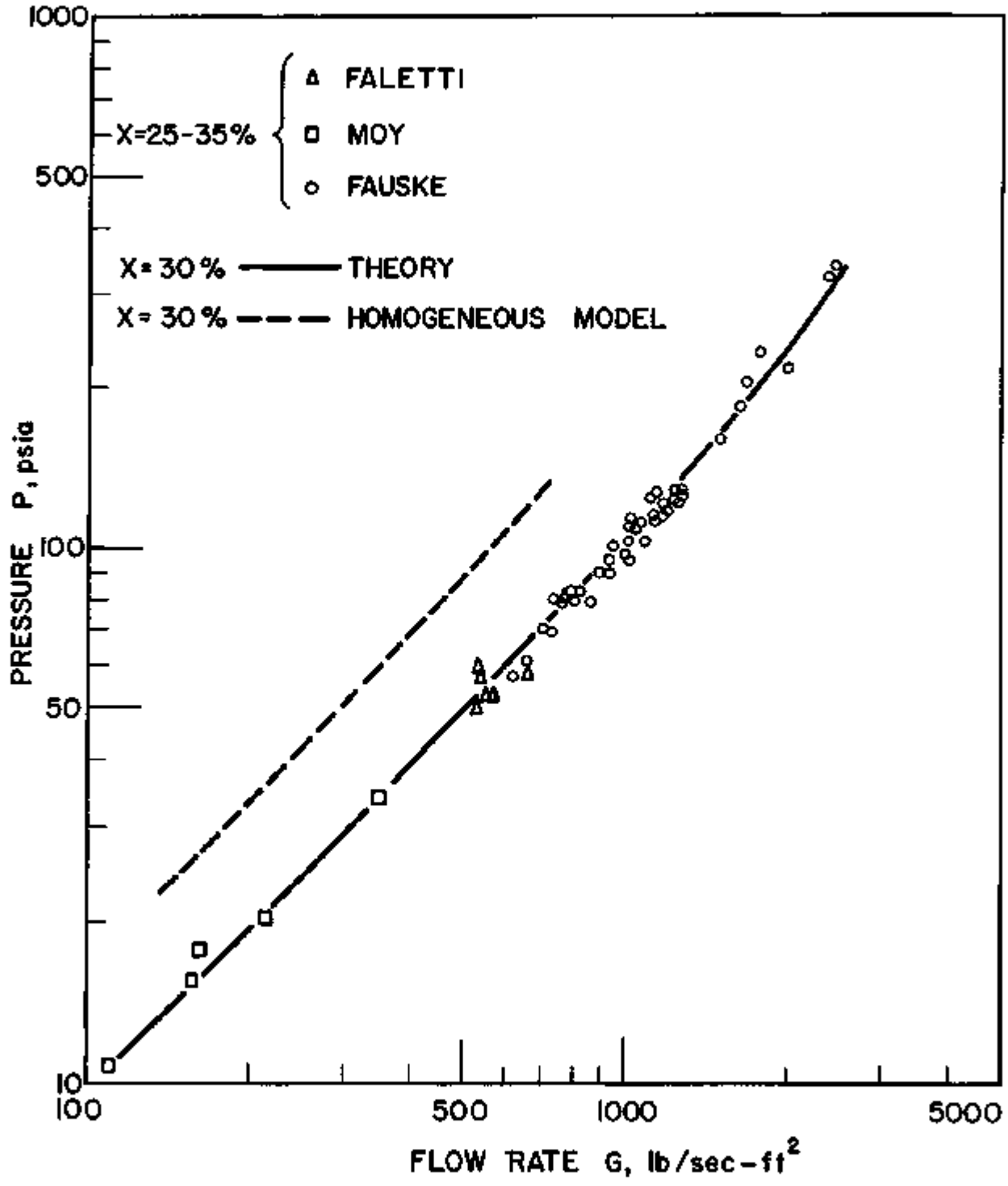

Figure 35. Comparison between the Data and the Author's Theory

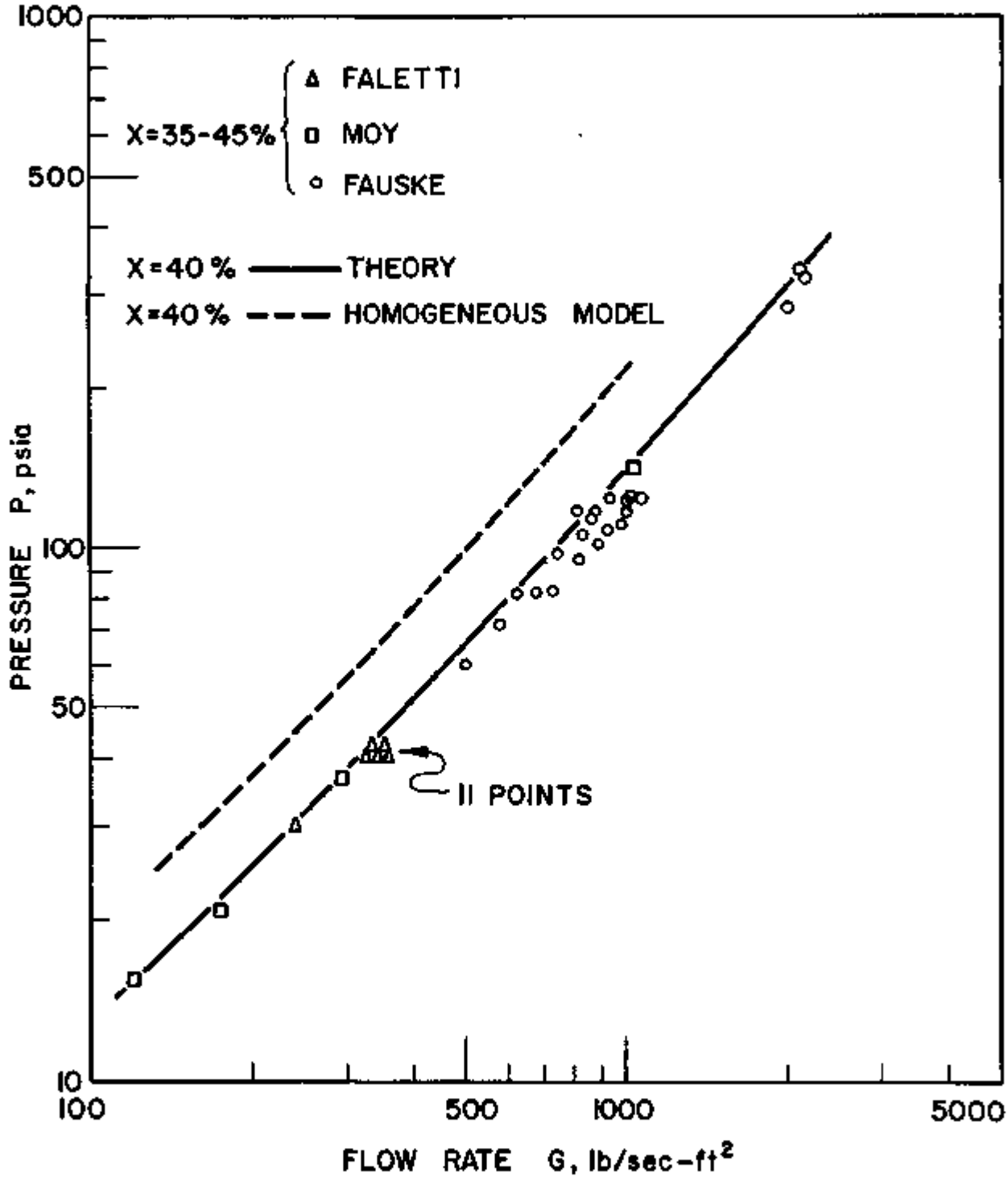

Figure 36. Comparison between the Data and the Author's Theory

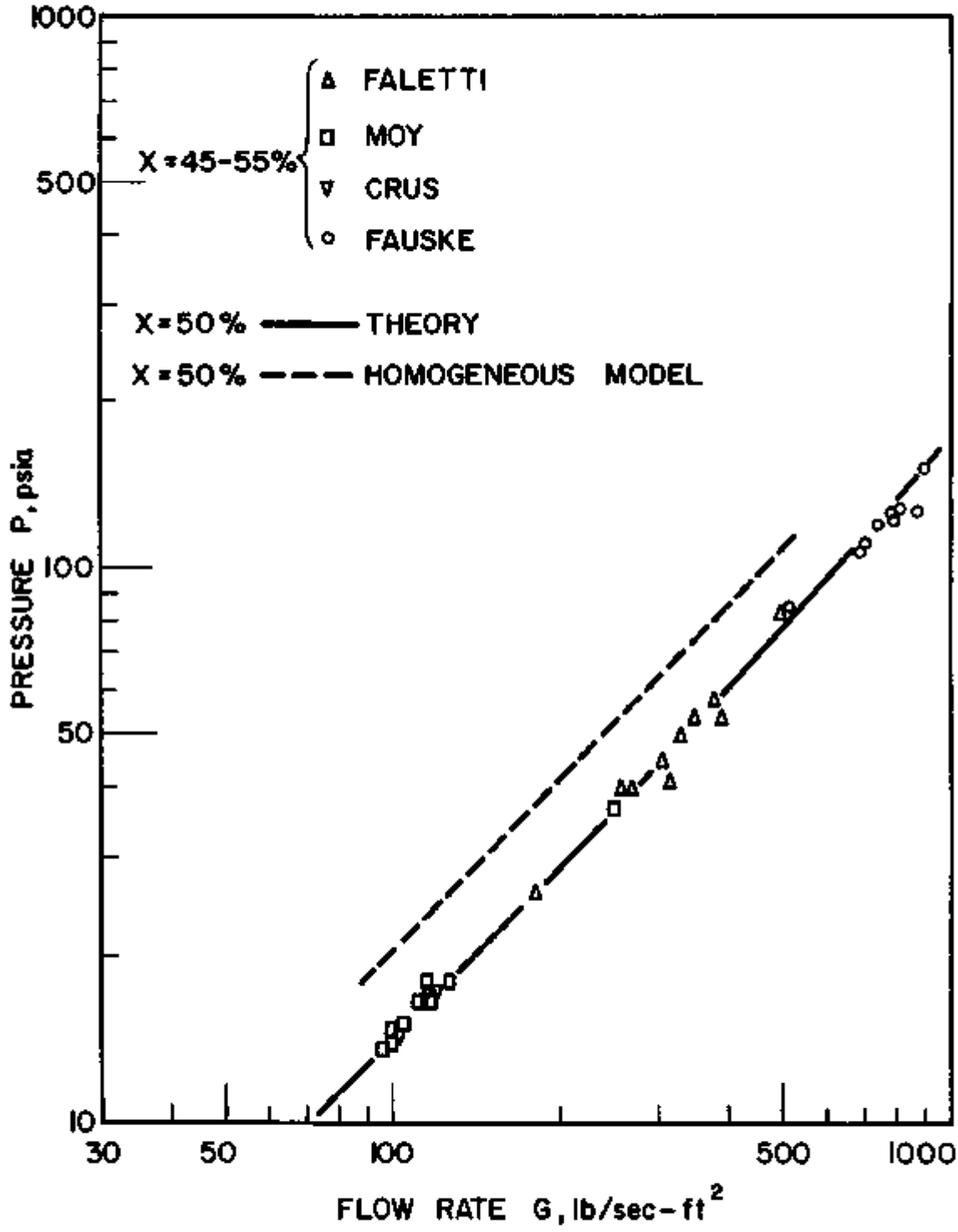

Figure 37. Comparison between the Data and the Author's Theory

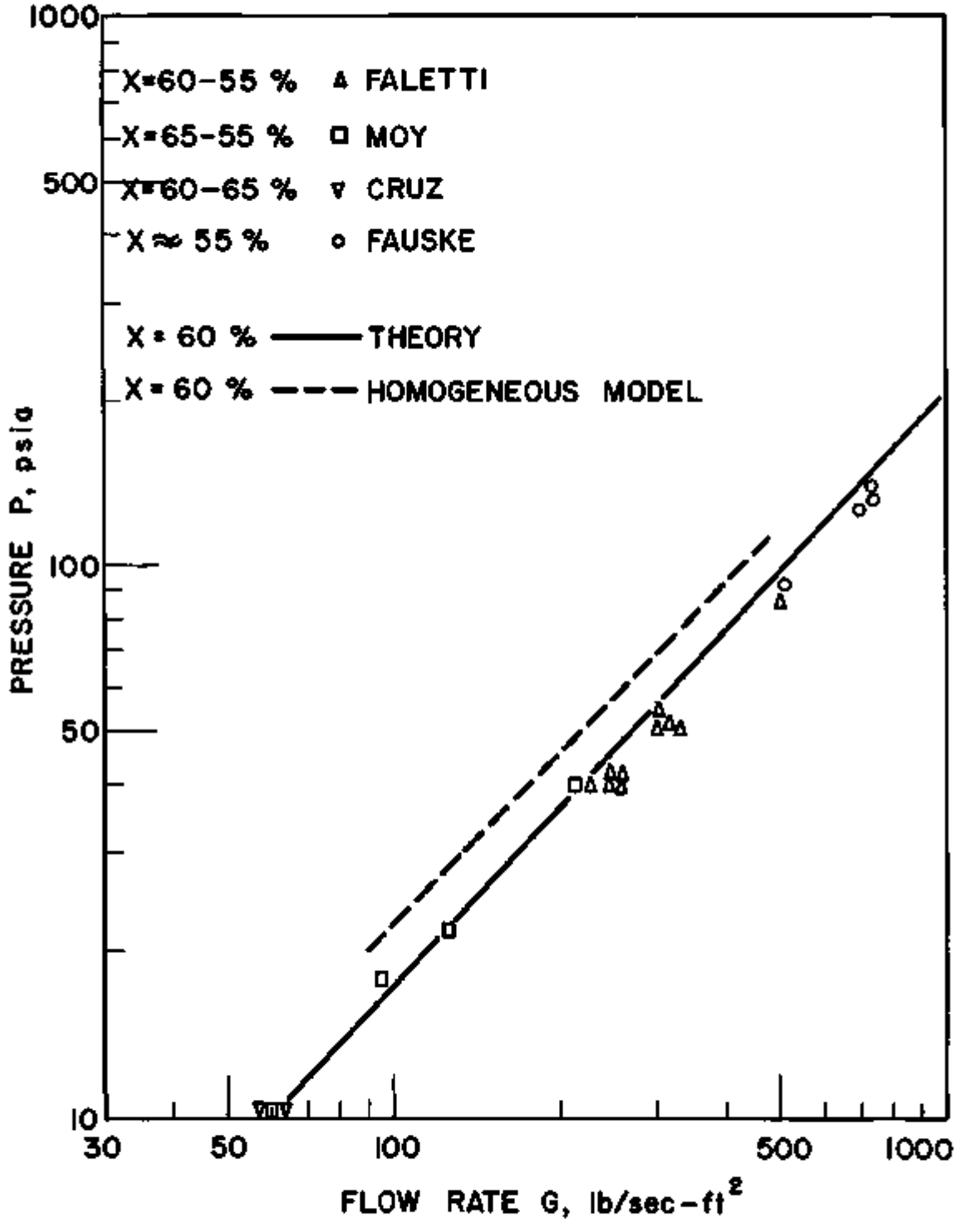

Figure 38. Comparison between the Data and the Author's Theory

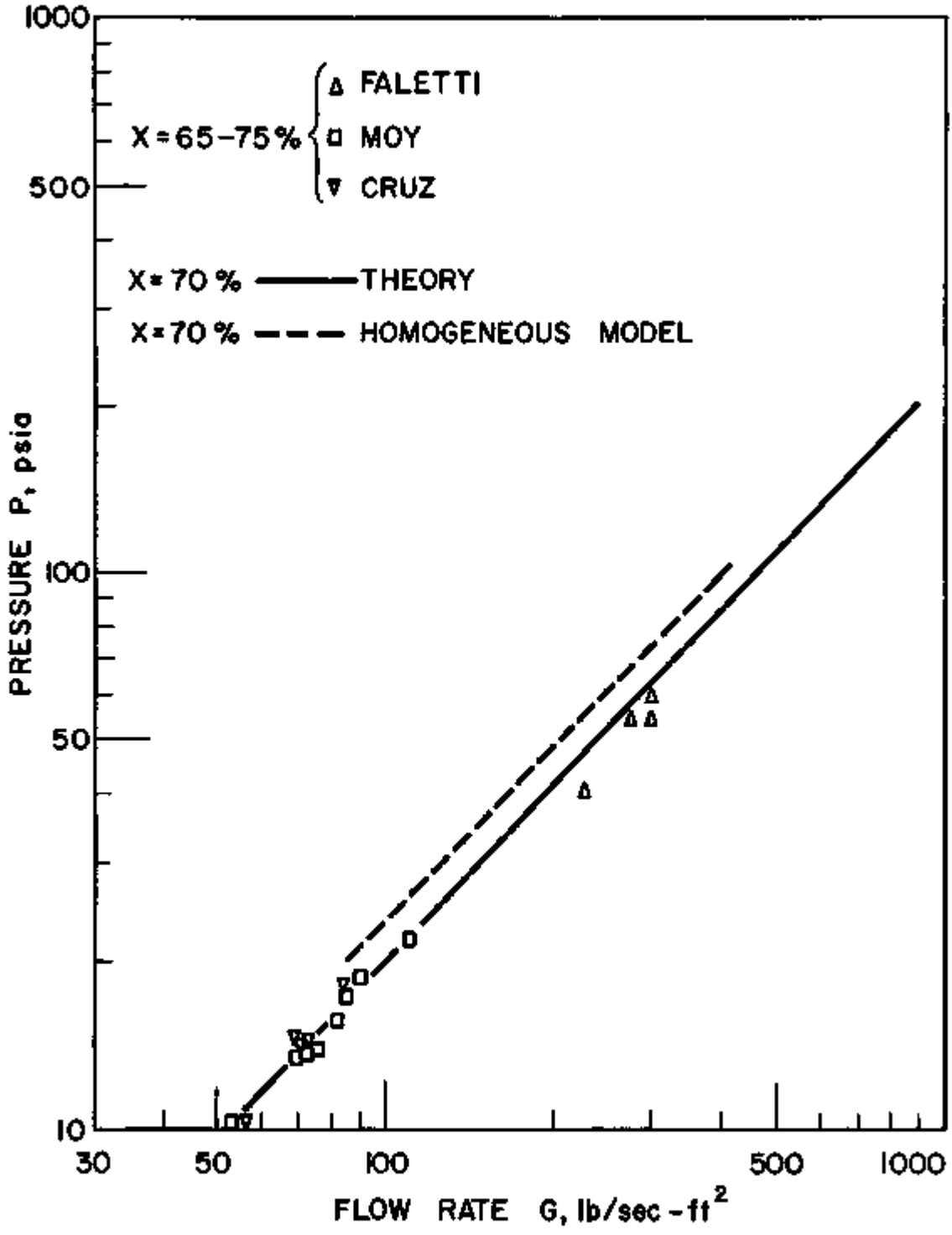

Figure 39. Comparison between the Data and the Author's Theory

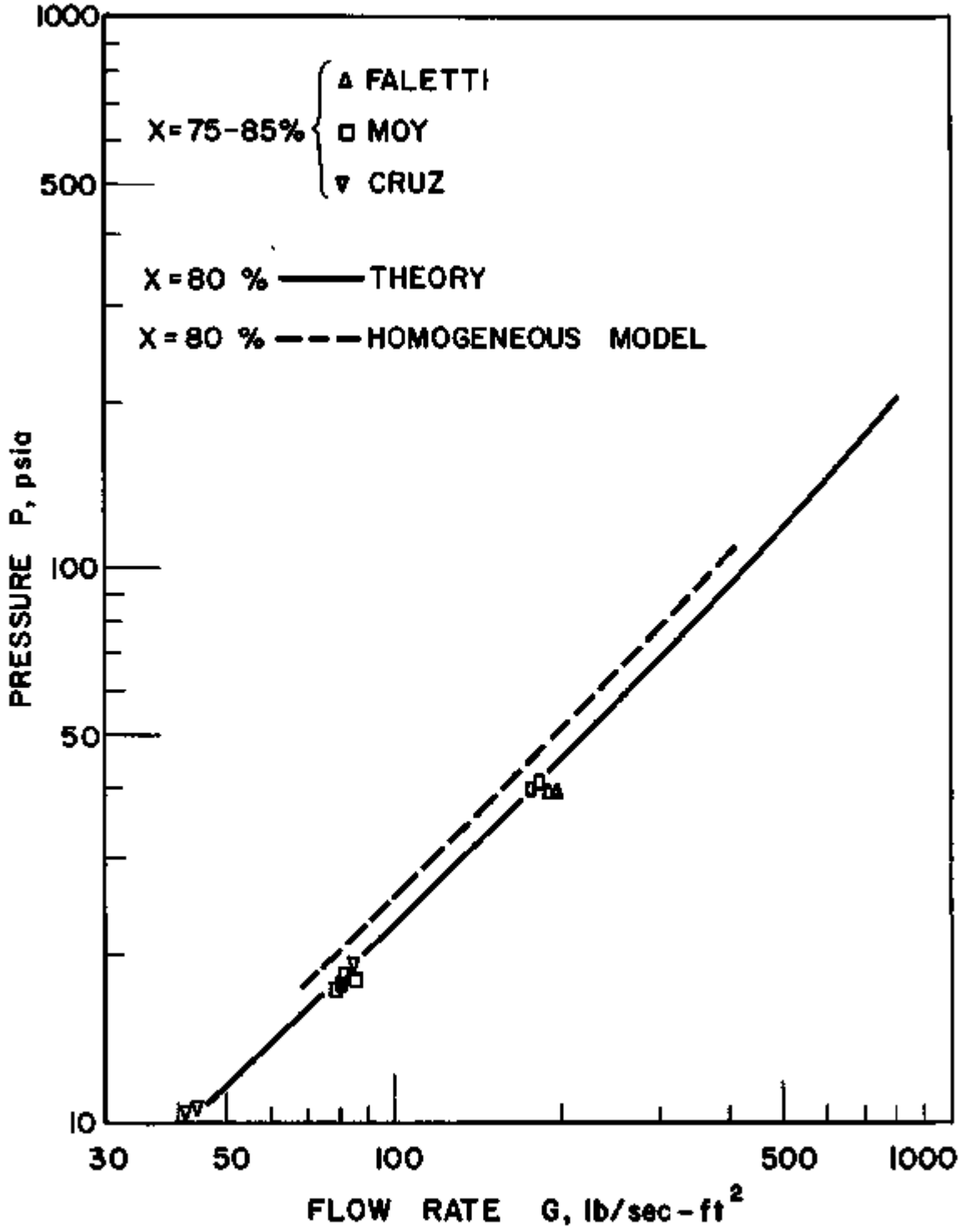

Figure 40. Comparison between the Data and the Author's Theory

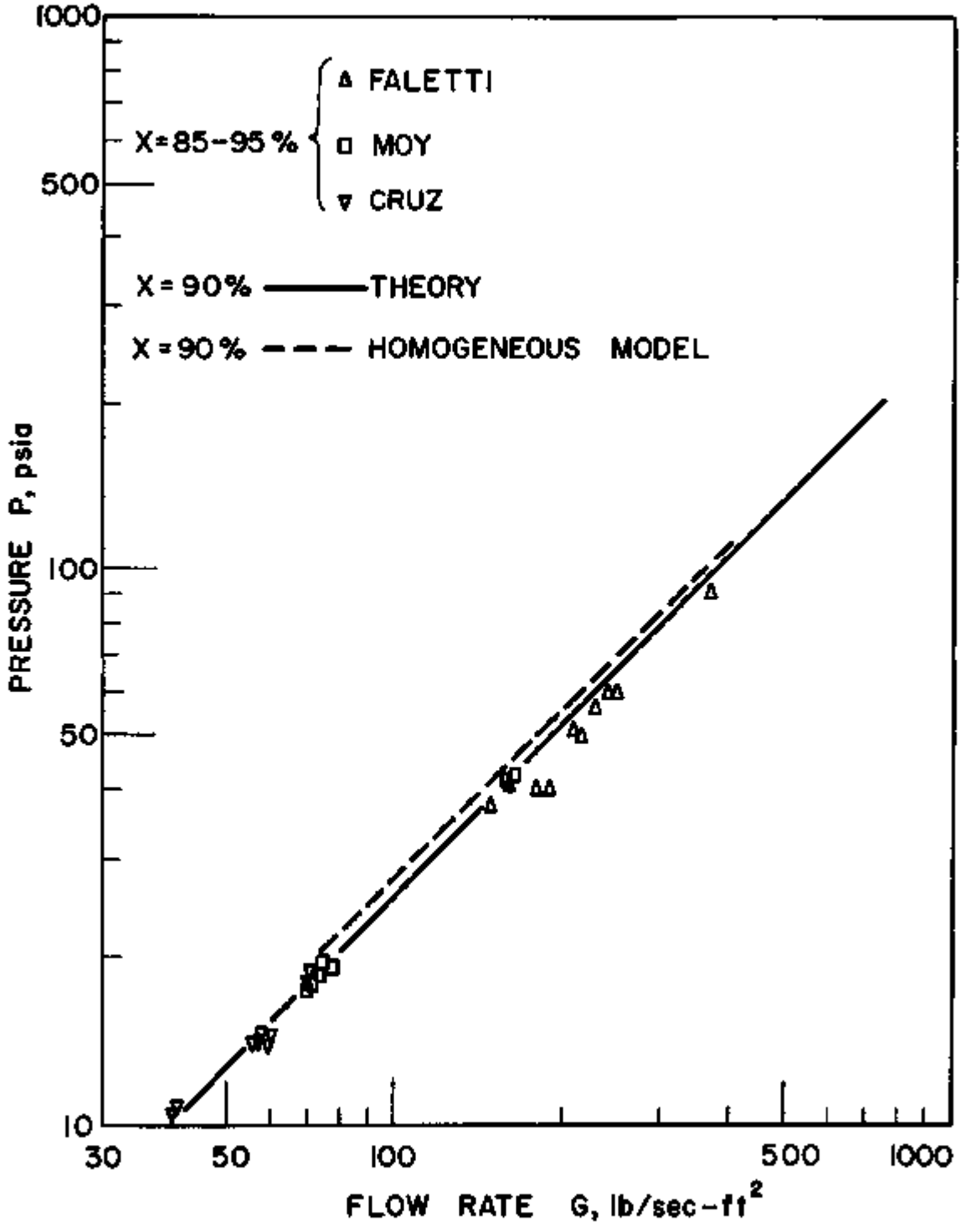

Figure 41. Comparison between the Data and the Author's Theory

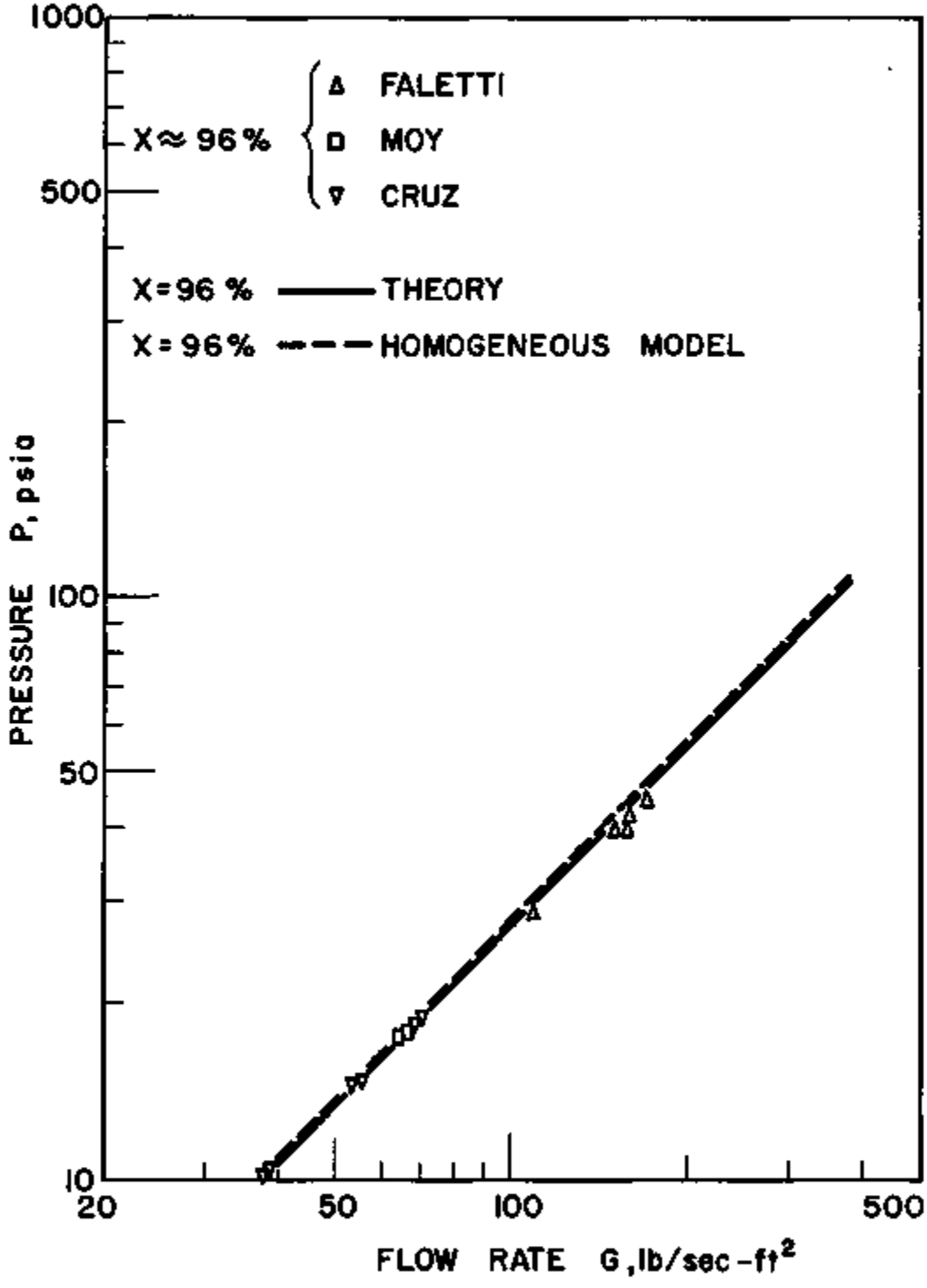

Figure 42. Comparison between the Data and the Author's Theory

parameter for different ranges, these being 1, 2, 3, 4, 5-15, 15-25, 25-35, 35-45, 45-55, 55-65, 65-75, 75-85, 85-95, and 96%. The reasoning for grouping the data in the above-mentioned quality ranges should be quite clear from an analysis of the obtained data. At low qualities (1-5%), the critical flow rates are very sensitive to changes in quality, whereas as the quality becomes larger, the corresponding changes in the critical flow rates are smaller. It should be pointed out here that the qualities reported are based on the homogeneous flow model, at least as regards the kinetic-energy term. These qualities were found to be numerically the same or within about 0.01 below the values calculated when slip was included. An appreciation of the labor saved by doing so and the estimation of the error involved are illustrated in Appendix F.

In the work of Cruz,[27] which represents one of the first nonclassified studies undertaken explicitly to measure critical flows of steam-water mixtures over a wide range of quality, the data were plotted in the following way. The ordinate gave the per cent deviation between observed and "theoretical" critical discharges, defined as $(G_{obs} - G_{TH})\,100/G_{obs}$, and the abcissa represented the steam fraction, quality, ranging from 1 to 100% on the same plot. Theoretical critical discharges were calculated from the socalled "Homogeneous Flow Model," which, previous to this work, was the only theoretical model existing. Later, Moy[77] extended Cruz's work and presented his experimental data by adopting Cruz's procedure. One of the most recentworks on two-phase critical flow is presented by Faletti.[33] This investigator also adopted Cruz's method in presenting the data, although in a little-changed form. Faletti plotted the ratio of the observed mass velocity to the theoretical mass velocity, G_{obs}/G_{TH}, versus the quality x, where x ranged from 1 to 100%. He points out in his work that Cruz's correlating ratio, $(G_{obs} - G_{TH})/G_{obs}$, has the advantage of always lying between zero and unity if G_{obs}/G_{TH} is greater than unity, since

$$\frac{G_{obs} - G_{TH}}{G_{obs}} = 1 - \frac{G_{TH}}{G_{obs}} \quad .$$

Faletti further points out that this technique tends to obscure the amount of scatter by reducing it at low qualities and magnifying it at high qualities.

Therefore, this investigator made use of the G_{obs}/G_{TH} ratio in presenting the data rather than Cruz's $(G_{obs} - G_{TH})/(G_{obs})$. In this fashion, the above-mentioned investigators found the deviation from the flow rates predicted by the "Homogeneous Flow Model" and observed values, and used this as a correlation curve. The presentation of the critical-flow data in this form is questionable. First of all, the data became condensed, and little or no pressure dependency was discernible. Secondly, to correlate the data against a model which is not correct gives no additional insight on the critical phenomenon. The "correlation curves" as obtained by these investigators could be in serious error if applied to pressures higher than 100 psia (which is the highest critical pressure investigated previous to this work).

This method of presentation chosen by the writer is believed to be a detailed accounting. The data are plotted with quality as parameter, and the full pressure dependency can be observed over all ranges of qualities. Furthermore, by representing the data in this manner, as will be seen later, a more critical comparison is obtained between the experimental data and the theory developed for critical two-phase flow. Hence, previous critical-flow data[33,47] were replotted and compared with the writer's own data and theory.

6.4. Effect of Pipe Geometry on Critical Flow

As mentioned before, the purpose of using a rather small pipe size, such as the $\frac{1}{8}$-in.-ID pipe, in this work was to obtain as high a critical pressure at the outlet as possible with the high-pressure equipment. Before taking the data on TSIV, some investigators believed that the critical flow rate obtained could be predicted by the "Homogeneous Flow Model"; however, by an analysis of graphs 29 through 42 in which the data are plotted, no significant difference is noticeable in the critical flow rates obtained by TSII and TSIV. Hence, when plotting these data, no separation was made

to indicate data from TSII or TSIV. Since these two test sections had different lengths, one can also conclude that the length of the pipe causes no changes in the critical flow conditions. These observations are in agreement with previous work on the subject. Isbin, Cruz, and Moy[47] state in their work that the critical flow rate is independent of the pipe sizes for the conditions tested. The pipe sizes investigated were 1, $\frac{3}{4}$, $\frac{1}{2}$, and $\frac{1}{4}$-in. full bore and $1\frac{1}{4}$ and $3/4$-$\frac{1}{4}$-in. annulus. For the $\frac{1}{4}$-in. full bore, a pressure range from 3.9 to 43 psia was covered. Faletti,[33] who studied the critical flow of steam-water mixtures in concentric annuli having center rods of 0.188- and 0.375-in.-OD and 0.574-in.-ID test section, made the following statement: "For test sections longer than nine inches, interchanging a three-sixteenth inch center rod for a three-eighth inch center rod had no effect on the critical mass velocity. Therefore, it seems likely that the correlation will be applicable to small bore pipes near one-half inch in diameter, and, furthermore, that critical mass velocities in full bore pipes may not be a strong function of diameter." Isbin, Cruz, Moy, and Faletti's data are included in graphs 29 through 42, and what has been stated above can indeed be verified from these plots. These significant observations observed previously and supported in this work are in complete agreement with the theory presented. As one can see from Eq. (5.11-8), the critical flow rate is only a function of pressure P and quality x, with no dependency upon the geometry of the system. Furthermore, these observations support the theoretical relations obtained for void fraction and slip ratio under critical flow conditions, since these are also independent of diameter and length of the pipe. However, for ordinary two-phase flow, experimental data[67] indicate that void fraction and slip ratio may depend upon the size of the system.

6.5. Comparison of Results with Other Investigators

As already mentioned, the first most thorough study of critical flow in pipes was carried out by Cruz[27] and Moy[77] under the guidance of Isbin. The results of this study have been summarized.[47] Critical

pressures ranging from 4 to 43 psia were examined, with qualities ranging from 1 to 100%. The next extensive and most recent work on critical two-phase flow of steam-water mixtures in pipe was done by Faletti.[33] Critical throat pressures ranged from 26 to 100 psia, and qualities ranged from 1 to 98%. Most of the data of these investigators are plotted together with the author's own data in graphs 29 through 42. Since the writer's own critical throat pressures ranged from 50 to 360 psia, a direct comparison of the results is possible only with Faletti's data in the range from 50 to 100 psia. This comparison can be seen in graphs 29 through 38, and good agreement is obtained for all qualities available in this pressure range, considering the scattering in the data. The scatter found in these graphs, both in the data of previous investigators and of the author, is not excessive when one considers the unsteadiness of the upstream conditions and takes into account the size of the pressure fluctuations, which are characteristic for such a two-phase flow system. As for the data above 100 psia, which includes the major part of the data in this work, no extensive comparisons can be given. However, it can be said, from analysis of the graphs 29 through 42, that the results obtained above 100 psia show the same trends and indications as the data obtained below 100 psia. This will be clearly seen later when the comparison of the data with the theory is presented.

Several other investigations have been published, which partly have been devoted to two-phase critical flow studies. These include the works of Benjamin and Miller,[13] Bottomley,[20] Burnell,[23] Linning,[66] Hoopes,[45] and Agostinelli and Salemann.[1]

Benjamin, Miller, and Bottomley studied the flow of initially saturated water flowing through 4-in.-diameter pipes. Cruz, Moy, and Faletti state in their works that the measured critical flow rates of these investigators fall considerably below their own, and, hence, it can also be concluded that the data of Benjamin and Miller, and Bottomley are not in agreement with the results of the writer. This could be caused by the large bore size; however, it should be mentioned that these investigators

used thermocouple wells inserted into the flowing stream to get the temperature profile, and, by assuming thermodynamic equilibrium, the pressure profile was obtained. It seems plausible that they may have missed the steep drop in pressure at the exit and therefore have made estimates of the critical pressure which are too high; hence, the flow rates are correspondingly low.

Burnell's critical-flow data, obtained with pipes of diameters between half inch and one inch and a half, were compared by Cruz, Moy, and Faletti with their own data and found to agree satisfactorily; hence, the same can be said to be the case for the writer's data.

Faletti further showed in his work that the experimental data of Linning fall well below his own data and, consequently, below the writer's data. This can probably be explained by the fact that Linning used temperature measurements to obtain temperature profiles. Then, by use of steam tables and assuming no metastability, he was able to convert these profiles to pressure profiles. The possibility that the axial flow of heat gave him erroneous, large values of the exit temperature, and hence of pressure, cannot be dismissed.

The observations of Hoopes[45] that no sign of a "sonic jump" or critical pressure was observed at flow rates up to 4 times the theoretical (homogeneous theory) could be in accord with the conclusions of this work. Since his qualities ranged from 2.6 to 34 percent, it could be possible that the large flow rates he speaks of are at the lower qualities where, indeed, G_{obs}/G_{TH} does approach a value of 4. However, no comparison can be made because his experimental data were not tabulated.

Agostinelli and Salemann[1] studied the flow of initially saturated water through fine annular clearances (diametral clearances of 0.006-0.017 in.). It shall be mentioned that these investigators obtained flow rates below or equal to the values predicted by the homogeneous theory and hence do not agree with the writer's observations. The reasons for this can be pointed out as follows: (1) With the fine clearances used,

the chances for a homogeneous flow pattern to develop is possible. (2) It appears that they took their critical pressures to be the pressure at which the flow no longer increased. (3) Their test sections did not have pressure taps at the throat. They made use of three taps along the test section and one in the chamber just downstream of the throat. In the event that they extrapolated the lowest pressure profile to the exit, they could well be overestimating the pressure at the throat, as their last tap was many equivalent diameters upstream of the exit.

6.6. Comparison between Observed Data and Theory

So far certain important indications about the critical phenomenon have arisen from the developed theory and have been compared with experimental observations; in all cases they have been verified satisfactorily. The next step, therefore, is to compare the complete theory with the experimental data, not only taken by the writer, but also including work of previous investigators. Therefore, the theoretical critical flow rates as calculated from Eq. (5.11-8) are plotted in graphs 29 through 42 in the same manner as the experimental data is presented. This is also done for the flow rates predicted by Eq. (5.4-3), corresponding to the "Homogeneous Flow Model" (dotted line in the graphs). As must appear clear, this comparison of experimental data and theory can be said to be rather decisive, since each quality interval from 1 to 100% from the three major investigations done on the subject in the past, in addition to the author's own data, are compared. From these graphs it can be seen that the "Homogeneous Flow Model" does not predict the experimental results in any quality range except when one approaches a quality of 100%, which is expected, since this model describes single-phase flow satisfactorily.

Earlier investigators, as mentioned before in this work, have verified that this model is invalid for pressures up to 100 psia, and it has here been proved to be invalid for pressures as high as 360 psia, for all qualities. Hence, one or more assumptions in this model can be said to be incorrect. The major assumptions in this model are as follows:

1. homogeneous flow (no slip occurs);
2. thermodynamic equilibrium; and
3. isentropic expansion.

Graphs 29 through 42 indicate that the author's theory predicts the critical-flow conditions rather well in all ranges of qualities. Most noticeable is the extremely good comparison between theory and experimental data in the quality range from 1 to 5%, in which all other semi-empirical models have failed to predict the critical-flow rates. It is therefore logical to compare the assumptions in this theory with the previous one. These are as follows:

1. annular flow (slip occurs);
2. thermodynamic equilibrium; and
3. isenthalpic expansion.

As for assumption number 3, little difference is obtained in both theories, as discussed earlier in this paper, by using either restriction in calculating $\frac{dv}{dP}$ and, hence, the critical flow rate. Certainly, assumption number 1 for the "Homogeneous Flow Model" does not hold. Although slip has not in fact been measured at critical flow, the extensive background data on slip measurements in two-phase flow are sufficiently impressive to conclude that slip exists during critical flow. The decision regarding assumption number 2, the attainment of equilibrium, is more difficult to justify. Within the author's experiences, it appears reasonable to assume that the thermodynamic equilibrium is approached. The final justification is based upon the results obtained using these premises.

Furthermore, since the theory presented here predicts the experimental data for all pressures and qualities so far investigated, without including any parameters based on experiments, it is the author's opinion that this theory can be applied to higher pressures without any serious errors. There exist no reasons that indicate that the assumptions in the theory, tested up to 360 psia, should not be valid for higher pressures.

Hence, graph 22, representing the author's theory from atmospheric up to the critical point, 3206 psia, should be valuable in designing modern nuclear reactors, where, in the event of rupture in cooling system, etc., this must be taken into account in the design method. These reactors may operate anywhere from 1000 to 2000 psia, and a sudden rupture in such a system will eventually cause critical flow to occur.

Faletti,[33] who finished his studies on two-phase critical flow in 1959, compared his results, which have been shown to agree favorably with the author's, with existing semi-empirical models, but in all cases fair or poor agreements were obtained in the quality region from 20 to 100% and rather poor agreement in the quality range from 1 to 20%. These included comparisons with Linning's Method,[66] Modified Linning Model,[47] Stuart's Model,[33] and Firey's Model.[33] The two first-mentioned models, which are the most promising ones, are hampered by the lack of void fraction or slip data for high-velocity flow, since no theoretical relationship was developed.

Stuart developed a curve for predicting critical pressures of boiling water flowing through pipes from a knowledge of the saturation pressure. If this curve is correct, only one critical pressure would be possible for a given saturation pressure, which certainly is not true.

Firey's approach to the prediction of the critical mass velocity is to assume that the vapor travels at the speed of sound for vapor alone and that the liquid travels at somewhat lower velocity. This model does not predict the experimental data; hence, it is reasonable to state that his assumptions are wrong. This is in accordance with the conclusions of this work, namely, that no true sonic choking occurs and, therefore, the velocity of the vapor phase is less than that of sound.

Hence, it was not felt necessary to include these semi-empirical models in the comparison of results and theories in this work.

CHAPTER VII

THE MECHANISM OF CRITICAL TWO-PHASE PIPE FLOW

The question still remains to be answered as to whether or not critical flow occurs for two-phase flow with the same implications that it carries for one-phase flow. In the following pages some new ideas will be put forth in an attempt to answer this question by help of the theories presented in Chapter V and as supported by experimental observations.

Consider a flow system such as a pipe attached to a constant-pressure source on one end and to a large receiver on the other. Further, consider a compressible fluid alone. When the downstream pressure is reduced below that of the upstream end, flow begins and a pressure gradient is set up in the pipe. Dropping the downstream pressure further will result in an increased flow rate until a maximum flow rate is obtained. When this flow rate is reached, further reduction of the receiver pressure will no longer affect the flow rate. For a single-phase medium the equation giving this critical velocity is identical with the equation for the velocity of sound in the same medium. For a single-phase system, it can be said that the maximum flow and critical pressure are reached when the velocity of the stream is equal to that of a rarefaction wave in the same medium. Because of this, the downstream pressure can no longer be transmitted up into the pipe; therefore, the critical throat pressure for single-phase flow is independent of all pressures below the back pressure for which the maximum flow is first obtained.

Since one-phase critical flow can be explained from the fact that sonic velocity is sustained at the throat of the conduit, it becomes necessary to examine the theory developed for two-phase critical flow to obtain some information about the phase velocities. This is also of particular interest since measurements of void fraction have not been carried out under critical flow conditions, insofar as the author knows. As already noted in Chapter V, the absolute velocities calculated from the theory developed in

this work are below sonic velocities, except when the quality approaches 1.0. In Figure 24, the linear vapor velocity as calculated from the procedure outlined in Chapter V is plotted versus quality with pressure P as parameter. Figure 24 shows that no sonic velocities occur for two-phase critical flow of steam-water mixtures, if the assumed model is correct.

Therefore, one cannot adopt the method of sonic velocities to explain the maximum flows of steam-water mixtures.

Therefore, again consider the flow system as mentioned earlier; however, this time have a two-phase mixture coming from the constant-pressure source with a quality x anywhere between zero and one. Again, when the downstream pressure is reduced below that of the upstream end, flow begins and a pressure gradient is set up in the pipe, this being determined by the momentum and frictional pressure drops which are restricted by the void fraction or the slip ratio. Further drop in the downstream pressure will result in a steeper pressure gradient and increased flow rate until a maximum pressure gradient or flow rate is obtained. During the period before the maximum flow rate is obtained, the void fraction is changing and the slip ratio k is increasing. However, when a value $k = (v_g/v_l)^{1/2}$ is reached, the sum of the momentum and the frictional pressure losses have attained its maximum possible value and, hence, the steepest pressure gradient is achieved. When the kinetic-energy dissipation per unit volume in each fluid is equal, the flow system can be said to be stable, and critical two-phase flow is, indeed, sustained. At this point the velocities of the two phases have also obtained their maximum values; however, they are less than the sonic velocities in the same two media and differ, therefore, radically from single-phase flow. In other words, the extra freedom available compared with a single-phase compressible system, namely, the slip ratio, restricts the flow of the multiphase system in advance. Hence, the individual fluid phases cannot be accelerated sufficiently high to accommodate velocities experienced in single-phase flow. The p-v path for two-phase

critical flow is presumably dictated by the flow history of the fluid (void fraction), whereas in single-phase sonic flow the infinitesimal pressure pulse is assumed to be transmitted isentropically. At high frequencies the latter will always be greater than the former. Consequently, a pressure pulse will be propagated upstream, and no choking effect can exist in the same sense as for the flow of a single-phase fluid through a pipe.

The next question that will arise in the reader's mind is what will happen when the back pressure is reduced below the value where the maximum flow is first obtained. This pressure change will, indeed, be felt upstream, since the impulses caused by this pressure change are travelling with a greater velocity than those of the two phases leaving the exit of the pipe. However, the changes in the upstream conditions, like void fraction, slip ratio, etc., will be highly unstable, since any decrease or increase in the slip ratio will always result in a decrease of the absolute value of the pressure gradient, which cannot be sustained. If maximum flow occurs and there is a change in downstream conditions, it will not be possible for a steady-state flow to exist. After a transient period of readjustment, a steady-state condition will be established for which maximum flow does again occur. In other words, the system is only stable when the dissipated energy per unit volume is the same in each fluid phase, when no mechanical restriction exists at the exit of the pipe. Therefore, changes in downstream pressure, no matter how small, or how small the back pressure is compared with the critical throat pressure, will always be transmitted upstream. However, if the back pressure is kept constant after the change is carried out and is smaller than the value of the back pressure that caused maximum flow, the two-phase flow system will always force itself back to the stable conditions $[k = (v_g/v_l)^{1/2}]$ and will sustain its finite maximum pressure gradient or maximum flow.

That the pressure impulses are transported upstream when changes in back pressure are carried out have, indeed, been noticed during the experimental work and by previous investigators,[33,77] but have apparently

been interpreted differently. This has led to some confusion, since these authors were not sure whether or not critical flow for one phase and two phases are carried out with the same implications. It is not possible to produce a differential pressure between the discharge plane and the receiver so large that a change of back pressure will not affect the overall axial pressure profile to some degree. Differential pressures as large as 360 psi were achieved between the end of the test section and the expansion section.

Therefore, when the experimental data were taken in this work, the back pressure was kept to as low a value as possible, such that with this pressure the attainment of the maximum pressure gradient or maximum flow rate was assured. Further, the conditions of stability at the throat do not depend only upon the upstream conditions, but also upon how invariant one can keep the back pressure. This last restriction was believed to be satisfied by operating the condenser connecting the downstream expansion section at same conditions at all times.

As a conclusion from what has been stated above, the implications for one-phase and two-phase critical flow differ significantly.

CHAPTER VIII

SUMMARY AND CONCLUSIONS

8.1. Summary

This investigation starts with a brief introduction to the various problems associated with two-phase flow and critical flow in particular.

In Chapter II, a literature survey of two-phase critical flow is presented which covers the most extensive studies carried out on this subject up to date. Void fraction, flow pattern, and pressure drop in two-phase flow are also briefly discussed.

In Chapter III and IV the experimental apparatus and operating procedure are described in detail.

In Chapter V the author's theory of two-phase critical flow is presented.

In Chapter VI an analysis of the critical-flow data, including previous major investigations and extensive comparisons of theory with experimental values, are carried out.

In Chapter VII some new ideas are presented concerning the mechanism of two-phase critical flow.

Critical two-phase, steam-water flows have been measured over a range of quality from 0.01 to 0.7, total flows from 500 to 4,300 $lb/sec\text{-}ft^2$, pressures from 40 to 360 psia, pipe diameters of 0.125-, 0.269-, and 0.4825-in. inside diameter, and pipe lengths of 110 and 56 $\frac{1}{4}$ in. A theory has been developed for the two-phase critical-flow phenomenon, and extensive comparisons of predicted with experimental values show substantial agreement over the whole range of qualities and pressures.

8.2. Conclusions

1. From an analysis of the literature concerning two-phase flow, one concludes that data on critical two-phase flow over 100 psia are needed.

2. Previous to the author's theory, no theory was available that could satisfactorily predict the critical two-phase flow data of Cruz,[27] Moy,[77] and Faletti,[33] which are the three most extensive experimental investigations made on the subject.

3. Therefore, the goal of this research is believed to have been reached inasmuch as equipment was built where critical-flow data above 100 psia were obtained and a theory developed that predicts the experimental values satisfactorily.

4. Theoretical expressions for the specific volume, void fraction, and slip ratio for critical steam-water mixtures have been derived. Therefore, the first complete analytical solution was made possible for estimating the critical two-phase flow rate, including slip between the two phases.

5. The pressure profiles for runs at critical flow were all characterized by extremely steep pressure gradients near the throat; however, the pressure gradients are definitely finite and approach absolute maximum values, these depending only upon critical flow rate and quality.

6. Sonic velocities are not achieved in critical two-phase flow of steam-water mixtures. Therefore, the phenomenon of two-phase critical flow differs significantly from that of single-phase critical flow.

7. A new theory has been postulated in an effort to explain the mechanism of two-phase critical flow.

8. The geometry of the system to be investigated has apparently no effect on the critical-flow phenomenon for the diameters and lengths of pipes used in this work. The same observations have been made by previous investigators and are in agreement with the developed theory.

9. The experimental data obtained in this work compare favorably with previous investigations in the range of variables where such a comparison is possible (data below 100 psia).

10. The "Homogeneous Flow Model" is found to be unsatisfactory for all critical throat pressures and qualities examined. The assumption of no slip between the phases, therefore, can be said to be definitely incorrect.

11. Since the theory presented in this work describes the critical phenomenon satisfactorily for all pressures and qualities examined so far, and no parameters depending on experimental values are needed in the theory, Eq. (5.11-8) or graph 22 is believed by the author to be highly valuable in determining the maximum discharge of steam-water mixtures from conduits and "breaks" in vessels and pipes. The applications are subjects of considerable concern in the evaluation of nuclear reactor accidents and containment among others.

BIBLIOGRAPHY

1. Agostinelli, A., and Salemann, V., Prediction of Flashing Water Flow through Fine Annular Clearances, Trans. Am. Soc. Mech. Engrs., 80, 1138-1142 (1958).

2. Allen, C. M., Hooper, L. J., Piezometer Investigation, Trans. Am. Soc. Mech. Engrs., 54, Hyd-54-1, 1932.

3. Allen, W. F., Flow of Flashing Mixture of Water and Steam through Pipes and Valves, Trans. Am. Soc. Mech. Engrs., 73, 257 (1951).

4. Alves, G. E., Co-current Liquid-Gas Flow in a Pipe-line Contactor, Chem. Eng. Progress, 50, 449 (1954).

5. Ambrose, T. W., Literature Survey of Flow Patterns Associated with Two-phase Flow, HW-52927.

6. Anson, D., Belin, R. E., and Horlor, M. L., Dept. Sci. Ind. Research, Dominion Physical Lab., Rept. R-239, Lower Hutt, New Zealand (Feb 1955).

7. Armand, A. A., Resistance during Movement of Two-phase System Along Horizontal Pipes, Vsesoiuznyi Teplotekhnichesku Institut Izvestia, No. 1, 16-23 (1946).

8. Badger, W. L., How Long-tube Evaporator Works, Chem. and Met. Engrg., 46, 640 (1949).

9. Bailey, J. F., Metastable Flow of Saturated Water, Trans. Am. Soc. Mech. Engrs., 73, 1109 (1951).

10. Bailey, R. V., Zmola, P. C., Taylor, F. M., and Planchet, R. J., Transport of Gases through Liquid-Gas Mixtures, CF-55-12-118, (Dec 1955).

11. Baker, O., Design of Pipelines for the Simultaneous Flow of Oil and Gas, The Oil and Gas Journal (July 26, 1954).

12. Barbet, E., Evaporation in the Sugar Industry, Bull. Assoc. Chim. Sucr., 32, 111 (1914).

13. Benjamin, M. W., and Miller, J. G., The Flow of Saturated Water through Throttling Orifices, Trans. Am. Soc. Mech. Engrs., 63, 419-429 (1941).

14. Benjamin, M. W., and Miller, J. G., The Flow of a Flashing Mixture of Water and Steam through Pipes, Trans. Am. Soc. Mech. Engrs., 64, 657-669 (1942).

15. Bennett, J. A. R., Two-phase Flow in Gas-Liquid Systems, AERE-CE/R-2497.

16. Bergelin, O. P., and Gazley, C., Jr., Co-current Gas-Liquid Flow. I-Flow in Horizontal Tubes, Heat Transfer and Fluid Mechanics Institute, Berkeley, California meeting, pp. 5-18 (1949).

17. Bergelin, O. P., Kegel, P. K., Carpenter, F. G., and Gazley, C., Jr., Co-current Gas-Liquid Flow. II-Flow in Vertical Tubes, Heat Transfer and Fluid Mechanics Institute, Berkeley, California meeting, 19-28 (1949).

18. Bolstad, M. M., and Jordan, R. C., Theory and Use of the Capillary Tube Expansion Device, Refrigerating Engrg., 56, 519 (1948).

19. Bolstad, M. M., and Jordan, R. C., Theory and Use of the Capillary Tube Expansion Device. Part II-Nonadiabatic Flow, Refrigerating Engrg., 57, 577 (1949).

20. Bottomley, W. T., Flow of Boiling Water through Orifices and Pipes, Trans. North-East Coast Inst. Engrs. and Shipbuilders, 53, 65-100 (1937).

21. Bridge, T. C., How to Design the Piping for Conveying Flashing Hot Water, Heating, Piping and Air Conditioning, 69-73 (March 1949); 92-96 (April 1949); 98-100 (May 1949).

22. Brooks, C. H., and Badger, W. L., Heat Transfer Coefficients in the Boiling Section of a Long-tube, Natural-circulation Evaporator, Trans. Am. Inst. Chem. Engrs., 33, 392 (1937).

23. Burnell, J. G., Flow of Boiling Water through Nozzles, Orifices and Pipes, Engineering, 164, 572 (1947).

24. Chrisholm, D., The Flow of Steam-Water Mixtures through Sharp-edge Orifices, Eng. and Boiler House Rev., 73, 252-256 (1958).

25. Collier, J. G., A Review of Two-phase Heat Transfer (1935-1957), AERE-CE/R-2496.

26. Cook, W. H., Boiling Density in Vertical Rectangular Multichannel Sections with Natural Circulation, ANL-5621 (Nov 1956).

27. Cruz, A. J. R., Critical Discharges of Steam-Water Mixtures, M. S. Thesis, Univ. of Minnesota (1953).

28. Dengler, C. E., Heat Transfer and Pressure Drop for Evaporation of Water in a Vertical Tube, Ph.D. Thesis, Mass. Inst. Tech. (1952).

29. Dittus, F. W., and Hildebrand, A., A Method of Determining the Pressure Drop for Oil-Vapor Mixtures Flowing through Furnace Coils, Trans. Am. Soc. Mech. Engrs., 64, 185 (1942).

30. Dixon, A. D., Gamma Absorption Techniques Applied to Steam Dryness Determinations, IGR-TN/W-489 (March 1957).

31. Dodge, B. F., Chemical Engineering Thermodynamics, McGraw-Hill Company, Inc., New York and London (1944).

32. Egen, R. A., Dingee, D. A., and Chastain, J. W., Vapor Formation and Behavior in Boiling Heat Transfer, BMI-1163 (Feb 1957).

33. Faletti, D. W., Two-phase Critical Flow of Steam-Water Mixtures, Ph.D. Thesis, Univ. of Washington (1959).

34. Fauske, H. K., Analysis of Burnout in Two-phase Flow, M. S. Thesis, Univ. of Minnesota (1959).

35. Fauske, H. K., Critical Two-phase, Steam-Water Flows, 1961 Proc. Heat Transfer and Fluid Mech. Inst. Stanford University Press, Stanford, U. S. A., p. 79.

36. Galegar, W. G., Stovall, W. B., and Huntington, R. L., More Data on Two-phase Vertical Flow, Petroleum Refiner (Nov 1954).

37. Galson, A. E., Steam Slip and Burnout in Bulk Boiling Systems, GEAP-1076 (1957).

38. Goodenough, G. A., Supersaturation and the Flow of Steam, Power, 66, 466-469 (1927).

39. Gresham, W. A., Foster, P. A., Kyle, R. J., Review of the Literature on Two-phase (Gas-Liquid) Fluid Flow in Pipes, WADC-TR-55-422 (1955).

40. Hall, N. A., Thermodynamics of Fluid Flow, Prentice Hall, Inc., New York (1951).

41. Harvey, B. F., and Foust, A. S., Two-phase One-dimensional Flow Equations and Their Application to Flow in Evaporator Tubes, Heat Transfer Symposium, A.I.Ch.E., Atlantic City, N. J., 49, 289-329 (1951).

42. Haubenreich, P. N., Flow of a Flashing Mixture of Steam and Water at High Pressure, CF-55-5200 (1955). Taken from (33).

43. Haywood, R. W., Research into the Fundamentals of Boiler Circulation Theory, Inst. of Mech. Engrs. (London), Gen. Discussion on Heat Transfer, September 11-13, pp. 20-22 (1951).

44. Hodkinson, B., The Flow of Hot Water through a Nozzle, Engineering, 143, 629-630 (1937).

45. Hoopes, J. W., Jr., Pressure Drop for Flow of Steam-Water Mixtures in a Heated Annulus and through Orifices, GEH-22, 803, (1955).

46. Isbin, H. S., Moen, R. H., Mosher, D. R., Two-phase Pressure Drops, AECU-2994 (1954).

47. Isbin, H. S., Moy, J. E., and Cruz, A. J. R., Two-phase, Steam-Water Critical Flow, A.I.Ch.E. Journal, 3, 361-365 (1957).

48. Isbin, H. S., et al., Two-phase, Steam-Water Pressure Drops, Preprint 147, Section XXIV, Nucl. Eng. and Sci. Conf. at Chicago (1958), from A.I.Ch.E.

49. Isbin, H. S., Sher, N. C., Eddy, K. C., Void Fractions in Two-phase, Steam-Water Flow, A.I.Ch.E. Journal, 3, 136-142 (1957).

50. Isbin, H. S., Rodriquez, A., Larson, H. C., and Pattie, B. D., Void Fractions in Two-phase Flow, A.I.Ch.E. Journal, 5, 427-432 (1959).

51. Isbin, H. S., Vanderwater, R., Fauske, H. K., and Singh, S., A Model for Correlating Two-phase, Steam-Water, Burnout Heat Transfer, Presented at the A.I.Ch.E. Summer Meeting, June, 1960, Mexico City, Mexico Journal of Heat Transfer (May 1961).

52. Isbin, H. S., Fauske, H. K., Grace, T., and Garcia, I., Two-phase, Steam-Water Pressure Drops for Critical Flows, Symposium on Two-phase Fluid Flow, February 7, 1962, Institution of Mech. Eng., London, England.

53. Isbigai, S., and Sekoguchi, K., On the Flashing Flow of Saturated Water, Trans. Japan. Soc. Mech. Engrs., 2, No. 8, 563-568 (1959).

54. Jacobs, J., Heat Transfer and Fluid Flow, TID-3305 (1958).

55. Jaroschek, K., and Brandt, F., Untersuchungen über den Reibungsdruckverlust von Wasser/Dampf-Gemischen und die Voreilgeschwindigkeit des Dampfes in senkrechten Kessel-rohren, B.W.K., Bd. 11, No. 9, 407-454 (Sept 1959).

56. Jens, W. H., and Leppert, G. J., Am. Soc. Naval Engineers, 67, 437 (1955).

57. Kirschbaum, E., Kranz, B., and Stark, D., Heat Transfer with a Vertical Vaporizing Tube, Zeitschrift des Vereines Deutscher Ingenieure, Forschungsheft 375 (1935).

58. Kittredge, A. E., and Dougherty, E. S., Discharge Capacity of Traps, Combustion, 6, 14-19 (Sept 1934).

59. Koel, J. C., Ingenieur, 66, No. 13, 19 (1954).

60. Kosterin, S. I., An Investigation of the Effect of the Diameter and Inclination of a Pipe on Friction Factors and the Flow Structure of a Gas-Liquid Mixture, Izvestia Akad. Nauk SSSR, OTN, 12, 1824-1831 (1949).

61. Krasiakova, L. T., Some Characteristic Flows of a Two-phase Mixture in a Horizontal Pipe, Zhurnal Technicheskoi Fiziki, 22, No. 4, 654-669 (1952).

62. Larson, H. C., Void Fractions of Two-phase, Steam-Water Mixtures, M.S. Thesis, Univ. of Minnesota (1957).

63. Leppert, G., Pressure Drop during Forced-circulation Boiling, Ph.D. Thesis, Ill. Inst. Tech. (1954).

64. Levy, S., Theory of Pressure Drop and Heat Transfer for Two-phase Two-component Annular Flow in Pipes, Ohio State Univ. Engrg. Exp. Station Bull. No. 149, Proceedings of the Second Mid-western Conference on Fluid Mechanics, 337 (1952).

65. Lewis, W. Y., and Robertson, S. A., The Circulation of Water and Steam in Water-Tube Boilers, and the Rational Simplification of Boiler Design, Proc. Inst. Mech. Engrs. (London), 143, 147 (1940).

66. Linning, D. L., The Adiabatic Flow of Evaporating Fluids in Pipes of Uniform Bore, Proc. Inst. Mech. Engrs., 1B, 64-75 (1952-1953).

67. Lottes, P. A., Petrick, M., and Marchaterre, J. F., Lecture Notes on Heat Extraction from Boiling Water Power Reactors, Presented at the Advanced Summer Institute at Kjeller, Norway, August 17-29, 1959, ANL-6063.

68. Marcy, G. P., Pressure Drop with Change of Phase in a Capillary Tube, Refrigerating Engrg., 57, 53 (1949).

69. Markson, A. A., Ravese, T., and Humphreys, C. G. R., A Method of Estimating the Circulation in Steam-Boiler-Furnace Circuits, Trans. Am. Soc. Mech. Engrs., 64, 275 (1942).

70. Martinelli, R. C., Boelter, L. M. K., Taylor, T. H. M., Thomsen, E. C., and Morrin, E. H., Isothermal Pressure Drop for Two-phase, Two-component Flow in a Horizontal Pipe, Trans. Am. Soc. Mech. Engrs., 66, 139 (1944).

71. Martinelli, R. C., Lockhart, R. W., Proposed Correlation of Data for Isothermal Two-phase, Two-component Flow in Pipes, Chem. Eng. Prog. 45, 39-50 (1949).

72. Martinelli, R. C., and Nelson, D. B., Prediction of Pressure Drop during Forced Circulation Boiling of Water, Trans. Am. Soc. Mech. Engrs., 70, 695 (1948).

73. Masnovi, R., Literature Survey of Two-phase Flow, Univ. of Pittsburgh (1957).

74. McAdams, W. H., Woods, W. K., and Heroman, L. C., Jr., Vaporization inside Horizontal Tubes. II-Benzene-Oil Mixtures, Trans. Am. Soc. Mech. Engrs., 64, 193 (1942).

75. Mellanby, A. L., and Kerr, W., The Supersaturated Condition as Shown by Nozzle Flow, Proc. Inst. Mech. Engrs., 2, Part 2, 855-883 (1922).

76. Mosher, D. R., Two-phase, Steam-Water, Pressure Drops, M. S. Thesis, Univ. of Minnesota (1954).

77. Moy, J. E., Critical Discharges of Steam-Water Mixtures, M. S. Thesis, Univ. of Minnesota (1955).

78. Pasqua, P. F., Metastable Flow of Freon-12, Refrigerating Engrg., 61, 1084A (1953).

79. Pattie, B. D., Two-phase Flow, Critical Discharges and Void Fractions, M. S. Thesis, Univ. of Minnesota (1957).

80. Rateau, A., Experimental Researches on the Flow of Steam through Nozzles and Orifices, to which is added a Note on the Flow of Hot Water, A. Constable and Co., Ltd., London (1905). Taken from (46).

81. Rettaliatta, Undercooling in Steam Nozzles, Trans. Am. Soc. Mech. Eng., 58, 599 (1936).

82. Reveal, W. S., Heat Transmission Studies in a Natural Circulation Evaporator, Ph.D. Thesis, Univ. of Minnesota (1946).

83. Rodriquez, H. A., Void Fractions in Two-phase, Steam-Water Flow, M.S. Thesis, Univ. of Minnesota (1957).

84. Rogers, J. D., Two-phase Flow of Hydrogen in Horizontal Tubes, AECU-2203.

85. Sauvage, Ecoulement de l'eau des chaudieres, Annales des Mines, 9, Vol. II (1892). Taken from (27).

86. Schneider, F. N., White, P. D., and Huntington, R. L., Horizontal Two-phase Oil and Gas Flow, Pipe Line Industry (Oct 1954).

87. Schwarz, K., Investigations of the Density Distribution, Water and Steam Velocity, and the Frictional Pressure Drop in Vertical and Horizontal Boiler Riser Tubes, Vereines Deutscher Ingenieure, Forschungsheft 445, 20 (1954).

88. Schweppe, J. L., and Foust, A. S., Effect of Forced Circulation Rate on Boiling Heat Transfer and Pressure Drop in a Short Tube, Heat Transfer Symposium, A.I.Ch.E., Atlantic City, N. J., 49, 242-288 (1951).

89. Shapiro, A. H., The Mechanics and Thermodynamics of Steady One-dimensional Gas Flow, Vol. 1, The Ronald Press Co., New York (1953).

90. Shugaev, V., and Sorokin, S., The Hydraulic Resistance of a Two-phase Mixture, Zhurnal Tekhnicheskoi Fiziki, Vol. IX, No. 20, 1854 (1939).

91. Silver, R. S., Temperature and Pressure Phenomenon in the Flow of Saturated Liquid, Proc. Roy. Soc. (London), A194, 464 (1948).

92. Silver, R. S., and Mitchell, J. A., Discharge of Saturated Water through Nozzles, Trans. Northeast Coast Institution of Engineers and Shipbuilders, 62, 51-72, D15-30 (1945-1946).

93. Smith, G. M., and Hoe, Y. L., Water Velocities in the Two-phase Flow of Steam and Water in 4.06 and 6.06 inch Diameter Horizontal Pipelines, C. E. 174, Report No. DL 1186, Dominion Laboratory, Dept. of Scientific and Industrial Research, New Zealand (Sept 1956).

94. Stanton, T. E., The Flow of Gases at High Speeds, Proc. Roy. Soc. (London), A111, 306-339 (1926).

95. Stein, R. P., Hoopes, J. W., Markels, M., Selke, W. A., Bendler, A. J., and Bonilla, C. F., Pressure Drop and Heat Transfer to Non-boiling and Boiling Water in Turbulent Flow in an Internally Heated Annulus, Chem. Eng. Progress Symposium Series, No. 11 50, 115-126 (1954).

96. Stroebe, G. W., Baker, E. M., and Badger, W. L., Boiling-film Heat Transfer Coefficients in a Long-tube Vertical Evaporator, Ind. Eng. Chem., 31, 200 (1939).

97. Stuart, M. C., and Yarnell, D. R., Fluid Flow through Two Orifices in Series, Mech. Eng., 58, 479 (1936).

98. Stuart, M. C., and Yarnell, D. R., Fluid Flow through Two Orifices in Series. II, Trans. Am. Soc. Mech. Engrs., 66, 387-395 (1944).

99. Tangren, R. F., Dodge, C. H., and Seifert, H. S., Compressibility Effects in Two-phase Flow, J. Appl. Phys. 20, 637 (1949).

100. Untermeyer, S., Use of Boiling Water as a Reactor Coolant, Am. Soc. Mech. Engrs., 57-NESC-80 (March 1957).

101. Uren, L. C., Gregory, P. P., Hancock, R. A., and Feskov, G. V., Flow Resistance of Gas-Oil Mixtures through Vertical Pipes, Trans. Am. Inst. Mining Met. Engrs. (Petroleum Dev. and Tech.), 86, 209 (1930).

102. Versluys, J., Mathematical Development of the Theory of Flowing Oil Wells, Trans. Am. Inst. Mining Met. Engrs. (Petroleum Dev. and Tech.), 86, 192 (1930).

103. Woods, W. K., and Worthington, H., Boiling in the Pile, du H 10, 169 (1943). Taken from Moulton, Dr. R. W., and Firey, J. C., General Electric Co., HW-47681 (1957).

104. Yagi, Sakae, Shirai, Takashi, Sasaki, and Teiji, Vertical Tube Reactor. I. Flow Pattern and Hold-up in Gas-Liquid Two-phase Flow, Chemical Engineering (Japan), 15, 317 (1951).

105. Yellott, J. J., Supersaturated Steam, Trans. Am. Soc. Mech. Engrs., 56, 411-430 (1934).

106. Zinzen, A., Der Wasserumlauf in Röhrenkesseln, B.W.K. Bd. 3, No. 7 (July 1951).

107. Zinzen, A., and Schubert, F., Neuer Ansatz zur Auswertung von Versuchen über den naturlichen Wasserumlauf in Dampfkesseln, B.W.K., Bd. 10, No. 5 (May 1958).

APPENDIX A

TABULATION OF CRITICAL-FLOW DATA

Table IV

CRITICAL-FLOW DATA FROM RUNS MADE WITH TSII - LONG

Run No	P_{th} psia	x_{Th} %	G_{ab} lbm/ft²-sec
TSII-1	95	20 0	1067 3
-2	107	24 1	1119 3
-3	106	20 2	1205 5
-4	94	15 68	1182 3
-5	98	22 8	1148 5
-6	104	23 34	1078 4
-7	124	25 87	1230 9
-8	124	38 45	1022 6
-9	125	26 9	1265 4
-10	125	31 96	1115 5
-11	129	26 0	1232 5
-12	127	30 2	1148 5
-13	124	24 94	1250 6
-14	112	31 10	1055 4
-15	115	24 94	1165 4
-16	113	32 72	1014 0
-17	82	31 35	786 1
-18	85	23 88	914 9
-19	69	28 25	723 5
-20	82	36 16	723 5
-21	83	29 05	815 5
-22	109	31 06	1046 5
-23	113	25 92	1130 0
-24	107	37 05	925 5
-25	90	26 73	936 8
-26	Equipment failed - aborted		
-27	90	29 50	889 5
-28	78	22 38	907 1
-29	110	35 41	979 9
-30	113	44 33	862 1
-31	135	28 62	1126 0
-32	116	36 23	993 7
-33	116	45 27	872 6
-34	117	55 88	758 0
-35	Not reliable		
-36	110	31 90	1065 8
-37	110	30 97	1012 0
-38	117	25 02	1184 4
-39	61	27 16	654 5
-40	65	20 67	763 6
-41	65	16 41	858 2
-42	54	23 97	645 2
-43	97	28 31	908 6
-44	98	20 44	1259 1
-45	95	22 65	1106 5
-46	95	24 56	1065 8
TSII-47	95	27 43	1005 1
-48	95	32 15	926 1
-49	95	36 1	862 8
-50	95	40 01	814 9
-51	103	52 25	698 8
-52	Not reliable		
-53	73	23 07	854 8
-54	70	31 57	705 5
-55	71	43 53	576 4
-56	99	23 24	1188 6
-57	103	26 10	1062 5
-58	103	29 33	1017 6
-59	101	33 39	949 4
-60	101	37 53	888 1
-61	105	42 43	828 3
-62	106	53 46	718 5
-63	Equipment failed - aborted		
-64	142	43 61	1027 5
-65	146	52 20	976 13
-65A	129	24 69	1276 8
-66	121	29 54	1171 3
67	122	35 67	1059 9
-68	121	40 56	998 9
-69	123	45 57	928 6
-70	125	50 26	872 0
-71	121	55 94	810 0
-72	127	60 13	781 0
-73	127	61 79	766 2
-74	Not Reliable		
-75	57	15 79	785 6
-76	56	14 18	821 7
-77	57	16 79	760 9
-78	57	19 10	716 8
-79	57	22 78	656 3
-80	57	24 79	626 3
-81	59	34 90	516 6
-82	79	18 04	1002 3
-83	80	21 63	922 5
-84	79	25 26	854 9
-85	79	28 15	807 5
-86	79	31 43	760 4
-87	80	31 32	730 5
-88	81	38 34	678 2
-89	81	44 20	620 7
-90	82	56 71	527 5

Table V

CRITICAL-FLOW DATA FROM RUNS MADE WITH TSIV - SHORT

Run No.	P_{th}, psia	x_{Th}, %	G_{ob}, lb/ft^2-sec	Run No.	P_{th}, psia	x_{Th}, %	G_{ob}, lb/ft^2-sec
TSIV-1	87	2.9	2211.8	TSIV-29	160	24.90	1529.0
-2	115	4.1	1985.0	-30	170	17.00	1908.1
-3	110	13.9	1701.2	-31	175	10.64	2182.1
-4	130	20.94	1415.8	-32	175	5.64	2408.2
-5	205	8.76	2520.0	-33	135	3.34	2685.5
-6	190	13.6	2296.6	-34	102	2.47	2969.3
-7	220	5.15	2831.6	-35	185	27.40	1613.5
-8	185	4.0	3123.6	-36	195	17.40	1956.0
-9	258	13.9	2784.3	-37	195	10.44	2282.2
-10	275	10.15	3000.0	-38	195	7.50	2464.9
-11	268	4.43	3270.0	-39	233	34.50	1785.4
-12	215	2.61	3575.3	-40	242	23.80	2127.9
-13	185	2.05	3911.3	-41	247	17.80	2505.4
-14	150	1.6	4201.7	-42	252	14.40	2719.7
-15	160	24.9	1534.9	-43	270	9.60	2987.2
-16	172	15.3	1883.9	-44	243	5.40	3271.0
-17	188	11.1	2223.5	-45	330	42.80	2104.1
-18	195	6.8	2465.9	-46	340	31.50	2446.7
-19	167	4.14	2734.7	-47	348	22.60	2727.2
-20	205	29.5	1669.3	-48	352	19.50	3043.0
-21	210	20.36	2027.5	-49	361	14.30	3334.0
-22	213	14.6	2328.2	-50	320	40.12	2135.0
-23	222	11.0	2582.4	-51	325	29.40	2373.3
-24	227	6.1	2850.0	-52	330	20.9	2641.7
-25	280	39.06	1954.0	-53	320	17.3	2900.6
-26	217	28.20	1949.5	-54	330	12.04	3200.0
-27	243	20.90	2122.4	-55	310	7.06	3600.7
-28	232	18.5	2448.9				

APPENDIX B

TABULATION OF UPSTREAM PRESSURES

Table VI

TABULATION OF UPSTREAM PRESSURE FOR RUNS MADE WITH TSII - LONG

Distance from throat, in.	4	1/4	$6\frac{1}{4}$	$12\frac{1}{4}$	$24\frac{1}{4}$	$36\frac{1}{4}$	$48\frac{1}{4}$	
Run No.	Back Pressure	P_1, psig	P_2, psig	P_3, psig	P_4, psig	P_5, psig	P_6, psig	x, %
TSII- 1	0	85	132	152	185	200	215	20.0
- 2	0	100	160	182	220	250	260	24.1
- 3	0	97	156	177	215	235	250	20.2
- 4	0	83	132	150	185	205	227	15.7
- 5	0	92	148	167	205	225	240	22.8
- 6	0	95	152	172	210	231	250	23.34
- 7	0	120	192	222	262	286	325	25.9
- 8	0	120	193	222	265	286	325	38.45
- 9	0	124	200	231	275	297	335	26.9
-10	0	117	185	216	255	276	310	37.0
-11	0	120	181	219	261	284	315	26.0
-12	0	117	176	212	251	272	310	30.2
-13	0	120	192	222	262	287	320	24.94
-14	0	104	167	193	233	246	277	31.10
-15	0	107	172	198	242	261	290	24.94
-16	0	104	167	191	233	248	280	32.72
-17	0	72	117	136	165	183	195	31.35
-18	0	74	120	138	172	179	210	23.88
-19	0	57	92	106	128	144	167	28.25
-20	0	72	117	137	167	184	205	36.16
-21	0	72	116	133	158	181	200	29.06
-22	0	102	167	189	230	246	275	31.06
-23	0	107	172	194	235	251	280	25.92
-24	0	100	162	187	225	246	270	37.05
-25	0	80	128	148	180	200	222	26.73
-26	0	Equipment failed-aborted						
-27	0	80	128	149	178	197	220	29.50
-28	0	68	117	137	166	188	210	22.38
-29	0	102	165	190	230	246	274	35.41
-30	0	104	167	196	235	256	280	44.33
-31	0	107	171	198	237	259	285	28.62
-32	0	109	174	200	242	261	290	36.23
-33	0	100	177	204	246	266	295	45.27
-34	0	110	179	209	255	276	310	55.88
-35	0	Not reliable						
-36	0	104	168	191	230	265	295	31.90
-37	0	99	161	181	215	255	280	31.97
-38	0	107	173	194	242	276	310	25.02
-39	0	49	65	95	118	156	175	27.16
-40	0	52	80	104	129	169	188	20.67
-41	0	52	80	107	132	171	190	16.41
-42	0	41	70	84	108	144	158	23.97
-43	0	90	147	169	202	240	268	28.31
-44	0	94	156	179	220	259	290	20.44
-45	0	92	153	177	215	256	285	22.65

Table VI (Cont'd.)

Distance from throat, in.	4	1/4	6¼	12¼	24¼	36¼	48¾	
Run No.	Back Pressure	P_1, psig	P_2, psig	P_3, psig	P_4, psig	P_5, psig	P_6, psig	x, %
TSII-46	0	91	149	173	210	252	280	24.56
-47	0	90	143	167	200	243	265	27.43
-48	0	90	143	167	198	240	260	32.15
-49	0	91	149	171	205	245	265	36.10
-50	0	91	149	170	205	244	265	40.01
-51	0	94	158	179	218	261	288	52.25
-52	0	Not reliable						
-53	0	64	105	126	155	198	220	23.07
-54	0	61	96	116	138	179	195	31.57
-55	0	62	103	121	145	189	208	43.53
-56	0	97	160	186	225	264	300	23.24
-57	0	95	154	177	216	255	285	26.10
-58	0	94	153	174	210	250	275	29.33
-59	0	94	155	176	210	252	275	33.33
-60	0	95	158	180	215	255	275	37.93
-61	0	97	160	183	220	258	285	42.41
-62	0	99	163	188	231	269	295	53.46
-63	0	Equipment failed-aborted						
-64	0	133	202	241	284	329	370	43.61
-65	0	141	218	254	295	339	380	52.20
-65A	0	122	196	228	270	296	335	24.69
-66	0	117	190	217	252	275	310	29.54
-67	0	116	186	217	255	275	310	35.87
-68	0	116	189	218	255	275	310	40.56
-69	0	118	195	228	270	286	320	45.37
-70	0	122	200	233	280	310	348	50.26
-71	0	120	203	239	290	312	365	55.94
-72	0	122	200	237	290	314	365	60.13
-73	0	122	198	236	290	312	365	61.79
-74	0	Not reliable						
-75	0	45	81	96	121	132	155	15.79
-76	0	43	78	95	120	129	150	14.18
-77	0	45	81	96	122	132	155	16.79
-78	0	44	81	96	122	132	155	19.10
-79	0	44	77	91	119	130	155	22.78
-80	0	44	77	89	112	125	150	24.79
-81	0	46	75	90	110	122	145	34.90
-82	0	67	110	139	170	190	210	18.04
-83	0	68	117	139	170	190	210	21.63
-84	0	67	115	129	165	182	210	25.26
-85	0	66.5	109	127	156	173	197	28.15
-86	0	68	111	128	156	173	195	31.41
-87	0	68	110	126	156	175	195	31.32
-88	0	69	115	130	160	178	195	38.34
-89	0	69.5	115	131	160	178	195	44.20
-90	0	70.5	120	141	170	188	215	56.71

Table VII

TABULATION OF UPSTREAM PRESSURES FOR RUNS MADE WITH TSIV - SHORT

Distance from throat, in.	4	1/8	6 1/8	12 1/8	24 1/8	36 1/8	48 1/8	
Run No.	Back Pressure	P_1, psig	P_2, psig	P_3, psig	P_4, psig	P_5, psig	P_6, psig	x, %
TSIV- 1	0	72	97	107	120	132	148	2.9
- 2	0	100	140	150	160	170	180	4.1
- 3	0	95	180	202	220	230	240	13.9
- 4	0	115	223	259	310	342	370	20.94
- 5	0	190	320	355	405	425	440	8.76
- 6	0	175	228	380	445	462	480	13.6
- 7	0	205	289	300	335	350	380	5.15
- 8	0	170	230	240	265	290	320	4.0
- 9	0	243	450	490	585	600	648	13.90
-10	0	260	427	480	530	555	580	10.15
-11	0	253	358	390	415	445	480	4.43
-12	0	202	270	293	330	360	405	2.61
-13	0	170	225	245	290	335	380	2.05
-14	0	135	172	195	243	290	345	1.6
-15	0	145	275	335	397	450	490	24.9
-16	0	157	295	365	418	455	485	15.3
-17	0	173	305	350	395	415	435	11.1
-18	0	180	272	295	310	340	370	6.8
-19	0	152	205	220	235	250	265	4.14
-20	0	190	350	415	500	570	630	29.5
-21	0	195	360	425	500	555	600	20.36
-22	0	198	365	435	510	550	600	14.6
-23	0	207	365	435	475	500	530	11.0
-24	0	212	305	345	360	375	390	6.1
-25	0	265	450	545	645	735	830	39.06
-26	0	202	380	455	560	640	700	28.20
-27	0	228	420	500	590	655	715	20.90
-28	0	222	410	495	585	625	665	18.50
-29	0	145	275	340	395	450	480	24.90
-30	0	155	295	360	415	460	490	17.00
-31	0	160	285	335	355	370	380	10.64
-32	0	160	225	250	260	275	300	5.64
-33	0	120	160	180	190	200	210	3.34
-34	0	87	115	140	160	180	200	2.47
-35	0	170	320	385	465	530	590	27.40
-36	0	180	340	400	470	530	570	17.40
-37	0	180	325	380	440	450	460	10.44
-38	0	180	295	340	360	375	390	7.50
-39	0	218	385	465	565	635	700	34.50
-40	0	227	410	490	595	650	700	23.80
-41	0	232	425	500	585	640	700	17.80
-42	0	237	425	500	575	595	620	14.40
-43	0	255	415	475	500	525	550	9.60
-44	0	228	315	355	375	390	420	5.40
-45	0	315	535	635	755	860	940	42.80
-46	0	325	540	645	775	880	950	31.50
-47	0	333	565	670	795	880	960	22.60
-48	0	337	575	670	795	865	940	19.50
-49	0	346	580	670	755	820	860	14.30
-50	0	305	515	605	725	820	920	40.12
-51	0	310	525	615	735	830	920	29.40
-52	0	315	535	625	745	830	920	20.90
-53	0	305	520	620	715	770	820	17.3
-54	0	315	525	610	670	720	760	12.04
-55	0	295	427	455	485	520	550	7.06

APPENDIX C

CALCULATION PROCEDURE FOR GRAPH 14, REPRESENTING THE "HOMOGENEOUS FLOW MODEL"

The conditions on which Figure 14 are based are as follows:

1. adiabatic and reversible expansion;
2. thermodynamic equilibrium; and
3. equal phase velocities.

The general method of calculation consisted in calculating the critical, or maximum, mass velocity of a steam-water mixture of a given quality x at a given pressure P.

As shown in Chapter V, the theoretical critical mass velocity as derived from the "Homogeneous Flow Model" is given by

$$G_{max} = \left[\frac{-g_c}{\left(\frac{dv}{dP}\right)_{sm}}\right]^{1/2} ,$$

where

$$v = v_l (1 - x) + v_g x \quad .$$

A method which gives good results is to approximate

$$\left(\frac{dv}{dP}\right)_{sm} \text{ by } \left(\frac{\Delta v}{\Delta P}\right)_{sm} \quad .$$

The best means of describing this is to carry out a sample calculation.

A. Intermediate-quality Points

Let

P_c = 11 psia

x = 25% .

For P_c = 11 psia, the Steam Tables give

$$s_f = 0.2903 \quad ; \quad s_{fg} = 1.4897 \quad .$$

Also,

$$s_m = s_f + s_{fg}\, x \quad .$$

In order to calculate dP/dv, the variation in volume v will be determined over a pressure gradient at constant entropy. Thus, for a pressure P' sufficiently close to P, we have

$$s_m = s_f' + s_{fg}'\, x' \quad .$$

Hence,

$$x' = \frac{s_m - s_f'}{s_{fg}'} \quad .$$

Putting in the proper values,

for P = 10 psia, x' = 0.25211;

for P = 12 psia, x' = 0.2479.

The specific volume of the mixture is then calculated by the formula

$$v = v_l (1-x) + v_g\, x \quad ;$$

for P = 10 psia, v = 9.6982 ft^3/lb

for P = 11 psia, v = 8.7974 ft^3/lb

for P = 12 psia, v = 8.0444 ft^3/lb

Next, dP/dv can be obtained graphically as the slope of the tangent to the curve resulting from a plot of P versus v, at the point corresponding to P = 11 psia. From such a plot,

$$dP/dv = 176.69\ lb^2/ft^5 \quad .$$

Then

$$G_{max} = (g\, dP/dv)^{1/2} = 75.4\ lb/ft^2\text{-sec}.$$

Since dP/dv is calculated by a graphical method, its accuracy cannot be assured. The error committed in this evaluation was minimized by "smoothing" the existing values by means of plots of dP/dv versus P and of dP/dv versus v.

As any remaining error would carry over to the determination of G, a correction was made in this variable by plotting P versus G with quality x as a parameter.

B. Saturated Water

It is obvious that, at saturation conditions, the partial derivative dP/dv cannot be calculated by considering pressures just above and just below a given saturation pressure, inasmuch as water would be below its saturation point for any pressure higher than its saturation pressure.

In this case, indirect means were used to evaluate that quantity. Critical mass velocities were plotted against quality with pressure as a parameter, and the resulting curves were extrapolated to quality $x = 0$. The extrapolation, from $x = 0.07$ to $x = 0.00$, though small, was in the steepest portion of the curve, and the values of G so obtained proved to be not too reliable.

Reliability was improved by plotting P versus G and drawing a smooth curve through the points available. These corrected values of G, together with the water enthalpy at given critical pressures (in this case equal to the total energy), constituted all the required data to identify the saturated water line.

C. Saturated Steam

The derivative dP/dv cannot be expected to vary in the same way in both the saturated and superheated regions, and, therefore, the method selected in determining the mass velocity at saturated steam conditions is of importance.

It was thought that the best approach consisted in extrapolating the mixture properties in the saturated region to saturated steam conditions. The adopted procedure was the same as described in Section B, except that the extrapolation was this time in the least steep portion of the curve, and the extrapolated values of G were found to lie on a smooth curve when plotted against P. All other calculations were performed as outlined in Section A.

APPENDIX D

CALCULATION PROCEDURE FOR GRAPH 22, SHOWING THE AUTHOR'S THEORY FOR PREDICTING CRITICAL TWO-PHASE FLOW RATES

The conditions on which Figure 22 is based are as follows:

1. annular flow model where different velocities exist;
2. specific volume of the steam-water mixture given by

$$v = \frac{x^2 v_g}{\alpha_g} + \frac{(1-x)^2 v_l}{1-\alpha_g} \quad ;$$

3. $\left(\frac{dG}{dP}\right)_{\text{constant enthalpy}} = 0$;

4. $\left|\frac{dP}{dl}\right|_{G,x} = \left\{\text{Max}\right\}_{\text{finite}}$; and

5. thermodynamic equilibrium.

The general method of calculation consisted in calculating the critical, or maximum, mass velocity of a steam-water mixture of a given quality x at a given pressure P.

As shown in Chapter V, the theoretical critical mass velocity as derived from the author's theory is given by

$$G_{crit} = \left[\frac{-g_c k}{\{(1-x+kx)x\}\, dv_g/dP + \{v_g(1+2kx-2x)+v_l(2xk-2k-2xk^2+k^2)\}\, dx/dP + \{k[1+x(k-2)-x^2(k-1)]\}\, dv_l/dP}\right]^{1/2} .$$

where

$$k = \left(\frac{v_g}{v_l}\right)^{1/2} .$$

A method which gives good results is to approximate

$$\frac{dv_g}{dP} \text{ by } \frac{\Delta v_g}{\Delta P}, \quad \frac{dv_l}{dP} \text{ by } \frac{\Delta v_l}{\Delta P}, \text{ and } \frac{\Delta x}{dP} \text{ by } \frac{\Delta x}{\Delta P}$$

under isenthalpic conditions.

The best means of describing this is to carry out a sample calculation.

Let P_c = 600 psia and x = 1, 5, 10, 20, 40, 60, and 80%. The thermodynamic properties used in carrying out this sample calculation are tabulated in Table VIII.

Table VIII

THERMODYNAMIC PROPERTIES

Pressures, psia	620	600	580
v_g (ft^3/lb)	0.744	0.7698	0.7973
v_l (ft^3/lb)	0.0202	0.0201	0.0201
h_{fg} (Btu/lb)	727.2	731.6	736.1
h_f (Btu/lb)	475.7		467.4

The quantity $(\Delta P/\Delta v)_H$, the approximation to $(dP/dv)_H$ is calculated by calculating the new specific volumes of a mixture, originally at x_{600} and 600 psia, when expanded isenthalpically to 580 psia and compressed isenthalpically to 620 psia. Then Δv_H is simply equal to the difference between the specific volumes at 580 psia and 620 psia. During this process, x, v_g, and v_l change. The change in x shall be calculated first.

Calculation of $(dx/dP)_H$ at 600 psia

For constant mixture enthalpy,

$$\left(\frac{dx}{dP}\right)_H = -\frac{1}{h_{fg}}\left(\frac{dh_f}{dP} + x\,\frac{dh_{fg}}{dP}\right)$$

$$\approx -\frac{1}{h_{fg}}\left(\frac{\Delta h_f}{\Delta P} + x\,\frac{\Delta h_{fg}}{\Delta P}\right)$$

$$= -\frac{1}{731.6}\left(\frac{475.7 - 467.4}{(40)(144)} - x\,\frac{736.1 - 727.2}{(40)(144)}\right)$$

$$= \frac{10^{-6}}{4.214}\left[-8.3 + (x)(8.9)\right] \quad .$$

Hence the values shown in Table IX can be calculated.

Table IX

TABULATION OF $(dx/dP)_H$ FOR VARIOUS VALUES OF QUALITY AT 600 psia

Quality x, %	$(dx/dP)_H$
1	-1.9485×10^{-6}
5	-1.8640×10^{-6}
10	-1.7584×10^{-6}
20	-1.5472×10^{-6}
40	-1.1248×10^{-6}
60	-0.7024×10^{-6}
80	-0.2800×10^{-6}

Calculation of $(dv_g/dP)_H$ at 600 psia

$$\left(\frac{dv_g}{dP}\right)_H \approx \left(\frac{\Delta v_g}{\Delta P}\right)_H = -\frac{0.7973 - 0.7440}{(40)(144)} = -9.2535 \times 10^{-6} \quad .$$

Calculation of $(dv_l/dp)_H$ at 600 psia

$$\left(\frac{dv_l}{dP}\right)_H \approx \left(\frac{\Delta v_l}{\Delta P}\right)_H = \frac{0.0202 - 0.0201}{(40)(144)} = 1.7361 \times 10^{-8} \quad .$$

Calculation of slip ratio k at 600 psia

$$k = \left(\frac{v_g}{v_l}\right)^{1/2} = \left(\frac{0.7698}{0.0201}\right)^{1/2} = 6.19 \quad .$$

By substituting in the above values for the derivatives and k, for different qualities x, in the equation for determining G_{crit}, Table X is obtained.

Table X

TABULATION OF CALCULATED CRITICAL FLOW RATES FOR VARIOUS VALUES OF QUALITY AT 600 psia

Quality x, %	Critical Flow Rate G, lb/ft^2-sec
1	8960
5	7605
10	6510
20	5100
40	3570
60	2740
80	2235

If the term including dv_l/dP is neglected in the equation giving the critical flow rate, Table XI is obtained.

Table XI

TABULATION OF APPROXIMATE CRITICAL FLOW RATES FOR VARIOUS VALUES OF QUALITY AT 600 psia

Quality x, %	Critical Flow Rate G, lb/ft^2-sec
1	8760
5	7425
10	6408
20	5040
40	3540
60	2730
80	2230

By a comparison of Tables X and XI, it can be seen that the error is less than 3% by neglecting the dv_l/dP term in calculating the critical mass velocity. Furthermore, this error decreases with decreasing pressure. At 400 psia, the error is less than 1%. Hence, all mass velocities below 400 psia can be calculated safely by discarding the dv_l/dP term, which was done in preparing graph 22.

As for calculating the critical flow rates of saturated steam, see Appendix C, since the author's equation for critical flow rate at $x = 1$ converges to that of the "Homogeneous Flow Model."

APPENDIX E

THE ERROR INTRODUCED BY EVALUATING dv/dP FROM STEAM TABLE

The quantities v_f, v_g, h_f, h_{fg}, s_f, and s_{fg} needed to estimate critical flow rates are found in the steam tables of Keenan and Keyes.*

The derivative of a quantity is obtained by a linear approximation from adjacent lines in the tables; thus,

$$\left(\frac{dv_g}{dP}\right)_n \cong \frac{(v_g)_{n+a} - (v_g)_{n-b}}{P_{n+a} - P_{n-b}} \quad ,$$

where P_n, etc., refer to the values in the n^{th} line of the table. In general, a and b were taken as unity, that is, values were computed from adjacent lines in the table except where the intervals were suddenly changed. In that case, a or b was chosen so that

$$P_{n+a} - P_n = P_n - P_{n-b} \quad .$$

The error introduced by this technique is partly due to the fact that the slope of the chord differs slightly from the slope of the tangent at the midpoint of the arc, and partly due to the small difference between adjacent variables. Curve fitting with approximate analytical expressions and differentiation may eliminate the first error, but not the second; that is, one cannot fit any curve any more accurately than the given points. The error due to the linear approximation in evaluating the derivatives dv_f/dP, dh_f/dP, and dh_{fg}/dP is practically zero since the quantities v_f, h_f, and h_{fg} vary approximately in a linear fashion with respect to pressure in limited regions. The errors due to the difference between chord and tangent can be shown to be of the order of $(\Delta P/P)^2$ for evaluating dv_g/dP, ds_f/dP, and ds_{fg}/dP.

First, consider the difference of slope between the chord and the tangent. The chord is chosen to be symmetric about the point of interest.

*Keenan, J. H., Keyes, F. G., Thermodynamic Properties of Steam, John Wiley and Sons, Inc., New York (1936).

Over a limited region the value of v_g varies approximately as $1/P$, and s_{fg} and s_f vary approximately as log P. For both these types of functions one can show the error to be equal to $(\Delta P/P)^2$.

Case I

$$y = x^n;$$

$$y + \Delta y = \Delta y = (x + \Delta x)^n = x^n\left[1 + n\frac{\Delta x}{x} + \frac{n(n-1)}{1\cdot 2}\left(\frac{\Delta x}{x}\right)^2 + \text{------}\right] \quad ;$$

$$y - \Delta y = (x - \Delta x)^n = x^n\left[1 - \frac{n\Delta x}{x} + \text{------}\right] \quad ;$$

$$2\Delta y = x^n\left[2\frac{n\Delta x}{x} + 2\frac{n(n-1)(n-2)}{1\cdot 2\cdot 3}\left(\frac{\Delta x}{x}\right)^3 + \text{------}\right] \quad ;$$

$$\frac{\Delta y}{\Delta x} = nx^{n-1}\left[1 + \frac{(n-1)(n-2)}{2\cdot 3}\left(\frac{\Delta x}{x}\right)^2 + \text{------}\right] \quad .$$

The definition of the tangent is the slope of the chord as $\Delta x \to 0$; thus,

$$1 + \frac{(n-1)(n-2)}{2\cdot 3}\left(\frac{\Delta x}{x}\right)^2 + \text{higher powers of } \frac{\Delta x}{x}$$

is the error in using a chord symmetrically disposed about the point of interest. Now, v_g varies approximately as P^{-1}. Hence, the chord differs from the tangent by a factor differing from unity by $(\Delta P/P)^2$.

Case II

$$y = \log x \quad ;$$

$$\Delta y = \log (x + \Delta x) - \log x \quad ;$$

$$\Delta y = \log \left(1 + \frac{\Delta x}{x}\right) \quad ;$$

$$-\Delta y = \log \left(1 - \frac{\Delta x}{x}\right) \quad .$$

Therefore,

$$2\Delta y = \log \left(1 + \frac{\Delta x}{x}\right) - \log \left(1 - \frac{\Delta x}{x}\right)$$

$$= \frac{\Delta x}{x} + \left(\frac{\Delta x}{x}\right)^2 + \left(\frac{\Delta x}{x}\right)^3 + \text{------} + \frac{\Delta x}{x} - \left(\frac{\Delta x}{x}\right)^2 + \left(\frac{\Delta x}{x}\right)^3 \text{----}$$

$$= 2\frac{\Delta x}{x} + 2\left(\frac{\Delta x}{x}\right)^3 + \text{----} \quad .$$

Hence,

$$\frac{\Delta Y}{\Delta x} = \frac{1}{x}\left[1 + \left(\frac{\Delta x}{x}\right)^2 + \text{------}\right] \quad .$$

Since s_{fg} and s_f approximate a log P function over limited regions, here again chord errors are of the form $(\Delta P/P)^2$.

It should be noted that if a nonsymmetrical chord is chosen to approximate the tangent, so that the one end of the chord is at a point of interest, then the error will become $\Delta P/P$ instead of $(\Delta P/P)^2$. This can be seen immediately in the above derivation since the first terms in the bionomial expression cancel.

APPENDIX F

SAMPLE CALCULATION SHOWING THE DETERMINATION OF CRITICAL MASS VELOCITY, CRITICAL PRESSURE, AND QUALITY AT ANY POINT ALONG THE TEST SECTION FROM THE EXPERIMENTAL DATA

Computations involved in determining the critical mass velocity, critical pressure, and quality are illustrated by the following sample calculation based on run TSII-42 (see Chapter IV).

1. Critical Mass Velocity

$W_m = W_s + W_{sL} = 322 + 595.5 = 917.5$ lb/hr.

Cross-sectional area of test Section II: $A = 0.000395$ ft^2.

Mass velocity: $G = \frac{917.5}{(0.000395)(3600)} = 645.2$ lb/sec-ft^2.

2. Critical Pressure

There are six pressure measurements along the test section to consider, namely, P_1, P_2, P_3, P_4, P_5, and P_6 (see Chapter IV). These pressure data are plotted versus distance from pressure tap 6, and the resulting curve is extrapolated to the outlet of the test pipe (1 diameter length) to obtain the critical pressure. Examples of this are shown in graphs 25 through 28. From such a plot, $P_{th} = 54$ psia.

3. Mixture Composition at Any Point along the Pipe

It can readily be recognized that, in order to arrive at true values of vapor and liquid mass fractions, void-fraction relationships are required, which indeed have been derived in this work. However, it will be shown here that by assuming homogeneous flow this causes no significant change in quality. Sample calculations of the quality at pressure tap 6 by means of both annular and homogeneous flow models follow:

a. Calculation of the quality at pressure tap 6 assuming homogeneous flow:

From Eq. (5.13-13), neglecting kinetic-energy terms, one has for a first approximation of x_6:

$$x_{0,6} = \frac{W_s H_s + W_{sL} H_{sL} - Q_{Loss} - W_m h_l}{W_m h_{fg}}$$

W_s = 322 lb/hr; P_s = 350 psia; T_s = 583.3°F; H_s = 1301.4 Btu/lb;
W_{sL} = 595.5 lb/hr; P_{sL} = 595 psia; T_{sL} = 98.0°F; H_s = 66 Btu/lb;
W_m = 917.5 lb/hr; P_6 = 173 psia; h_l = 342.6 Btu/lb; h_{fg} = 853.7 Btu/lb;
Q_{Loss} = 20.000 Btu/hr.

Heat losses, Q_{Loss}, for the system were determined with superheated steam. The heat losses over the system from the steam Flowrator to the inlet of the test section were found, in five separate trials, to vary from 15.000 to 25.000 Btu/hr or approximately 5% of the steam enthalpy at the Flowrator. The trials were done at different steam flow rates. For calculating the quality at the inlet to the test section in the two-phase runs, the enthalpy loss over this inlet section was taken to be 20.000 Btu/hr.

Under the same conditions as above, the heat losses over the total test section were measured and found to be negligible compared with the steam enthalpy at the Flowrator.

Heat losses for the water inlet line were assumed negligible.

$$x_{0,6} = \frac{(322)(1301.4)+(595.5)(66)-20.000-(917.5)(342.6)}{(917.5)(853.7)} = 0.1583 \quad .$$

Evaluation of kinetic energies at Flowrators:

v_s = 1.6699 ft³/lb; v_{g_6} = 2.630 ft³/lb;

v_{sL} = 0.016 ft³/lb: v_{l_6} = 0.0182 ft³/lb;

$KE_s = W_s^3 v_s^2 / 2gJA^2$;

g_c = 32.2 lb_m-ft/lb_f-sec²; J = 778 Btu/lb_f-ft

$A = \pi D^2/4 = (3.14)(1/12)^2/4 = 0.00545$ ft².

So the kinetic energy for the steam at the Flowrator becomes

$$KE_s = (322)^3(1.6699)^2/(2)(32.2)(778)(0.00545)^2(3600)^2 = 2.631 \text{ Btu/hr.}$$

For the subcooled water at the Flowrator;

$$KE_{sL} = (595.5)^3(0.016)^3/(2)(32.2)(778)(0.00545)^2(3600)^2 = \text{negligible.}$$

Evaluation of the kinetic energy of the steam-water mixture at pressure tap 6:

From "Homogeneous Flow Model,"

$$v_m = xv_g + (1-x)v_l = (0.1583)(2.630) + (0.8417)(0.016) = 0.4298.$$

$$A = \frac{\pi D^2}{4} = \frac{(3.14)(0.269/12)^2}{4} = 0.000395 \text{ ft}^2.$$

From Eq. (5.13-7), one gets:

$$(KE)_{TP\ Homogeneous} = \frac{W_m^3 v_m^2}{2g_c J A^2}$$

$$= \frac{(917.5)^3(0.4298)^2}{(2)(32.2)(778)(0.000395)^2} = 1374 \text{ Btu/hr} \quad .$$

Solving again for x in Eqs. (5.13-13) and (5.13-12), neglecting kinetic energy terms at Flowrators,

$$x_{1,6} = x_{0,6} - \frac{KE_{TPH}}{W_m h_{fg}} = 0.1583 - \frac{1374}{(917.5)(853.7)} = 0.1565$$

Repeating the procedure,

$$v_m = (0.1565)(2.630) + (0.8435)(0.016) = 0.4251.$$

$$KE_{TPH} = \frac{(917.5)^3(0.4251)^2}{(2)(32.2)(778)(3600)^2(0.000395)^2} = 1343 \text{ Btu/hr}$$

and

$$x_{2,6} = 0.1583 - \frac{1343}{(917.5)(853.7)} = 0.1566 \quad .$$

Hence, the quality at pressure tap 6 assuming homogeneous flow is equal to 0.1566.

b. Calculation of the quality at pressure tap 6 using the author's theoretical expression for the void fraction α_g.

Using Eq. (5.13-12),

$$x = x_0 + c \quad ,$$

where

$$x_0 = \frac{W_s H_s + W_{sL} h_{sL} - Q_{Loss} - W_m h_l}{W_m h_{fg}}$$

$$c = \frac{8}{\pi^2 g_c J W_m h_{fg}} \left[\frac{W_s^3 v_s^2}{D_s^4} + \frac{W_{sL}^3 v_{sL}^2}{D_{sL}^4} - \frac{W_m^3}{D^4} \left\{ \frac{x^3 v_g^2}{R_g^2} + \frac{(1-x)^3 v_l^2}{(1-R_g)^2} \right\} \right] \quad .$$

From Eq. (5.13-13), one has:

$$x_{0,6} = 0.1583 \quad .$$

The void fraction α_g is given by Eq. (5.9-13):

$$\alpha_g = \left[\frac{1-x}{x} \left(\frac{v_l}{v_g} \right)^{1/2} + 1 \right]^{-1} = \left[\left(\frac{0.8417}{0.1583} \right) \left(\frac{0.0182}{2.630} \right)^{1/2} + 1 \right]^{-1} = 0.6930 \quad .$$

The kinetic-energy correction factor c then becomes

$$c = \frac{(8)(3600)^{-2}}{(3.14)^2 (50103)(917.5)(853.7)}$$

$$\left[\frac{(322)^3 (1.670)^2}{(1/12)^4} + \frac{(595.5)^3 (0.016)^2}{(1/12)^4} - \frac{(917.5)^3}{(0.269/12)^4} \left\{ \frac{(0.1583)^3 (2.630)^2}{(0.6930)^2} + \frac{(8417)^3 (0.0182)^2}{(0.3070)^2} \right\} \right] = -0.0003 \quad ,$$

and, using Eq. (5.13-12) one gets

$$x_{1,6} = 0.1583 - 0.0003 = 0.1580.$$

Hence, the quality at pressure tap 6 assuming an annular flow model is equal to 0.1580.

As one can see, this iteration procedure converges quite rapidly. Furthermore, the error by assuming homogeneous flow in calculating the quality, which saves considerable labor, is less than 1%. In the same manner as described above, the quality x can be calculated at any point along the pipe where the static pressure is known.

APPENDIX G

CALCULATION PROCEDURE FOR EVALUATION OF THE FRICTION COEFFICIENT FROM EQUATION (5.12-7)

The two-phase friction coefficient will be calculated from Eq. (5.12-7), based upon the experimental data for run TSII-42 (see Chapter IV).

Equation (5.12-7) is

$$f_m = -\frac{2D}{L}\left\{\frac{g_c}{G^2}\left[\frac{k}{x[1+x(k-1)]}\right]_{\text{mean}}\left|\frac{p^{n+1}}{a}\sum_{m=0}^{\infty}\frac{\left(-\frac{\Gamma}{a}p^n\right)^m}{n(m+1)+1}\right|_{P_2}^{P_1} + \log\frac{v_1}{v_2}\right\} \quad ,$$

where

$$\Gamma = \frac{1-x}{x} v_l k \quad ; \quad v_g = a P^{-n} \quad ;$$

$$v = \frac{[(1-x)v_l k + x\, v_g][1+x(k-1)]}{k} \quad ; \quad k = \left(\frac{v_g}{v_l}\right)^{1/2}$$

Furthermore, for Eq. (5.12-7) to give a solution that converges, the following condition must be satisfied:

$$\left|\frac{\Gamma}{a} P^n\right| < 1 \quad .$$

As an example, the average friction coefficient between pressure taps 2 and 1 in run TSII-42 will be calculated, with $P_2 = 85$ psia and $P_1 = 56$ psia, and with $L = \frac{1}{2}$ ft.

The qualities at P_2 and P_1 are calculated in the same manner as is shown in Appendix F for P_6 and are

$$x_2 = 0.2173; \quad x_1 = 0.2382 \quad .$$

The constants a and n in $v_g = aP^{-n}$ are evaluated from steam tables and are

$$a = 5 \times 10^4; \quad n = 0.973 \quad .$$

Calculations of slip ratio at P_2 and P_1:

At P_2,

$$v_{g_2} = 5.168 \text{ ft}^3/\text{lb} \text{ and } v_{l_2} = 0.01761 \quad .$$

Hence

$$k_2 = \left(\frac{5.168}{0.01761}\right)^{1/2} = 17.13 \quad .$$

At P_1,

$$v_{g_1} = 7.656 \text{ ft}^3/\text{lb} \text{ and } v_{l_1} = 0.01733 \quad .$$

Hence

$$k_1 = \left(\frac{7.656}{0.01733}\right)^{1/2} = 21.02$$

Calculation of Γ_2 and Γ_1

$$\Gamma_2 = \frac{1 - x_2}{x_2} v_{l_2} k_2 = \frac{1-0.2173}{0.2173} (0.01761)(17.13) = 1.0864 \quad .$$

$$\Gamma_1 = \frac{1 - x_1}{x_1} v_{l_1} k_1 = \frac{1-0.2382}{0.2382} (0.01733)(21.02) = 1.1650 \quad .$$

Check on $\left|\frac{\Gamma}{a} P^n\right| < 1$:

$$\frac{\Gamma_1}{a} P_1^n = \frac{1.1650}{5 \times 10^4} (56 \times 144)^{0.973} = 0.14737 \quad .$$

$$\frac{\Gamma_2}{a} P_2^n = \frac{1.0864}{5 \times 10^4} (85 \times 144)^{0.973} = 0.20626 \quad .$$

Hence, the condition is satisfied for the solution to converge.

Calculation of $\left[\frac{k}{x\ 1 + x(k-1)}\right]_{\text{mean}}$:

$$\left[\text{Mean}\right] = \left[\frac{17.13}{(0.2173)\ 1 + 0.2173(17.13-1)} + \frac{21.02}{(0.2382)\ 1 + 0.2382(21.02-1)}\right]^{1/2}$$

$$= \left[17.4986 + 15.2969\right]^{1/2} = 16.3977 \quad .$$

Calculations of P_1^{n+1}/a and P_2^{n+1} :

$$\frac{P_2^{n+1}}{a} = \frac{(85 \times 144)^{1.973}}{5 \times 10^4} = 2354.0 \quad .$$

$$\frac{P_1^{n+1}}{a} = \frac{(56 \times 144)^{1.973}}{5 \times 10^4} = 1020.1 \quad .$$

Calculations of $\sum_{m=0}^{\infty} \frac{\left(-\frac{\Gamma}{a} P^n\right)^m}{n(m+1)+1}$ at P_2 and P_1:

$$\sum_{m=0}^{\infty} \frac{\left(-\frac{\Gamma}{a} P^n\right)^m}{n(m+1)+1} = \frac{1}{n+1} - \frac{\frac{\Gamma}{a} P^n}{(2n+1)} + \frac{\left(\frac{\Gamma}{a} P^n\right)^2}{(3n+1)} - \frac{\left(\frac{\Gamma}{a} P^n\right)^3}{4n+1} + \frac{\left(\frac{\Gamma}{a} P^n\right)^4}{5n+1} - \cdots\cdots$$

At P_2,

$$\sum_{m=0}^{\infty} \approx 0.5068 - 0.0700 + 0.0109 - 0.0018 + 0.0003 = 0.4462 \quad .$$

At P_1,

$$\sum_{m=0}^{\infty} \approx 0.5068 - 0.0500 + 0.0055 - 0.0006 + 0.0001 = 0.4618 \quad .$$

Then

$$\left| \frac{P^{n+1}}{a} \sum_{m=0}^{\infty} \frac{\left(-\frac{\Gamma}{a} P^n\right)^m}{n(m+1)+1} \right|_{P_2}^{P_1} = (1020.1)(0.4618) - (2354.0)(0.4462)$$

$$= 471.06 - 1050.35$$

$$= -579.29 \quad .$$

Calculation of $\log_e v_1/v_2$:

$$\frac{v_1}{v_2} = \frac{\left[(1 - x_1) v_{l_1} k_1 + x_1 v_{g_1}\right] \left[1 + x_1 (k_1 - 1) k_2\right]}{\left[(1 - x_2) v_{l_2} k_2 + x_2 v_{g_2}\right] \left[1 + x_2 (k_2 - 1) k_1\right]}$$

$$= \frac{[(1-0.2382)(0.01733)(21.02) + (0.2382)(7.656)][1+(0.2382)(21.02-1)](17.13)}{[(1-0.2173)(0.01761)(17.13) + (0.2173)(5.168)][1+(0.2173)(17.13-1)](21.02)}$$

$$= 1.6134 \quad .$$

Hence

$$\log_e v_1/v_2 = 0.47834 \quad .$$

Finally, the average two-phase friction coefficient between pressure tap 2 and 1 for run TSII-42 with a flow rate G=645.2 lb/sec-ft^2 and inside diameter of the pipe equal to 0.269 in. becomes

$$f_m = \left[\frac{-(2)(0.269)}{(6)}\right]\left[\frac{(32.2)}{(645.2)^2}(16.3977)(-579.29) + 0.47834\right]$$

$$= (-0.08967)\left[(0.73362) + (0.47834)\right]$$

$$= (-0.08967)(-0.25528)$$

$$= 0.0229 \quad .$$

Therefore, the above procedure shows how the developed theory in this work also can be used to calculate the two-phase friction coefficient. Also, the described procedure above was used to verify $\partial f/\partial k = 0$ for $k = (v_g/v_l)^{1/2}$ from experimental data. The friction factor f_m was calculated by choosing different values of k, each time carrying out the procedure above, and indeed a graph similar to graph 19 in Chapter V was obtained. This was carried out for a few extreme runs. For the run TSII-42 above, the average slip ratio between P_2 and P_1 calculated from Eq. (5.9-12) is $(17.13+21.02)/\frac{1}{2} = 19.075$ and gives a friction factor equal to 0.0229. For the same experimental data, using an average value of 15 for the slip ratio, the friction factor is found to be 0.0165, and for k_{av}, equal to 25, f_m becomes 0.0210, which shows that f_m obtains its maximum value for a value of k greater than 15 and less than 25.